The Interaction of Chlorophyll a with Lipids in Model and Natural Membrane Systems

Thesis by
Kenneth Eugene Eigenberg

In Partial Fulfillment of the Requirements
for the Degree of
Doctor of Philosophy

California Institute of Technology
Pasadena, California

1981
(Submitted October 23, 1980)

To Helen - My partner in all the truly important things

ACKNOWLEDGMENTS

If this work has enjoyed any success it was because it was initiated from a point of nearly complete ignorance about chlorophyll and photosynthetic membranes. Had we known more about what we were doing during the early stages a number of approaches which later proved fruitful would have been rejected off-hand as being impractical. Thus a good deal of credit is due to the entire Chan group for providing the kind of environment which encourages exploration and which recognizes that the risk of failure is an important component of success.

Bill Croasmun was a partner in this project from the very beginning and has contributed to this thesis by his friendship as well as his ideas. In addition to providing the necessary critical mass of two heads, Bill's temperate logic kept us on course several times when I would have eagerly run off on a tangent.

Special thanks to our group secretary Emily Olson, and to Henriette Wymar and Helen who went out of their way to help put this thesis together.

Finally, I wish to express my deepest regard to my parents who taught me the value of hard work, to my wife and friends who taught me the value of good fun, and to Sunney Chan who encouraged me to work hard all the while making me think it was fun.

ABSTRACT

Chlorophyll a is the principal photosynthetic pigment of plants and most algae. Despite its importance relatively little is known about its organization or environment within the photosynthetic membrane. A variety of evidence suggests that a significant portion of the chlorophyll may be associated with the lipid portion of the photosynthetic thylakoid membrane. The topic of the interaction of chlorophyll with lipid membranes, both model and natural, forms the basis of this thesis.

It is found that chlorophyll a can be incorporated into model phospholipid bilayer membranes at up to 40 mole percent. Both multilamellar and small vesicular bilayer forms can be prepared and characterized. The phase diagram of the chlorophyll a/distearoylphosphatidylcholine (DSPC) bilayer system, obtained by differential thermal analysis, is complex and indicates that below the solidus phase transition chlorophyll a and DSPC form a compound phase with a composition of 40 mole percent chlorophyll a. A thermodynamic simulation of the phase diagram yields an estimate for the strength of the chlorophyll a-DSPC interaction. Nuclear magnetic resonance studies, utilizing the shift effect on nearby nuclei due to the large ring current magnetic anisotropy of chlorophyll, demonstrate that compound formation results from a coordination interaction between the DSPC phosphate and the central magnesium atom of chlorophyll a which has an obligatory requirement for an additional axial ligand.

The optical properties of chlorophyll a are modified by its inclusion into bilayers and change at the bilayer phase transition. Compared to chlorophyll a in organic solution, chlorophyll a in bilayers has absorption maxima which are strongly red-shifted and a greatly reduced fluorescence. The red-shift is most pronounced and fluorescence is lowest below the solidus phase transition temperature. Several possible causes of these changes in optical properties are discussed. Because the optical properties of chlorophyll a/DSPC bilayers in the compound phase duplicate the optical properties of bulk in vivo chlorophyll quite well, this system constitutes an attractive model of the photosynthetic chlorophyll antenna.

Evidence for the location of a pool of chlorophyll in a lipid environment comes from the ^{13}C-NMR spectrum at 90.5 MHz of the photosynthetic thylakoid membrane from spinach. Specific lipid and chlorophyll resonances are observed and assigned but no protein resonances are found. It can be estimated that at least 30% of the plant chlorophyll contributes to the high resolution spectrum with the remainder presumably broadened by association with membrane proteins. The resonance linewidths of the observed chlorophyll phytol chains are approximately the same as those of the lipid hydrocarbon chains indicating that their motional states are similar and suggesting that this fraction of chlorophyll is lipid bound or at most only loosely associated with membrane proteins.

TABLE OF CONTENTS

TABLE OF CONTENTS

TABLE OF CONTENTS

TABLE OF CONTENTS

FOREWORD

The mutual orientation of chromophores within photosynthetic membranes must be an important determinant of their spectral properties and photochemical function. A conceptual "blueprint" of the molecular architecture of the membrane could therefore contribute substantially to an understanding of the light-reaction events in photosynthesis. Unfortunately, no such blueprint exists and the molecular organization of photosynthetic membranes is only incompletely understood at present. In particular, the important questions of how individual membrane components, especially chlorophylls, are oriented vis-a-vis each other and how this organization affects photochemical properties are yet to be answered. The objective of this dissertation is to consider these questions and to report research efforts which provide a partial answer.

Chapter I discusses the properties of chlorophyll a in relation to its role in photosynthesis. The question of how chlorophyll is bound to the photosynthetic membrane is considered and evidence is presented to suggest that a portion of the chlorophyll a is involved with the membrane lipids. This conclusion is later supported in chapter VI by the finding that some chlorophyll phytol chains have a motional state similar to that of the lipids.

Chapters III, IV, and V then consider the organization of chlorophyll a in model phospholipid bilayer membranes and the interactions between chlorophyll a and the lipids. In chapter III the binary phase

diagram of the chlorophyll a/phospholipid bilayer system is determined by calorimetric techniques. Chapter IV provides additional interpretation of the phase behavior and shows evidence for a specific chemical interaction between chlorophyll a and lipids. Chapter V shows that the spectral properties of chlorophyll a are substantially altered by incorporating it into a bilayer and reports the spectral changes that occur upon varying the temperature through the region of the thermal phase transition.

Appendices A and B report some collateral observations which appeared during the course of this work. While they do not contribute substantially to the theme of chlorophyll a in membranes, they are interesting enough to stand on their own merit and are therefore included as supplementary appendices.

CHAPTER I

General Introduction - The Role of Chlorophyll in Photosynthesis

Photosynthetic organisms, which have the unique capability of harvesting solar energy and converting it into biosynthetically useful chemical energy, provide the primary source of nearly all energy consumed in the biosphere. Without photosynthesis it is unlikely that any significant level of biological activity could be sustained. The photosynthetic process is largely constructed around one particular class of molecules, the chlorophylls, whose special properties seem to be uniquely adapted to their intended function. Thus we might say (with necessary apologies) that without chlorophyll, life itself would be impossible.

In this chapter we will first consider the general process of photosynthesis and in particular the special role that chlorophylls play in harvesting the necessary energy from sunlight. Second, we will describe the specialized membrane structures which photosynthetic organisms have developed for this purpose and discuss their molecular components. We will then consider in more detail the properties of chlorophyll and, finally, speculate on the question of how chlorophyll is organized in the photosynthetic membrane.

A. PHOTOSYNTHESIS

Photosynthesis may be defined as the process by which phototrophic organisms utilize sunlight to produce fuels necessary for the biosynthesis of cell components. In green plants this process couples the catalytic oxidation of water to molecular oxygen with the fixation of atmospheric CO_2 by reduction to the form of carbohydrates. The overall reaction is described by the well known equation:

$$6CO_2 + 6H_2O \xrightarrow{h\nu} C_6H_{12}O_6 + 6O_2.$$

This reaction is accomplished in two separate phases.[1] In the first, energy from sunlight is stored in a high potential reductant as NADPH, and in the form of a high energy phosphate bond in ATP:

$$H_2O + NADP^+ + P_i + ADP \xrightarrow{h\nu} O_2 + NADPH + H^+ + ATP.$$

In the second phase, the products of the above reaction provide energy for the enzyme-catalyzed reduction of CO_2 to carbohydrates:

$$CO_2 + NADPH + H^+ + ATP \rightarrow C_6H_{12}O_6 + NADP^+ + ADP + P_i.$$

The first phase requires sunlight and is therefore referred to as the light reaction. The second phase is analogous to the respiratory process in animals and is independent of light, requiring only CO_2 and the products of the light reaction. It is referred to as the dark reaction of photosynthesis.

The light reaction in plants uses electrons from the oxidation of water as the electron source for the reduction of $NADP^+$ to NADPH,

yet the reduction potential of water is some 1.2 volts positive with respect to $NADP^+$. This uphill electron transfer reaction is driven by the absorption of photon energy from sunlight. It is almost universally accepted that the boost in electron energy is accomplished in two separate steps by two functionally distinct systems of pigments and electron carriers, called photosystems I and II. The pathway of electron flow through these photosystems is depicted in Figure I-1. According to this scheme, an electron from the oxidation of water is raised to a higher potential by photosystem II. Transfer from photosystem II to photosystem I occurs through an electron transport chain of successively lower potential redox couples. The 0.4 volt of downhill energy is partially conserved by the phosphorylation of ADP to ATP. In photosystem I the potential of the electron is boosted once again, and it then enters a second electron transport chain of high potential electron carriers which eventually reduce $NADP^+$ to NADPH.

Photosystem I and photosystem II are composed of groups of pigments which function as a photosynthetic unit.[2] Foremost among these pigments are the chlorophylls which are the principal pigment of plants and are found in all photosynthetic organisms. The bulk ($> 99\%$) of the chlorophyll in the plant photosynthetic unit, called antenna or light-harvesting chlorophyll, functions to absorb photons and to funnel the resulting excitation energy through an energy transfer process to a special pair of chlorophyll molecules which constitute the reaction center. In the reaction center the excitation energy gathered by the antenna is used for a charge separation, either by loss of an electron to an acceptor, or by developing opposite charges on a separated pair

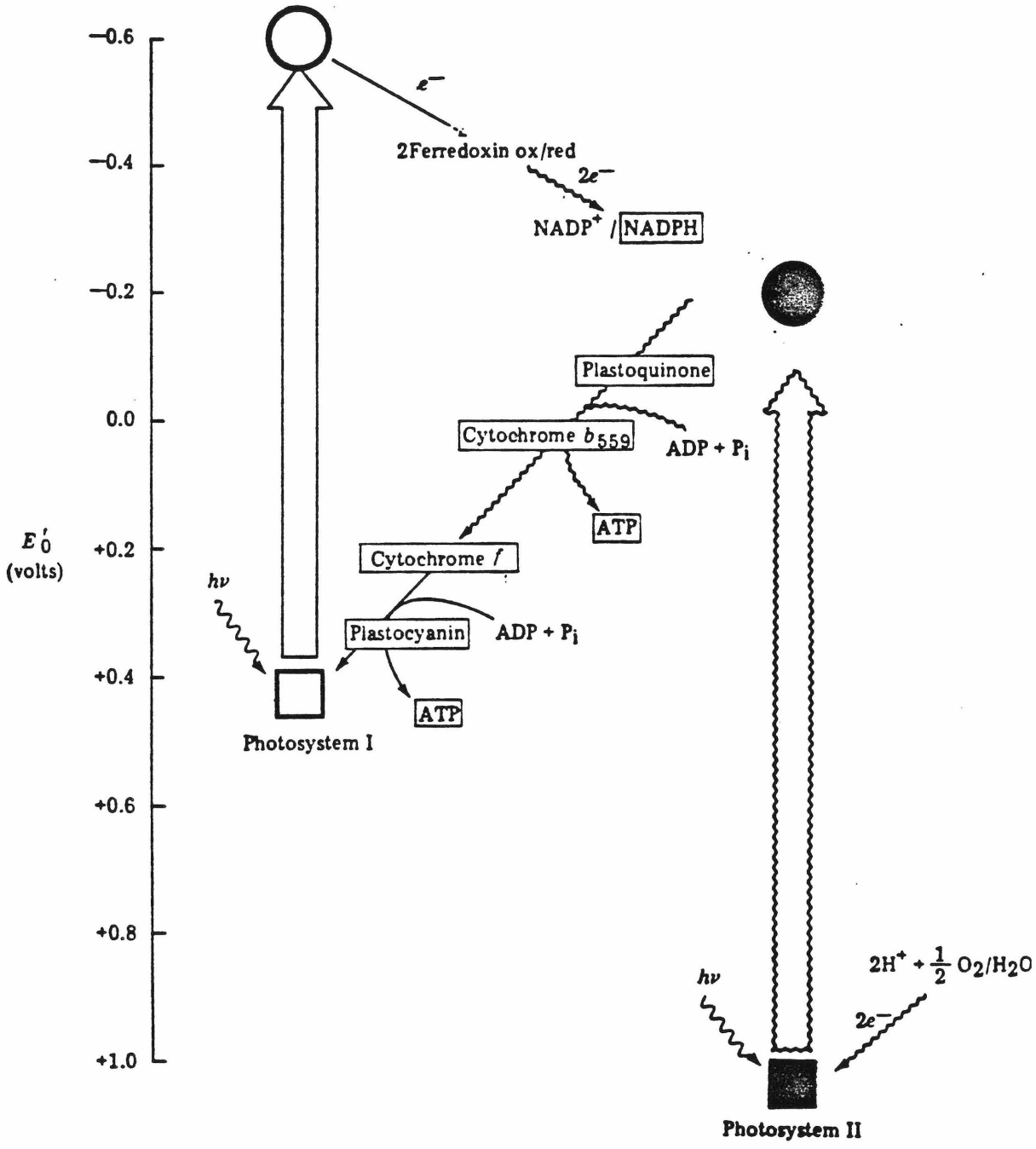

FIGURE I-1. Z-scheme of photosynthetic electron transport.

of chlorophyll molecules. Accessory pigments, such as carotenoids and biliproteins, provide a broad spectral coverage but ultimately transfer their excitation energy to chlorophylls. The pathway of energy flow through the photosynthetic pigments is schematized in Figure I-2. As shown in Figure I-2, the absorption of light by chlorophyll raises the molecule to either the first or second excited singlet state depending upon the energy of the absorbed photon. Rapid internal conversion occurs leaving all chlorophyll molecules in the ground vibrational level of the first excited state singlet. The singlet excitation then migrates among the antenna chlorophyll until it reaches one of the reaction centers which act as a lower energy 'trap' for the excitation. In order to balance the available energy between the two photosystems, excitation energy can also be transferred from one photosystem to another.[3] The exact mechanism of energy transfer is not known. Proposed mechanisms[4,5] vary from an exciton model in which the excitation is delocalized over a set of interacting chlorophyll molecules to a Förster mechanism[6] involving the discrete transfer of excitation energy between two chlorophylls.

B. PHOTOSYNTHETIC MEMBRANES

In all photosynthetic organisms the photosynthetic apparatus is associated with some form of membrane structure. The membrane serves a number of useful purposes. First, it provides a matrix for structural support and for the spatial organization of membrane components. Second, it provides partitions for the separation of metabolic products and allows the development of non-equilibrium chemical and

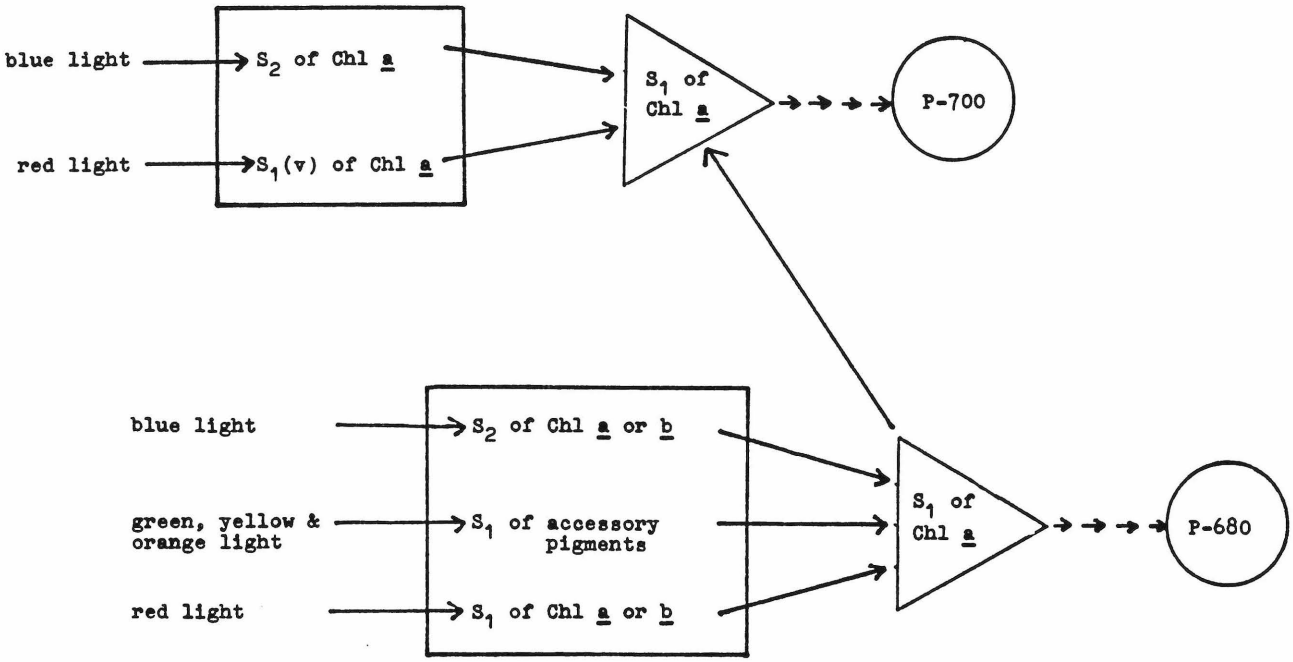

FIGURE I-2. Energy flow through the photosynthetic system of pigments.

electrical gradients.

In green plants the photosynthetic apparatus is contained in specialized plastids called chloroplasts.[7] The size, shape and number of chloroplasts vary from organism to organism, and to a certain extent may be influenced by the metabolic state and environmental conditions. The chloroplasts of spinach and of corn, one of which is shown in Figure I-3, are typical and used routinely for investigations. They tend to be oblately spheroidal in shape and may extend from 2-7 micrometers along the major axis. Chloroplasts are usually found with a double external membrane which is osmotically sensitive and selectively permeable to metabolic products. This outer membrane system is called the envelope membrane. Extending from one pole of the chloroplast to another is a second, highly organized and particularly striking system of membranes called the thylakoid system. As seen in Figure I-3, the thylakoids are collected in some regions into dense stacks of membranes called grana. It is quite generally thought that the grana resemble stacks of flattened membrane sacks interconnected by anastamosing membranes as illustrated in Figure I-4. The stacking structure has been verified by electron microscopy,[8] and by X-ray diffraction[9] it has been determined that the spacing between adjacent membranes is approximately 75 angstrons. The factors which control the stacking have been studied but are still unknown, although it is thought[8] that specific protein-protein interactions between membranes are involved.

The thylakoid system can be isolated from the chloroplast by osmotic lysis of the outer envelope membrane (see for example

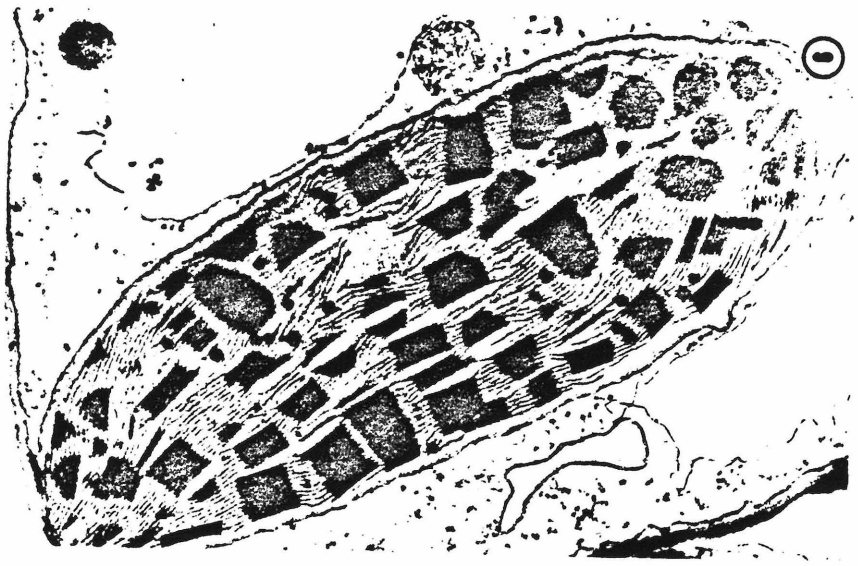

FIGURE I-3 (above). Typical chloroplast from corn.

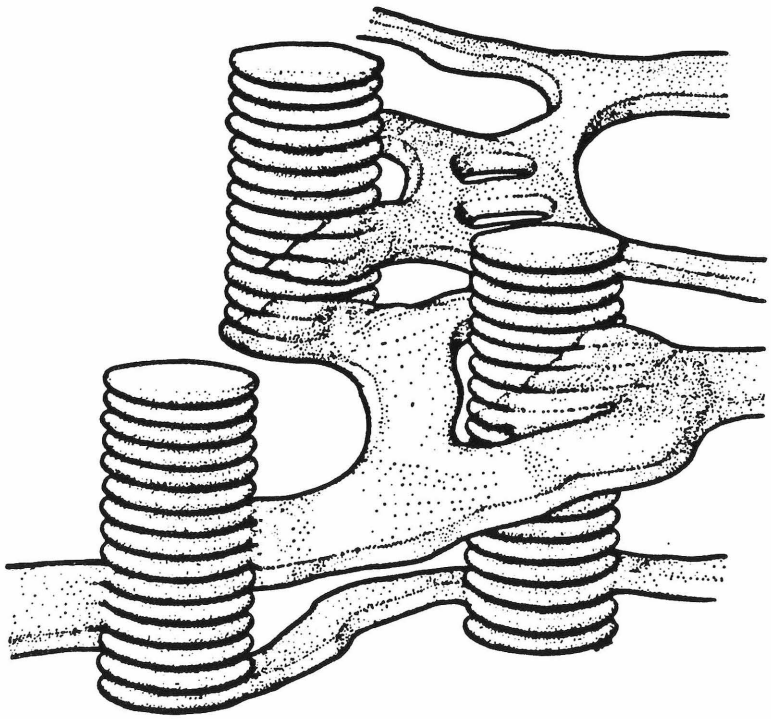

FIGURE I-4. Artist's conception of the thylakoid structures of chloroplasts.

Chapter II). Several important differences between the thylakoid and envelope membranes are apparent from the analytical lipid compositions of the isolated fractions. The compositions obtained from experiments by Hashimoto and Murakami[10] are shown in Figure I-5. First, we can conclude that the photosynthetic apparatus is associated exclusively with the thylakoid membrane since all of the chlorophylls are found in the thylakoid system. Second, we notice that monogalactosyl diglyceride (MGDG) is the predominant lipid of the thylakoid membrane and it is of quite low abundance in the envelope. In the envelope membrane phospholipids predominate, although the thylakoid membrane contains only a modest amount of these normally ubiquitous lipids. The significance of these abnormal compositions is not immediately obvious although we may speculate that monogalactosyl diglyceride must have an important role in the thylakoid membrane. Further speculation on this point will follow later in this chapter.

The structures of the principal lipids of the thylakoid membrane along with their approximate abundances are shown in Figure I-6. The glycolipids, monogalactosyl diglyceride (MGDG), digalactosyl diglyceride (DGDG) and sulfoquinonopyranosyl diglyceride (sulfolipid or SL) comprise nearly 70% of the total lipid mass. Phospholipids, principally represented by phosphatidyl glycerol (PG), are only present in small amounts. The fatty acid groups, R_1 and R_2, of the thylakoid lipids are highly unsaturated.[11,12] The fact that unsaturated fatty acids are characteristic of the photosynthetic membrane is remarkable since the high partial pressure of oxygen resulting from photosynthesis should make them particularly susceptible to oxidation. Apparently some

FIGURE I-5. Lipid compositions of the envelope and thylakoid membranes from spinach chloroplasts. The weight percentages given are from the average value of two experiments by Hashimoto and Murakami.[10]

LIPID	ENVELOPE (%)	THYLAKOID (%)
Monogalactosyl diglyceride	5.6	36.9
Digalactosyl diglyceride	21.8	20.7
Sulfoquinovosyl diglyceride	11.9	12.3
Phosphatidyl choline	30.6	7.8
Phosphatidyl glycerol	16.5	18.2
Phosphatidyl ethanolamine and/or phosphatidyl serine	+	N.D.
Chlorophyll(% of total lipids)	0.17	20.0
Carotenoid(mg/g protein)	4.7	26.0

(+; detectable, but not measured. N.D.; not detectable)

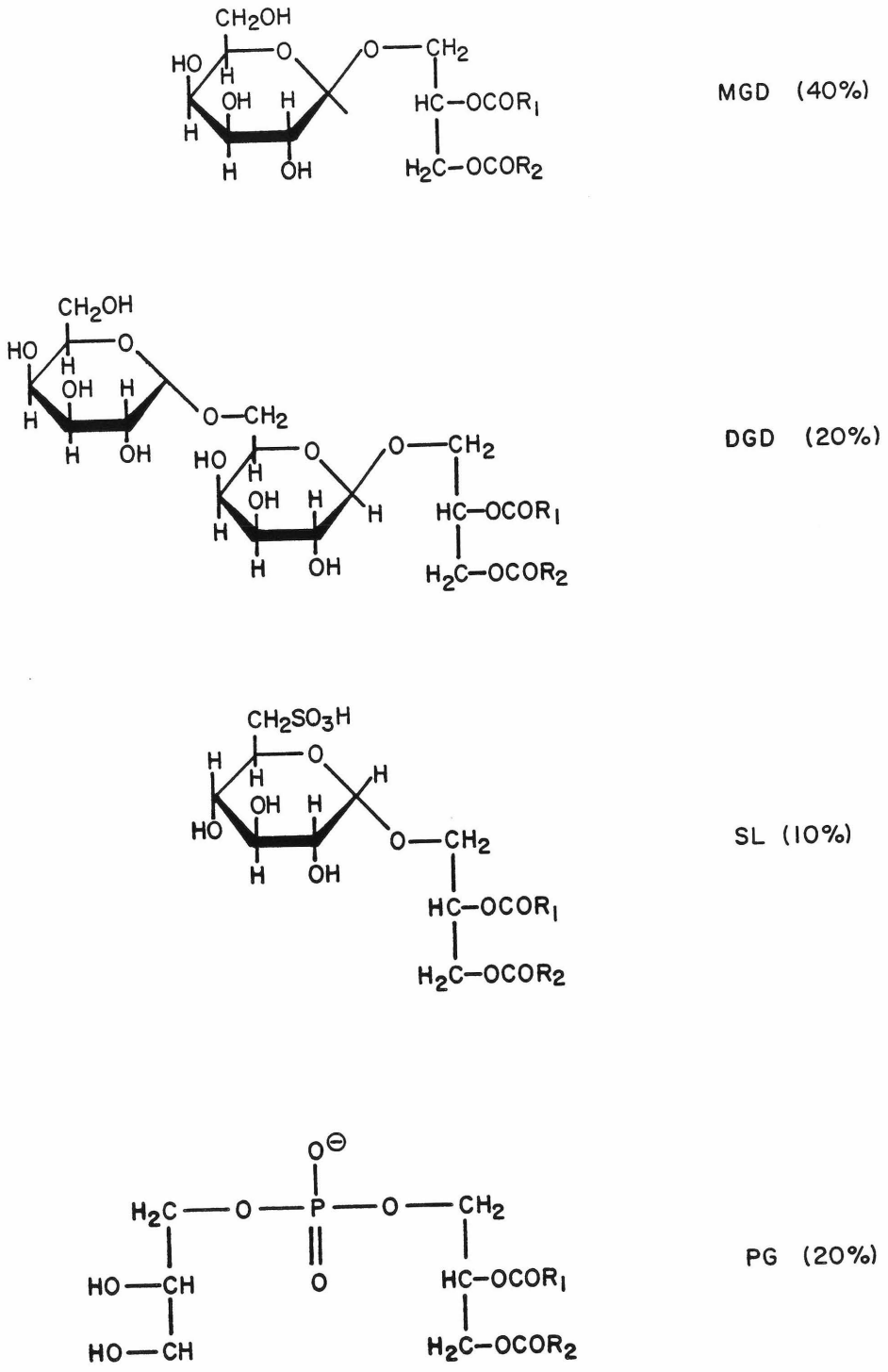

FIGURE I-6. Predominant lipids of the spinach thylakoid membrane with their approximate relative abundances (percent by weight of the total lipids). MGD: monogalactosyldiglyceride, DGD: digalactosyldiglyceride, SL: sulfoquinovopyranosyldiglyceride, PG: phosphatidylglycerol. R_1 and R_2 groups are unsaturated fatty acids.

protective mechanism exists which prevents this.

In addition to the lipids and pigments, the photosynthetic membrane contains a considerable amount of protein, on the order of 45% by weight. Two reasonably well characterized protein complexes which contain chlorophyll have been isolated from plants. The isolation and properties of these have been described by Thornber.[13,14] The first complex, called P700 - chlorophyll a - protein, contains only chlorophyll a and the reaction center of photosystem I. It has a molecular weight of about 100 kdaltons and contains a high proportion of hydrophobic amino acids. The content of chlorophyll a in this complex is quite variable. The second complex, called the light-harvesting chlorophyll a/b-protein, contains 3 chlorophyll a, 3 chlorophyll b and 1 carotene per 30 kdalton complex. Other pigment protein complexes have been hypothesized, but not shown conclusively to exist.

C. CHLOROPHYLL PROPERTIES

Depite the diversity of organisms which contain chlorophyll as an essential element of their photosynthetic unit, the actual number of structurally distinct chlorophylls is quite small[15] (see Figure I-7). As a class, the chlorophylls are all cyclic tetrapyrroles and as such belong to the porphyrin family of compounds. Figure I-8 shows the fundamental porphyrin structure and attempts to classify the more important chlorophylls based on their porphyrin side chains. The features common to all chlorophylls which distinguish them from other porphyrins are the central magnesium atom and the additional alicyclic ring V which contains a keto carbonyl at C-9 and a carbomethoxy group

FIGURE I-7. Distribution of chlorophylls among photosynthetic organisms.

	CHLOROPHYLLS				BACTERIOCHLOROPHYLL				
	a	b	c_1	c_2	a	b	c	d	e
Higher plants	+	+							
Chlorophyceae	+	+							
Conjugatophyceae	+	+							
Charophyceae	+	+							
Prasinophyceae	+	+							
Euglenophyceae	+	+							
Xanthophyceae	+		+	+					
Chloromonadophyceae	+		(+)						
Eustigmatophyceae	+								
Haptophyceae	+		+	+					
Chrysophyceae	+		+	+					
Phaeophyceae	+		+	+					
Bacillariophyceae	+		+	+					
Dinophyceae	+								
Cryptophyceae	+								
Rhondophyceae	+								
Cyanophyceae	+								
Chlorobacteriaceae					+		+	+	+
Thiorhodaceae					+				
Athiorhodaceae					+	+			

(A)

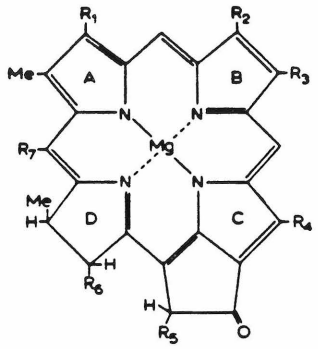

	R_1	R_2	R_3	R_4	R_5	R_6	R_7
Chlorophyll a	$-CH=CH_2$	$-CH_3$	$-CH_2CH_3$	$-CH_3$	$-CO-O-CH_3$	Phytol Ester[b]	-H
— b		-CHO					
— c_1		$-CH_3$	$-CH=CH_2$			Free Acrylic Acid	
— c_2							
Bacteriochlorophyll a	$-CO-CH_3$		$-CH_2CH_3$			Phytol[c] Ester[b]	
— b			$=CHCH_3$				
— c	$-CH-CH_3$ OH		Alkyl[a]	$-C_2H_5$	-H	Farnesol Ester[b]	$-CH_3$
— d							-H
— e		-CHO					$-CH_3$

FIGURE I-8. Classification of chlorophylls on the basis of their porphyrin side chains.

at C-10. A second carboxylic acid function at C-7 is esterified by an isoprenoid alcohol, phytol.

Chlorophyll a, shown in Figure I-9, is the most abundant of the chlorophylls, and is the most extensively studied. In addition to the features already discussed, chlorophyll a has a number of further modifications to the basic porphyrin structure. Ring IV is saturated at positions 7 and 8 to the dihydropyrrole level. The absolute configuration about these chiral centers has been established and it has been found that the 8-methyl and 10-carbomethoxy groups are directed toward opposite sides of the porphyrin plane from the 7-propionic ester. The crystal structure of ethyl chlorophyllide dihydrate, a derivative of chlorophyll a in which the phytol group is replaced by ethanol, has been obtained[16] and used to verify the stereochemistry.

The conjugated macrocycle in chlorophyll a constitutes an aromatic π-system of electrons. This produces a large anisotropy in magnetic shielding about the porphyrin, an effect which can be used to great advantage in NMR studies of chlorophyll. The ring system is modified by the saturation at positions 7 and 8 of ring IV with two important results: 1) two electrons are removed from the π-system which then follows the Hückel $(4n+2)$ rule of aromaticity and, 2) all symmetry elements of the porphyrin structure are eliminated. The crystallographic bond distances[16] of the chlorophyll a carbon skeleton suggest inequivalent bond orders, reflecting the contributions of at least three non-symmetric resonance structures. In addition, the central magnesium atom must also be at least partially conjugated into the ring system. As evidence of this, the ^{15}N-NMR signals are closer

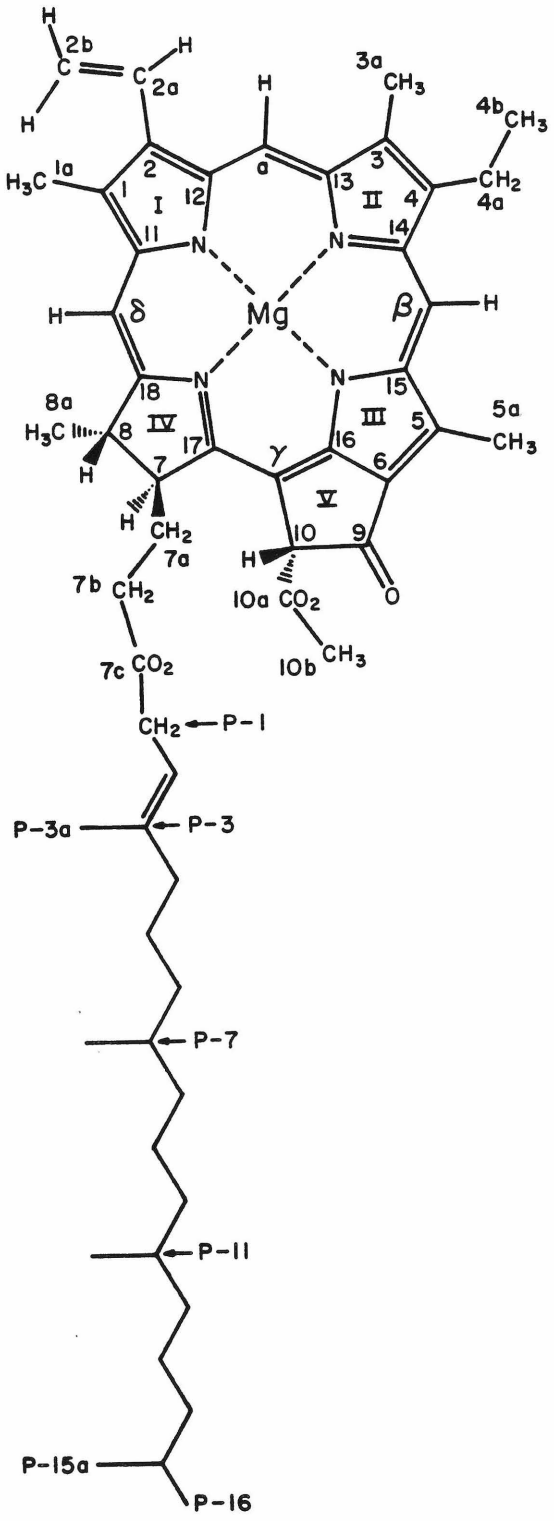

FIGURE I-9. Chemical structure of chlorophyll a.

together in chlorophyll a than in its magnesium-free derivative pheophorbide,[17] suggesting an equalizing effect of Mg on the charge distribution in the ring.

The electronic structure of chlorophyll has been of considerable interest because of the need to interpret the complex electronic absorption spectrum of in vivo chlorophyll. Weiss[18] has carried out extensive configuration interaction calculations based on the 'four-orbital model' which relates the absorption spectrum to the interaction of electrons in the two highest occupied and two lowest unoccupied porphyrin π-orbitals. Figure I-10 shows the visible absorption spectrum of chlorophyll in solution and identifies the various electronic transitions. In the four-orbital approximation Q_y and Q_x, the two lowest energy transitions, are weak and polarized perpendicular to each other. The Q_y transition dipole runs roughly between the ring I and ring III nitrogens and shows a vibronic envelope about 1130 cm^{-1} to higher energies. The next two transitions, B_x and B_y, are accidentally degenerate and contribute to the high energy Soret band. A satellite of the Soret band at 409 nm is assigned to another weaker transition, η, which becomes allowed from the combined perturbations of carbonyl substitution and ring distortion by Ring V.

The visible absorption spectrum of chlorophyll is sensitive to the environment[19] and state of ligation[20] of the chlorophyll molecule. In theory the spectrum contains much information which could provide clues to the organization of chlorophyll molecules in vivo. Unfortunately, the interpretation of spectra in terms of the electronic structure of chlorophyll is complicated by many indeterminable factors

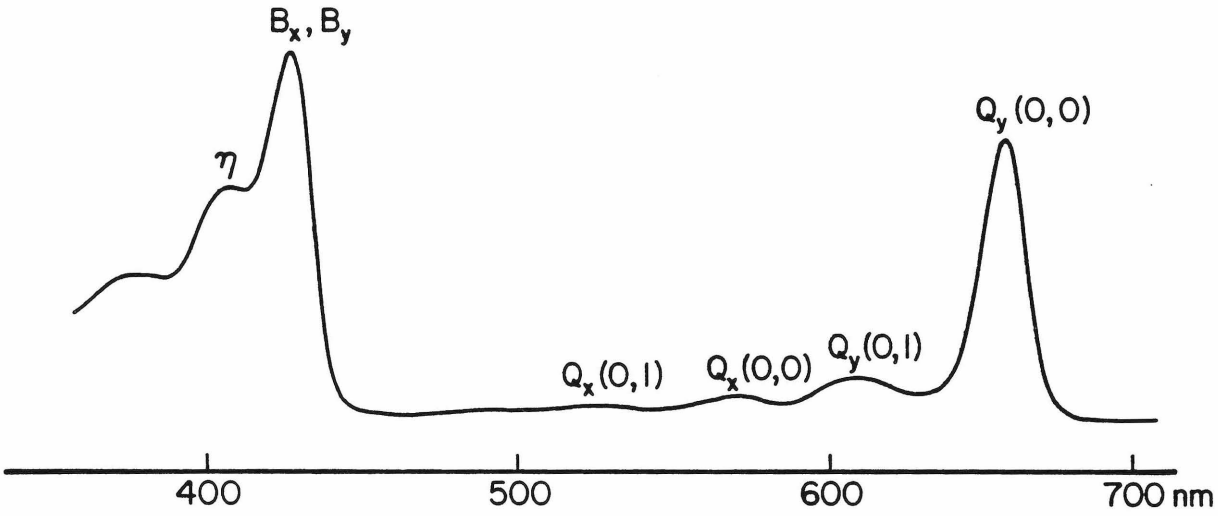

Positions of Maxima, 10^3 cm^{-1} (nm)	Heights of Maxima, 10^3 liter $mole^{-1}$ cm^{-1}	Assignment
24.45 (409)	66.4	η
23.31 (429)	104.2	B_x, B_y
18.86 (530)	3.8	Q_x (0,1)
17.40 (575)	7.1	Q_x (0,0)
16.31 (613)	13.0	Q_y (0,1)
15.17 (659)	84.9	Q_y (0,0)

FIGURE I-10. Visible absorption spectrum of chlorophyll a in diethyl ether.

such as the effects of porphyrin substitution, ring reduction and ligand binding to magnesium. Furthermore, the absorption spectrum of in vivo chlorophyll is complicated by contributions from many different spectral forms. As a result, considerable caution must be exercised in reaching conclusions about the organization of chlorophylls based on absorption spectra. More work is required to determine the effects of orientation, electronic interaction, different solvents and various ligands on the spectrum.

The central magnesium atom of chlorophyll a is shown in Figure I-9 as being bound only to the four nitrogen atoms of the tetrapyrrole system. However, it is well established[21] that 4-coordinate magnesium in chlorophyll is coordinatively unsaturated. For this reason chlorophylls are always found with a fifth and sometimes sixth axial ligand donating a lone pair of electrons to the strongly electrophilic magnesium. The resulting strong coordination interaction governs the interactions of chlorophyll with solvents and other molecules. This subject has been reviewed extensively by Katz.[22, 23] We may summarize by saying that in nucleophilic polar organic solvents, (such as ethers, alcohols, ketones, pyridine, or the like) a solvent molecule occupies one or both axial positions coordinated to magnesium by a lone pair of electrons from oxygen, nitrogen or sulfur. In general, the preference is toward 5-coordinate behavior although strongly nucleophilic solvents may cause the magnesium to assume a coordination number of six. The preference for 5-coordinate magnesium is quite possibly associated with the normal displacement of magnesium out of the plane of the porphyrin[16] which may limit the ligand accessibility from the backside of the porphyrin.

In non-polar solvents which cannot provide a nucleophilic ligand, the coordination requirement of one chlorophyll molecule is satisfied by interaction with the C-9 ketone of a second chlorophyll. This results in the formation of dimers (as in carbon tetrachloride) or higher oligomers (as in hydrocarbon solvents). However, the addition of equimolar amounts of a nucleophile is sufficient to disrupt these oligomers to produce monomeric chlorophyll. At this point it is fitting to point out that one of the keys to interpreting the organization of chlorophyll in the photosynthetic membrane is to identify the axial ligand to chlorophyll. We will next speculate on the possible identity of this ligand and the effect it may have on the in vivo organization of chlorophyll.

D. ORGANIZATION OF ANTENNA CHLOROPHYLL

Only a very small fraction of chlorophyll a molecules, on the order of one out of every three hundred,[24] actually participate in the basic photochemistry of the reaction center. However the remainder, which constitutes the bulk chlorophyll of the antenna, performs an essential function by collecting the energy required by the reaction center. Thus, in considering the properties of bulk chlorophyll in the photosynthetic membrane, it is likely that we are actually considering the properties of the photosynthetic antenna.

The optical properties of in vivo chlorophyll are unusual in many respects and suggest an unique organization of chlorophyll molecules within the photosynthetic membrane. The optical absorption spectrum of chlorophyll a in the in vivo antenna consists of a set of closely spaced

bands ranging from 662-705 nm.[25] The envelope of these bands is rather broad and featureless, and consequently a deconvolution into a set of distinct sub-bands is difficult. However, the Q_y-band absorption maximum is generally considered to be near 678 nm, shifted some 15-20 nm to the red of the corresponding absorption in most organic solvents. The origin of this red-shift has been the subject of much debate (see Chapter V). A further anomaly is the remarkable lack of fluorescence from *in vivo* chlorophyll. Dilute solutions of chlorophyll *a* in organic solvents are strongly fluorescent, whereas fluorescence from chlorophyll in intact chloroplasts is on the order of only 1% of that in solution.[26]

Polarized absorption and fluorescence studies[27-30] indicate that within the organizational framework of the *in vivo* antenna there is a considerable degree of orientation and interaction of chlorophyll chromophores. Measurements of the linear dichroism of chloroplasts[28] which have been aligned by a magnetic field show that at least 60% of the bulk chlorophyll *a* is oriented with their Q_y transition moments parallel or at a slight angle to the plane of the aligned thylakoid membranes. Circular dichroism is also observed for chloroplasts and is dependent on the orientation of the chloroplasts.[29] While these previous experiments indicate ordering of chlorophyll molecules with respect to the membrane plane, they cannot distinguish the ordering of chlorophyll molecules with respect to each other. However, by studying the fluorescence polarization of oriented and unoriented chloroplasts as a function of excitation and emission wavelengths, Becker *et al.*[30] could distinguish a moderate amount of intrinsic polarization and

concluded that Q_y transition moments of chlorophyll molecules are aligned with each other on at least a local level. In such experiments the possibility of energy transfer between chromophores must be considered. For example, a partial or complete depolarization of the fluorescence could result from two very different conditions: a) a large number of energy transfer steps between highly oriented chlorophyll molecules, or b) a smaller number of energy transfer steps between chlorophylls with a low degree of mutual order.

The low fluorescent yield from chloroplasts[26] must indicate an efficient transfer of energy to the reaction center trap. Since this transfer occurs from a relatively large array of some 300 chlorophyll molecules we may conclude that energy transfer is fast compared to the fluorescent lifetime, which itself is less than a nanosecond. Such an efficient energy transfer process could only occur among a system of highly oriented chromophores. Calculations by Beddard and Porter[31] suggest that chlorophyll molecules must be separated by at least 10 angstroms in order to prevent the formation of low energy traps by orbital overlap which would prevent further excitation migration. However the separation between chlorophylls must not be so great as to preclude a fast energy transfer step. Thus, not only must the antenna chlorophyll be ordered, it must also be oriented so as to provide the optimum separation between chromophores. The question we now wish to consider is how this ordering of chlorophyll molecules is accomplished <u>in vivo</u>.

It was previously noted that chlorophyll has an obligatory requirement for coordination by an axial nucleophilic ligand. Since the chloro-

phyll concentration in the thylakoid membrane is approximately 0.1-0.2 molar,[32] or at least 10% of the total membrane by weight,[33] there must be a large number of such nucleophilic groups. There are four classes of molecules present in the membrane at a high enough concentration to account for the total ligation of chlorophyll a: water, other chlorophyll molecules, protein side-chains, or lipid molecules. All of these have at one time or another been proposed to account for the complexation of in vivo chlorophyll, with the strength of conviction of the proponents usually greater than the strength of their evidence.

The first two possibilities, complexation by water or by other chlorophyll molecules, implicitly assume the presence of either hydrated or dry oligomers. The hydrated oligomer model, proposed by Strouse,[34,35] was based upon the crystal structure of ethyl chlorophyllide dihydrate and an erroneous calculation of exciton interactions within the structure which predicted an absorption at 680 nm, near the 678 nm absorption maximum of in vivo chlorophyll a. However, it is known that the actual absorption maximum of in vitro hydrated oligomers is in the 690-743 nm region,[36,37] considerably farther to the red than that of in vivo antenna chlorophyll. Furthermore, chlorophyll hydrates are ESR active, whereas in vivo antenna chlorophyll is not. The other model, based on anhydrous $(\text{chlorophyll})_n$ oligomers, assumes complexation by other chlorophyll molecules similar to the state of chlorophyll in dry hydrocarbon solvents. Evidence, extensively cited by Katz and co-workers,[22] is primarily based on a similarity between computer deconvolutions of the essentially featureless absorption bands of bulk in vivo chlorophyll and chlorophyll a in dry hexane. As pointed out by

Brown,[38] these authors are aware that unique computer deconvolutions of such spectra are impossible, yet persist in using them as presumptive evidence for the identity of antenna chlorophyll. Another problem with the oligomer model is the necessity to assume that chlorophyll is maintained in an anhydrous state, or that oligomers are not accessible to stronger nucleophiles such as galactolipids which are known to disrupt chlorophyll aggregates.[39,40] For these reasons, and because of the fact that the resonance Raman results of Lutz[41] preclude either hydrated or dry oligomers in vivo, we rule out these two possibilities. This leaves either protein or lipid groups as the means of complexation and orientation of chlorophyll in the in vivo antenna.

A substantial amount of effort has been devoted to the characterization of membrane protein complexes from the photosynthetic membranes of plants and algae. These studies, reviewed frequently by Thornber,[13-15] entail the gentle dissection of the membrane with detergent and separation of the detergent solubilized complexes by gel electrophoresis. Such studies find that much of the in vivo complement of chlorophyll a co-migrates with protein, although a significant fraction of chlorophyll is often found in a protein-free pigment band. These results have been taken as evidence that chlorophyll is conjugated with protein in situ. While such experiments do provide circumstantial support for the association of some chlorophyll with protein in an as yet unspecified manner, by no means do they conclusively establish chlorophyll-protein interactions as the sole means of organization of chlorophyll. In fact, detergent solubilization must necessarily cause a gross disruption of the membrane structure resulting in a loss

of information concerning membrane organization. Furthermore, it is possible that membrane components become artifactually associated with protein as a result of the detergent solubilization. Since chlorophyll-protein complexes often contain chlorophyll in a short wavelength, fluorescent form, they are apparently not physiologically intact.

To be sure, there is at least a strong indication from the previous studies that some amount of *in vivo* chlorophyll is conjugated with protein. This is especially likely in the case of the well characterized chlorophyll *a* - P700 - protein and chlorophyll *a*/*b* - protein complexes. However, these account for less than 75% of the total chlorophyll, and some of this chlorophyll may be associated peripherally or artifactually. The relevant issues then become a question of: 1) the manner in which chlorophyll is associated with protein (e.g., intrinsically or peripherally) and, 2) the extent to which chlorophyll is bound to protein, to lipids, or to both.

Judging from the ease with which most of the chlorophyll is extracted from thylakoids,[42] any intermolecular associations must be moderately weak. Any covalent bonds between chlorophyll and protein must be labile, if present at all. From the alignment of chlorophyll transition moments observed by fluorescence polarization experiments,[30] any chlorophyll bound to protein must be incorporated so as to orient all chlorophylls similarly, and furthermore the protein must be oriented within the membrane so as to align the chlorophyll transition moments parallel to the plane of the membrane. An additional consideration is whether there is sufficient protein to account for the complete complexation of chlorophyll. Considering that chlorophylls *a* and *b*

constitute 11% of the membrane mass,[33] and that protein accounts for 45% (20-25% if the amounts of electron-transport and CO_2-fixing enzymes are subtracted), it would be necessary for chlorophyll-containing proteins to be composed of approximately one-third chlorophyll by weight. While such a situation cannot be ruled out, it would be without precedent. Hence, the warrantable conclusion is that the complexation of all chlorophyll to protein as an intrinsic chromophore is an unlikely possibility.

An alternate theory, which forms the basis of this thesis and which constitutes the premise for the experimental work contained within, is the supposition that some amount of in vivo chlorophyll is associated with the lipid bilayer portion of the photosynthetic membrane as an amphiphilic lipid. This notion has been proposed in the past,[31,43,44] but has not been adequately investigated. Anderson proposed[43] in 1975 that chlorophyll was contained in the membrane as an extrinsic boundary lipid to protein. In this model, chlorophyll is pictured as being associated with the protein exterior through coordinative bonding of the porphyrin to nucleophilic protein side-chains and hydrophobic association of phytol with the protein hydrophobic exterior. Beddard and Porter[31] assumed that membrane bound chlorophyll behaved more as a traditional amphiphilic lipid rather than as a boundary lipid. They proposed in 1976 that chlorophylls are in fact bound to the membrane by lipid molecules which serve to separate them at an optimum distance for efficient energy transfer.

Both of the previous models recognize the importance of the amphiphilic character of chlorophyll. For comparison, Figure I-11

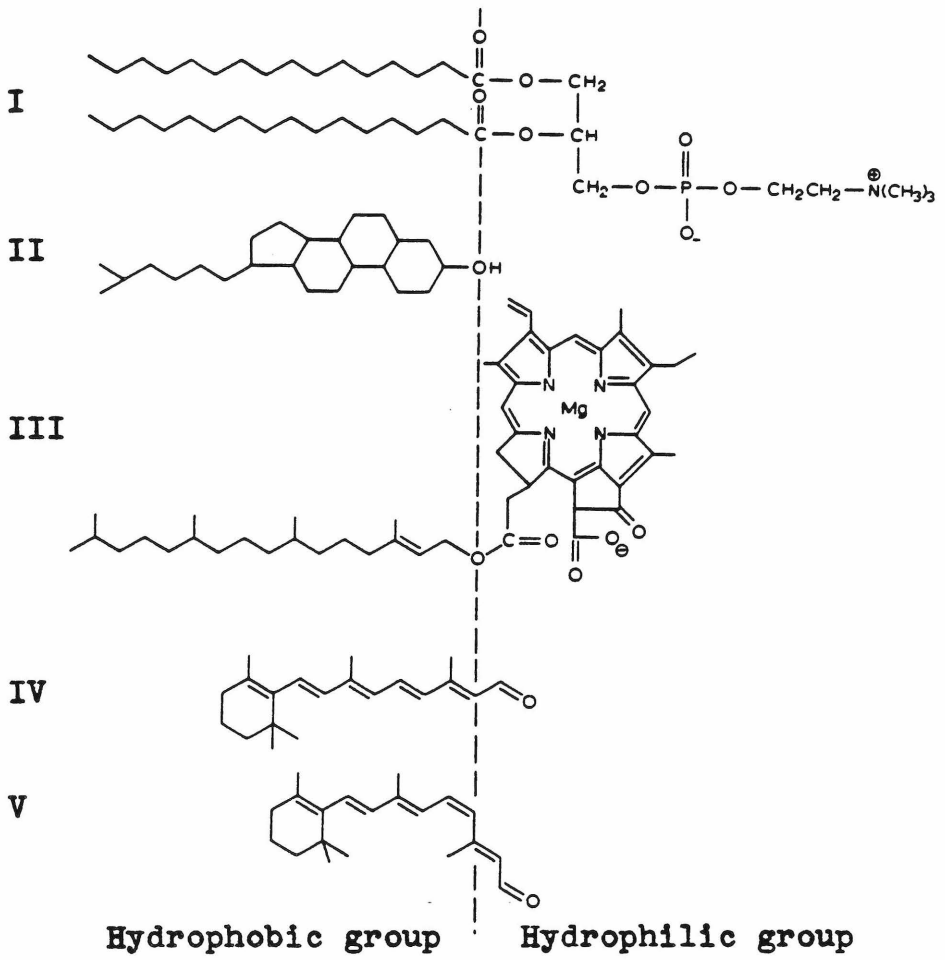

FIGURE I-11. Representative amphiphilic molecules: I, dipalmitoylphosphatidylcholine; II, cholesterol; III, chlorophyll a; IV, all-trans-retinal; V, 11-cis-retinal. Figure adapted from M. N. Jones, Biological Interfaces, Elsevier, Amsterdam, 1975, p. 13.

shows chlorophyll a along with some other typical amphiphilic molecules. Notice in chlorophyll a that there is a well defined interface between the non-polar phytol chain and the relatively polar porphyrin headgroup structure. It is this dual hydrophobic/hydrophilic nature which gives chlorophyll its amphiphilic character. Because chlorophyll a is amphiphilic, it is also expected to be surface active and, in fact, forms monolayers at an air-water interface.[45,46] As will be shown later, chlorophyll a can also interact with bilayer membranes.

Although both the Anderson and Porter models agree on the role of amphiphilicity in orienting chlorophyll, they disagree in their assumptions regarding the degree of involvement with other lipid molecules. A good deal of evidence suggests that lipids of the photosynthetic membrane, particularly the galactolipids, are important to photosynthetic function.[47] This in turn may suggest an involvement of the lipids with chlorophyll a. It is known that galactolipids are synthesized simultaneously with chlorophyll in greening Euglena and disappear simultaneously in the dark.[44] In chloroplasts, changes in lipid composition parallel the development of photosynthetic capability during the greening of dark-grown plants.[48-50] During the early stages of greening, fundamental chloroplast structures including proteins are already present. In the later stages chlorophyll and galactolipids are added to constitute the fully active membrane. Krupa and Baszynski[51] determined that removal of only 20% of the membrane galactolipids decreased photosystem I activity by 75%, This occurred either when lipids were selectively extracted with hexane, or when hydrolyzed enzymatically. Restoration back to the original full level of activity

resulted from reconstitution of the membrane. Bamberger and Park[52] determined that the decrease in activity upon treatment with galactolipase was a result of a decrease in the quantum efficiency. This suggests that the photosynthetic antenna, and therefore chlorophyll is affected. Ostrovskaya[53] found that treatment with galactolipase affected photosystem I while photosystem II remained unaffected. These results suggest an involvement of galactolipids with the antenna chlorophyll of photosystem I. There is as yet no conclusive evidence for interactions between chlorophyll and galactolipids in vivo, but it is known that galactolipids form strong complexes with chlorophyll in vitro.[39,40]

REFERENCES - CHAPTER I

1. A. L. Lehninger, in Biochemistry, 2nd ed., Worth Publishers, New York, 1975, chapter 22.
2. R. Emerson and W. Arnold, J. Gen. Physiol., 15, 391-420 (1932).
3. W. L. Butler, Brookhaven Symp. 28th, (J. M. Olsen and G. Hind, eds.), 1976, 338-346.
4. R. S. Knox, in Bioenergetics of Photosynthesis, (Govindjee, ed.), Academic Press, New York, 1975, pp. 183-221.
5. R. S. Knox, in Primary Processes of Photosynthesis, (J. Barber, ed.), Elsevier, Amsterdam, 1977, pp. 55-98.
6. L. L. Shipman and D. L. Housman, Photochem. Photobiol., 29, 1163-1167 (1979).
7. T. E. Weier, C. R. Stocking, and L. K. Shumway, Brookhaven Symp. 19th, 1966, 353-374.
8. L. A. Staehelin, P. A. Armond, and K. R. Miller, Brookhaven Symp. 28th, (J. M. Olson and G. Hind, eds), 1976, pp. 278-315.
9. D. M. Sadler, Biochim. Biophys. Acta, 298, 620-629 (1973).
10. H. Hashimoto and S. Murakami, Plant Cell Physiol., 16, 895-902 (1975).
11. A. T. James and B. W. Nichols, Nature, 210, 372-375 (1966).
12. C. F. Allen and P. Good, Methods Enz., 23, 523-547 (1971).
13. J. P. Thornber, Ann. Rev. Plant Physiol., 26, 127-158 (1975).
14. J. P. Thornber, J. P. Markwell, and S. Reinman, Photochem. Photobiol., 29, 1205-1216 (1979).

REFERENCES (continued)

15. J. P. Thornber and J. Barber, in Photosynthesis in Relation to Model Systems, (J. Barber, ed.), Elsevier, Amsterdam, 1979, pp. 27-70.

16. R. Serlin, H. Chow, and C. E. Strouse, J. Am. Chem. Soc., 97, 7237-7242 (1975).

17. S. G. Boxer, G. L. Closs, and J. J. Katz, J. Am. Chem. Soc., 96, 7058-7066 (1974).

18. C. Weiss, J. Mol. Spectroscopy, 44, 37-80 (1972).

19. G. R. Seely and R. G. Jensen, Spectrochimica Acta, 21, 1835-1845 (1965).

20. L. L. Shipman, T. M. Cotton, J. R. Norris, and J. J. Katz, J. Am. Chem. Soc., 98, 8222-8230 (1976).

21. J. J. Katz, Dev. Appl. Spectroscopy, 6, 201-218 (1968).

22. J. J. Katz, J. R. Norris, and L. L. Shipman, Brookhaven Symp. 28th, (J. M. Olson and G. Hind, eds.), 1976, pp. 16-55.

23. J. J. Katz, Inorg. Biochem., 2, 1022-1066 (1973).

24. R. P. F. Gregory, in Biochemistry of Photosynthesis, Wiley, London, 1977, pp. 43-45.

25. T. M. Cotton, A. D. Trifunac, K. Ballschmitter, and J. J. Katz, Biochim. Biophys. Acta, 368, 181-198 (1974).

26. L. Lavorel and A. L. Etienne, in Primary Processes of Photosynthesis, (J. Barber, ed.), Elsevier, Amsterdam, 1977, pp. 203-267.

27. A. Vermiglio, J. Breton, and P. J. Mathis, J. Supramol. Struct., 5, 109-116 (1977).

REFERENCES (continued)

28. N. E. Geacintov, F. Van-Nostrand, J. F. Becker, and J. B. Tinkel, Biochim. Biophys. Acta, 267, 65-79 (1972).

29. R. P. F. Gregory, in Primary Processes of Photosynthesis, (J. Barber, ed.), Elsevier, Amsterdam, 1977, pp. 465-492.

30. J. F. Becker, J. Breton, N. E. Geacintov, and F. Trentacosti, Biochim. Biophys. Acta, 440, 531-544 (1976).

31. G. S. Beddard and G. Porter, Nature, 260, 366-367 (1976).

32. E. Rabinowitch, in Photosynthesis, Vol. I, Interscience, New York, 1945, p. 412.

33. H. K. Lichtenthaler and R. B. Park, Nature, 198, 1070-1072 (1963).

34. C. E. Strouse, Proc. Natl. Acad. Sci. U.S., 71, 325-328 (1973).

35. C. E. Strouse, Prog. Inorg. Chem., 22, 159-177 (1976).

36. E. E. Jacobs, A. E. Vatter, and A. S. Holt, Arch. Biochem. Biophys., 53, 228-238 (1954).

37. E. A. Jacobs, A. S. Holt, and E. Rabinowitch, J. Chem. Phys., 22, 142-143 (1954).

38. J. S. Brown, Photochem. Photobiol., 26, 319-326 (1977).

39. J. Trosper and K. Sauer, Biochim. Biophys. Acta, 162, 97-105 (1968).

40. S. Aronoff, Photosynthetica, 12, 298-303 (1978).

41. M. Lutz, Biochim. Biophys. Acta, 460, 408-430 (1977).

42. A. A. Shlyk and G. N. Nikolayeva, Biofizika, 8, 201-211 (1963).

43. J. M. Anderson, Nature, 253, 536-537 (1975).

44. A. Rosenberg, Science, 157, 1191-1196 (1967).

REFERENCES (continued)

45. B. Ke, in The Chlorophylls, (L. P. Vernon and G. R. Seely, eds.), Academic Press, New York, 1966, pp. 253-279.

46. G. L. Gaines, W. D. Bellamy, and A. G. Tweet, J. Chem. Phys., 41, 538-540 (1964).

47. G. R. Seely, in Primary Processes of Photosynthesis, (J. Barber, ed.), Elsevier, Amsterdam, 1977, pp. 1-53.

48. A. Tremolieres and M. Lepage, Plant Physiol., 47, 329-339 (1971).

49. K. P. Heise and G. Jacobi, Planta, 111, 137-148 (1973).

50. J. C. Beck and R. P. Levine, Biochim. Biophys. Acta, 489, 360-369 (1977).

51. Z. Krupa and T. Baszynski, Biochim. Biophys. Acta, 408, 26-34 (1975).

52. E. S. Bamberger and R. B. Park, Plant Physiol., 41, 1591-1600 (1966).

53. L. K. Ostrovskaya, S. M. Kochubei, and T. M. Shodchina, Biokhimiia, 40, 143-147 (1975).

CHAPTER II

Isolation of Chlorophyll a and Preparation of Chlorophyll a-Containing Membranes

This chapter describes some of the procedures to obtain chlorophyll a and membranes which contain chlorophyll a. Many of the techniques described are based on established techniques which have been adapted and modified to obtain materials in a suitable form for the desired physical characterization. The information herein is included largely for the benefit of any succeeding workers who may wish to duplicate or extend this work. Be warned, however, that it is unlikely that successful preparations will be obtained when following published procedures for the first time. A degree of first-hand experience is required which can only be obtained in the laboratory.

Many of the difficulties in preparing and handling chlorophyll products are due to the diverse reactions which chlorophyll can undergo to yield chemically and spectroscopically similar alteration products. Chlorophyll is a rather unstable molecule and is particularly susceptible to attack by light, heat, dilute acids or bases, or certain organic solvents. Some of these reactions are illustrated in Figure II-1 and have been described in more detail in the many excellent monographs on chlorophyll.[1-3] It is often difficult to entirely avoid conditions under which chlorophyll might be altered, but the effects can usually be minimized by suitable precautions. For example, photo-oxidation and bleaching of chlorophyll under light can be reduced by removing oxygen

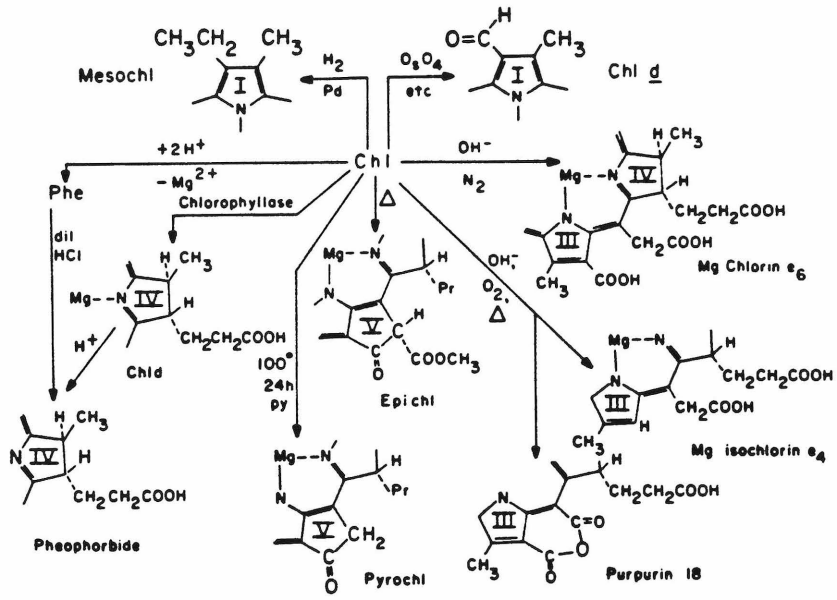

FIGURE II-1. Several of the possible reactions which can alter the chemical structure of chlorophyll a. Adapted from Seely.[3]

and using sealed containers. Heat is avoided whenever possible and large deviations from neutral pH are never allowed. Alcoholic solvents are used only when necessary and other organic solvents are freshly purified.

A. ISOLATION OF CHLOROPHYLL a

Chlorophyll a was isolated from spinach extracts by the dioxane precipitation procedure of Iriyama[4] and purified by chromatography on powdered sugar according to Strain et al.[5] Fresh spinach leaves free of midribs (5 kg) were washed and refrigerated. These were extracted in 900 gram batches with 1500 ml of ice-cold methanol by grinding for 1 minute in a pre-chilled Waring blender. The resulting extract was filtered through 8 layers of cheesecloth and then through pyrex wool to remove cell debris. The cell matter which was collected on the cheesecloth was re-extracted with a minimal amount of methanol until it became a colorless gray. On some occasions the leaves were boiled for 1 minute and immediately chilled prior to extraction. This facilitates the solvent extraction of the pigments but results in larger amounts of chlorophyll alteration products. Remaining cell debris which was not removed by filtration was eliminated by centrifugation of the extract at $2000 \times g$ for 5 minutes. The briliant deep green supernatant was decanted and combined into 3 liter batches. To these were added a $\frac{1}{7}$ volume (approximately 430 ml) of dioxane which had been purified on an alumina column. Then distilled water was added slowly with stirring until the solution became turbid with precipitated chlorophyll. The amount of water required, typically 500-700 ml, depends on the amount

of water which is extracted from the leaves. The precipitated solution was allowed to stand undisturbed at 4° C for several hours so as to allow the chlorophyll microcrystallites to grow and to sediment. The yellowish top portion (which contains most of the extracted lipids, carotenes, and xanthophyll pigments) was decanted from the thick lower mass of green crude chlorophyll precipitate. The precipitate was collected by continuous-flow centrifugation in a Sorvall SS-34 rotor at 15,000 × g with a flow rate of 50 ml/min. The green pellets were collectively dissolved in fresh diethyl ether which was then evaporated under dry nitrogen gas to yield about 3 grams of partially purified material which contained about 25% chlorophyll a by weight.

The crude material at this point contains chlorophylls a and b and small amounts of their isomerized or magnesium-free alteration products, as well as xanthophylls and a negligible amount of carotenoids. Chlorophyll a, or other desired pigments, can be obtained in a suitably pure form from the previously obtained crude extract by column chromatography on powdered sugar according to the procedures of Strain et al.[1,5] Other column materials were tried and found to be much less satisfactory than powdered sugar. A 6 cm × 60 cm column with a coarse bottom frit protected by filter paper was dry-packed under vacuum with approximately $3\frac{1}{2}$ pounds of commercial brand powdered sugar containing 3% starch. This is not a familiar laboratory procedure, but excellent results can be obtained with practice and an open mind. Packing a good column is the most critical step in isolating chlorophyll a. The powdered sugar should be sifted and the column packed under aspirator vacuum. The most even packing can be obtained

by tamping the powdered sugar with a rod to which is attached a flat-headed stopper slightly smaller than the column diameter. This is placed at the bottom of the column, powdered sugar is added and packed in even increments by small up-and-down motions of the glass rod. After close inspection for cracks, the column is then ready for the application of the crude spinach extract. Typically 0.4 grams of the previous spinach extract was dissolved in 20 ml of diethyl ether and then added to 60 ml of petroleum ether (20-40° b.p. fraction). This solution was applied to the column. Usually it is difficult to obtain an even pigment band at the top of the column. In these cases the top one or two centimeters of the column were stirred and allowed to settle to a level boundary. The column was eluted under vacuum with 0.5% n-propanol in petroleum ether. The pigments separated into the banding pattern illustrated in Figure II-2. Development of the column was continued, and the chlorophyll a fraction collected with special care to exclude other pigment bands.

The chlorophyll a elutriate required further treatment to exclude impurities from the powdered sugar which were leached from the column. The alcohol was extracted from the petroleum ether by gentle swirling with 3-200 ml portions of deionized water. This also served to remove most of the water soluble impurities. Then the petroleum ether was shaken vigorously with water in a separatory funnel. This resulted in an emulsion with chlorophyll a collecting on the surface of the water droplets. The separated aqueous layer was discarded and the emulsion collected. The petroleum ether was continually extracted in this fashion until it was nearly colorless. Usually 8-10 extractions

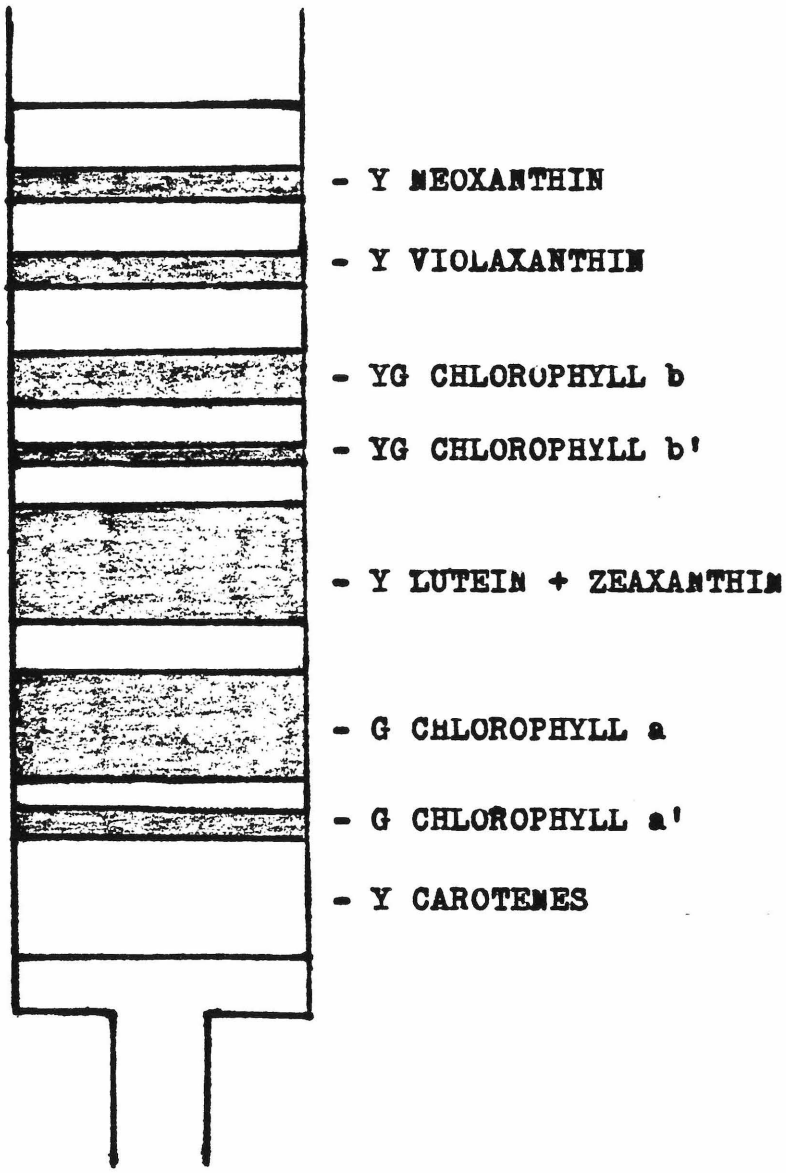

FIGURE II-2. Elution pattern of pigments from powdered sugar with 0.5% n-propanol in petroleum ether.

were required. During this time much of the water separated from the emulsion and could be discarded. Finally there resulted a small amount of petroleum ether with suspended solid chlorophyll and a little dispersed water. This was cooled on powdered dry ice, which froze the water, and precipitated chlorophyll _a_ from the petroleum ether layer which then collected on top of the ice layer. The petroleum ether plus chlorophyll _a_ was then decanted from the ice and the chlorophyll _a_ collected by centrifugation. The collected chlorophyll was dried under vacuum resulting in an average of 100 milligrams of chlorophyll _a_.

The final purity of the isolated product was determined from the optical absorption spectrum in diethyl ether. Molar extinction coefficients were determined from the absorption of a solution of chlorophyll _a_ (approximately 1 milligram weighed to 0.1 microgram) in 100 ml of fresh diethyl ether. Molar extinction coefficients found (literature values[6] in parentheses for pure chlorophyll _a_): $\epsilon^{M}_{660} = 8.56 \times 10^4$ (8.63×10^4), $\epsilon^{M}_{428} = 11.0 \times 10^4$ (11.2×10^4) indicate that the purity is greater than 98%. The ratios of the absorption bands correspond well with previously determined values (literature[7] in parentheses): $\epsilon^{M}_{428}/\epsilon^{M}_{660} = 1.29$ (1.31). This indicates that there are no colored impurities similar to chlorophyll _a_.

B. ISOLATION OF INTACT CHLOROPLASTS

Following the procedures of Hashimoto and Murakami,[8] whole chloroplasts were isolated from the leaves of fresh market spinach. Spinach leaves, with petioles removed, were carefully washed, chopped with scissors and refrigerated. Six-hundred grams of leaves were homogenized with 1800 ml of an ice-cold grinding medium (0.4 M sucrose, 5 mM $MgCl_2$, 10 mM $Na_4P_2O_7$, pH 8.0) for approximately 30 seconds in a Waring blender. The homogenate was filtered through 8 layers of cheesecloth and then through 16 layers in order to remove cell material. The filtrate was centrifuged rapidly by accelerating to $2000 \times g$ and then decelerating immediately in a GSA rotor with 500 ml bottles. The supernatant was decanted and a loose top layer of broken chloroplasts was also discarded. The remaining crude chloroplasts pellets were gently re-suspended and washed from the centrifuge bottles with a total of 30 ml of 1 M-medium (1 M sucrose, 5 mM $MgCl_2$, 75 mM NaCl and 10 mM $Na_4P_2O_7$, pH 7.2). The suspended chloroplasts were then centrifuged at $4000 \times g$ in an SS-34 rotor for 5 minutes. The purified intact chloroplasts were collected in the pellet. According to Hashimoto and Murakami,[8] this preparation is substantially free of other organelles such as mitochondria and nuclei.

C. SEPARATION OF THYLAKOID AND ENVELOPE MEMBRANES FROM INTACT CHLOROPLASTS

Purified spinach chloroplasts obtained by the previous procedure were used as starting material for the isolation of thylakoid and envelope membrane fractions. The outer envelope membrane was

osmotically ruptured in a hypotonic buffer medium and separated from thylakoids by centrifugation. All buffer media contained a cationic composition which prevents the dissociation and swelling of the thylakoid grana.[9] The preparations described were carried out at 4° C as much as was possible.

Intact chloroplasts from 600 grams of spinach leaves were suspended in 12 ml of 0 M-medium (5 mM $MgCl_2$, 75 mM NaCl, and 10 mM $Na_4P_2O_7$, pH 7.2). The suspension was then centrifuged at 7000 × g for 15 minutes. The yellow supernatant, containing separated envelope membranes, was decanted and saved for subsequent purification described in the next paragraph. The pelleted thylakoids were twice resuspended in 25 ml of 0.6-M medium (0.6 M sucrose, 5 mM $MgCl_2$, 75 mM NaCl and 10 mM $Na_4P_2O_7$, pH 7.2) and pelleted by centrifugation at 7000 × g for 15 minutes. When the thylakoid material was to be used for NMR studies, it was necessary to remove sucrose and to provide a deuterium signal to lock the spectrometer. Consequently, the pellet was thrice suspended in 0 M-D_2O buffer (5 mM $MgCl_2$, 75 mM NaCl and 10 mM $Na_4P_2O_7$, pH 7.7) and centrifuged as before.

In order to purify the envelope membrane fraction, the yellow supernatant obtained following the lysis of the chloroplasts was layered onto 10 ml of 0.9 M-medium (0.9 M sucrose, 5 mM $MgCl_2$, 75 mM NaCl and 10 mM $Na_4P_2O_7$, pH 7.2) in a cellulose nitrate tube and centrifuged in a swinging-bucket rotor at 60,000 × g for 2 hours in a Beckman L5-65 ultracentrifuge. The envelope membranes collected as a faint yellow band at the interface between the 0.6 M and 0.9 M

solutions. A small green pellet of thylakoids collected at the bottom of the tube. The yellow band was removed with a syringe, suspended in 0 M-medium and pelleted again at 20,000 ×g for 1 hour.

Figure II-3 shows the absorption spectrum of the envelope and thylakoid membrane fractions. The thylakoid spectrum shows contributions from chlorophyll a and carotenoids. The absorption maximum for bulk chlorophyll a is 679 nm, the same as for chloroplasts. The spectrum of the envelope membrane fraction is dominated by carotenoids and contains only a small contribution from chlorophyll a.

D. INCORPORATION OF CHLOROPHYLL a INTO MODEL BILAYER MEMBRANES

Natural biological membranes are exceedingly complex mixtures of lipid and protein components and, as in the case of the photosynthetic thylakoid membrane, there is usually a substantial degree of imposed biological order. Accordingly, characterization of their physical properties is complicated by difficulties in precisely controlling the large number of variables and in maintaining the required *in vivo* conditions. In recognition of the fact that the unit bilayer constitutes the fundamental element of nearly all biological membranes, simple aqueous suspensions of bilayer-forming phospholipids have been used as models for the more complex biological membranes. Even though such simple model systems sacrifice a fair degree of biological relevance, they at least make it possible to identify and control the critical variables in a well-defined homogeneous system. Chlorophyll can be incorporated into these model membranes as a means of studying the

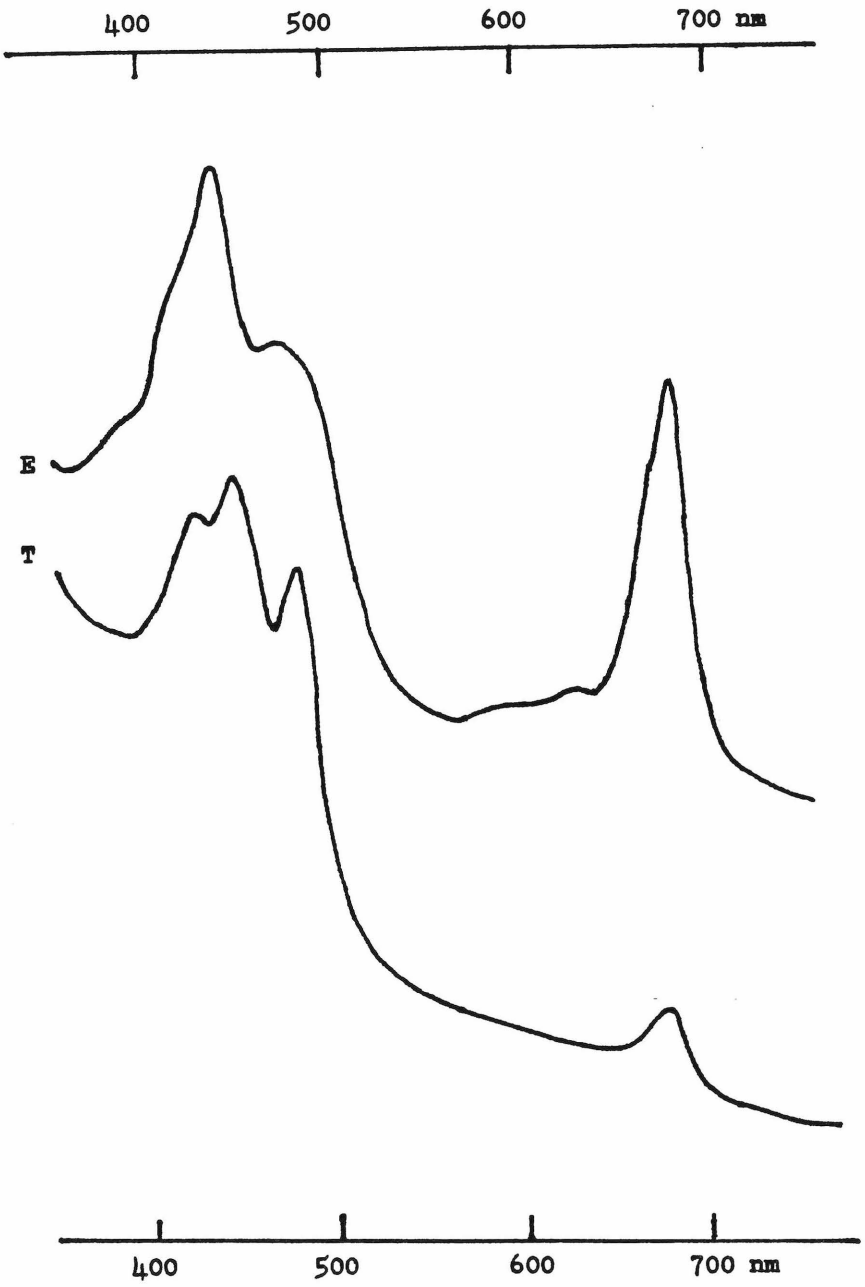

FIGURE II-3. Absorption spectra of envelope (top) and thylakoid (bottom) membranes from spinach chloroplasts.

organization of chlorophyll within the confines of a bilayer matrix and of determining how this organization affects its physical and spectroscopic properties. Information from these studies may then suggest appropriate protocols for future investigation of the more complex natural systems, or may suggest more suitable model systems which better assimilate the in situ characteristics.

In the studies described in the following chapters three types of model bilayer systems were prepared, namely planar multilayers, multilamellar vesicles, and small unilamellar vesicles. The first kind, planar multilayers, are the result of hydrating a lipid mixture with a minimum of water. Usually only 20-30% water by weight is required for full hydration. This type of bilayer system, diagrammed in Figure II-4, is composed of continuous sheets of bilayer membranes separated by layers of water. When lipids are suspended in excess water and gently shaken, a second type of structure similar to the first is formed in which the planar sheets are disrupted to form spherical aggregates with a number of concentric bilayers. Typically these multilamellar vesicles are on the order of a micron in outer diameter and composed of about 10 concentric layers. Such suspensions are convenient to prepare and are suitable for most physical studies. Unfortunately their large size can be a complicating factor in nuclear magnetic resonance studies since the characteristic long motional correlation times result in broad resonances due to incomplete motional averaging of the static dipolar couplings. For these NMR studies a third type of bilayer structure which consists of a much

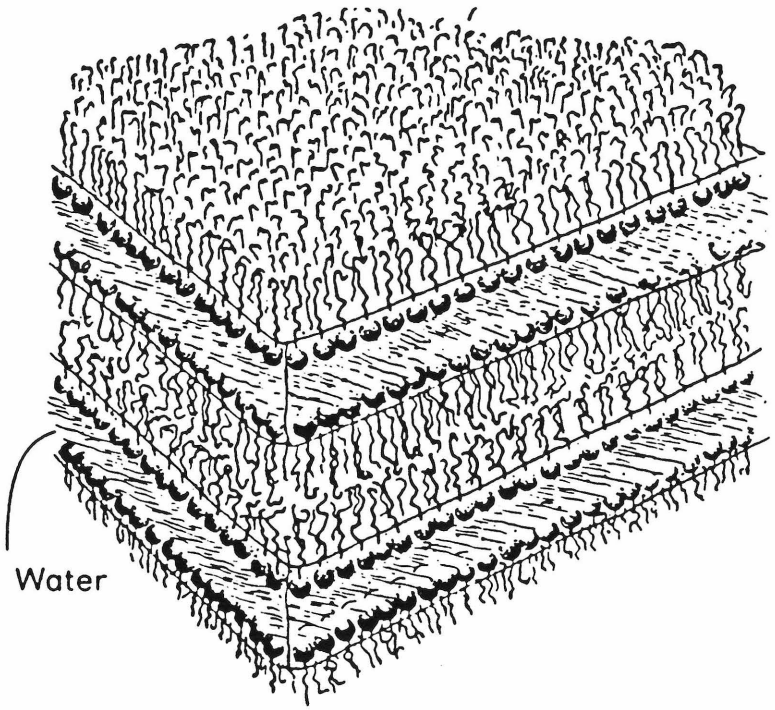

FIGURE II-4 (above). Multilamellar form of an aqueous dispersion of bilayer-forming lipids.

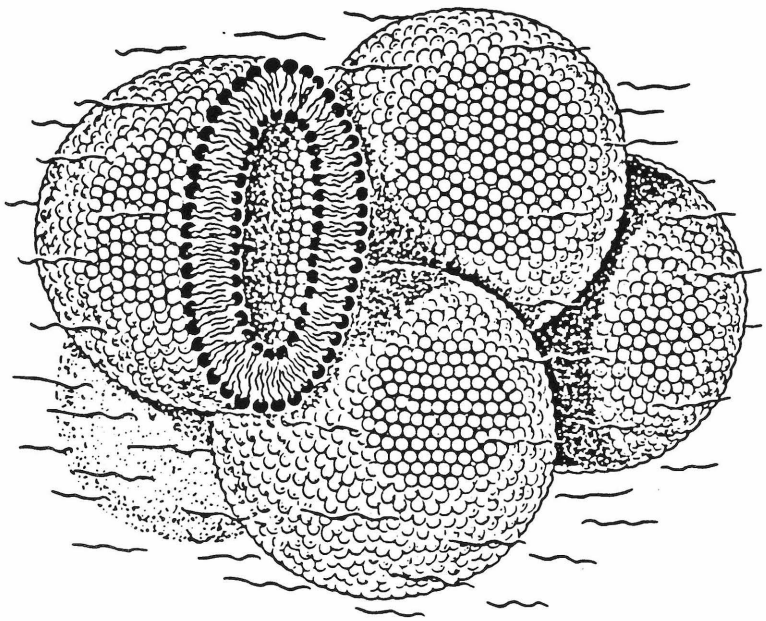

FIGURE II-5. Vesicles of bilayer-forming lipids prepared by sonication.

smaller single spherical bilayer is formed by sonication of dilute multimellar suspensions. These small unilamellar vesicles, diagrammed in Figure II-5, are typically a few hundred Angstroms in diameter, depending upon the lipid composition, and are stable for many hours eventually coalescing to form the more stable multimellar structures. The details of the preparation of these three types of bilayer systems may be found in the Materials and Methods sections of Chapters III, IV and V.

E. CHARACTERIZATION OF CHLOROPHYLL a/DSPC VESICLES

Small unilamellar vesicles prepared by sonication were characterized by determination of the vesicle size and by an analysis of the transbilayer distribution of components. Such a characterization is needed to demonstrate that the vesicular structure remains intact throughout the ranges of chlorophyll composition which were studied. It is also important to insure the uniformity of vesicle properties at different chlorophyll compositions.

DSPC vesicles containing from 5-40 mole percent chlorophyll a were prepared, as will be described in more detail in Chapter IV, by sonication in 0.1 M KCl, 0.01 M Tris-HCl buffer (pH 8.0) at a concentration of 1.0 milligram of total lipid per milliliter of buffer. A 0.25 ml portion of this vesicle suspension was then applied to a 1.0 × 13.0 cm Sepharose 4B column and eluted with buffer at a flow rate of 2 ml/hour. Fractions of 0.2 ml were collected and their absorbance measured at 670 nm to determine the elution profile of chlorophyll-containing vesicles. Similar experiments were performed with Blue

Dextran 2000 to determine the void volume, and with pure DSPC vesicles (diameter of 250 angstroms) and cytochrome c to provide reference points for sizing. The results of these experiments are shown in Figure II-6. All chlorophyll a/DSPC vesicles from 5-40 mole percent chlorophyll a gave essentially identical elution profiles.

The distribution of chlorophyll a between the inner and outer halves of the bilayer vesicle was then determined by selective chemical bleaching of outer layer chlorophyll a molecules with $K_2S_2O_8$, a non-permeable oxidant which causes bleaching of the chlorophyll a red absorption band.[10,11] Because the charged anion $S_2O_8^{2-}$ cannot penetrate the bilayer, externally added $K_2S_2O_8$ can only react with molecules in the outer layer. The peak fraction of each gel permeation experiment was diluted to 2 mls with buffer and the total amount of chlorophyll measured from the absorbance and the known extinction coefficients (assumed to be the same as in diethyl ether). The appropriate volume of a 0.05 M solution of $K_2S_2O_8$ in buffer was then added to give a 500-fold molar excess of $K_2S_2O_8$. The progress of the reaction was followed by monitoring the absorbance at 670 nm.
A typical set of results is shown in Figure II-7. Since there is a large excess of oxidant, the reaction follows pseudo-first order kinetics with an apparent rate constant of about 0.3 $hour^{-1}$. Eventually the reaction reaches completion with some amount of chlorophyll a in the inaccessible inner layer remaining unreacted. By comparison of the initial and final absorbances, a crude estimate can be made of the amounts of chlorophyll a in the inner and outer bilayer halves. These results are

FIGURE II-6 (next page). Elution profile of 15% chlorophyll a/DSPC sonicated vesicles from a 1.0 × 13.0 cm Sepharose 4B gel filtration column. Also shown are the elution profiles of Blue Dextran 2000 (to determine void volume) and of cytochrome c and pure DSPC sonicated vesicles (outer diameter about 250 angstroms).

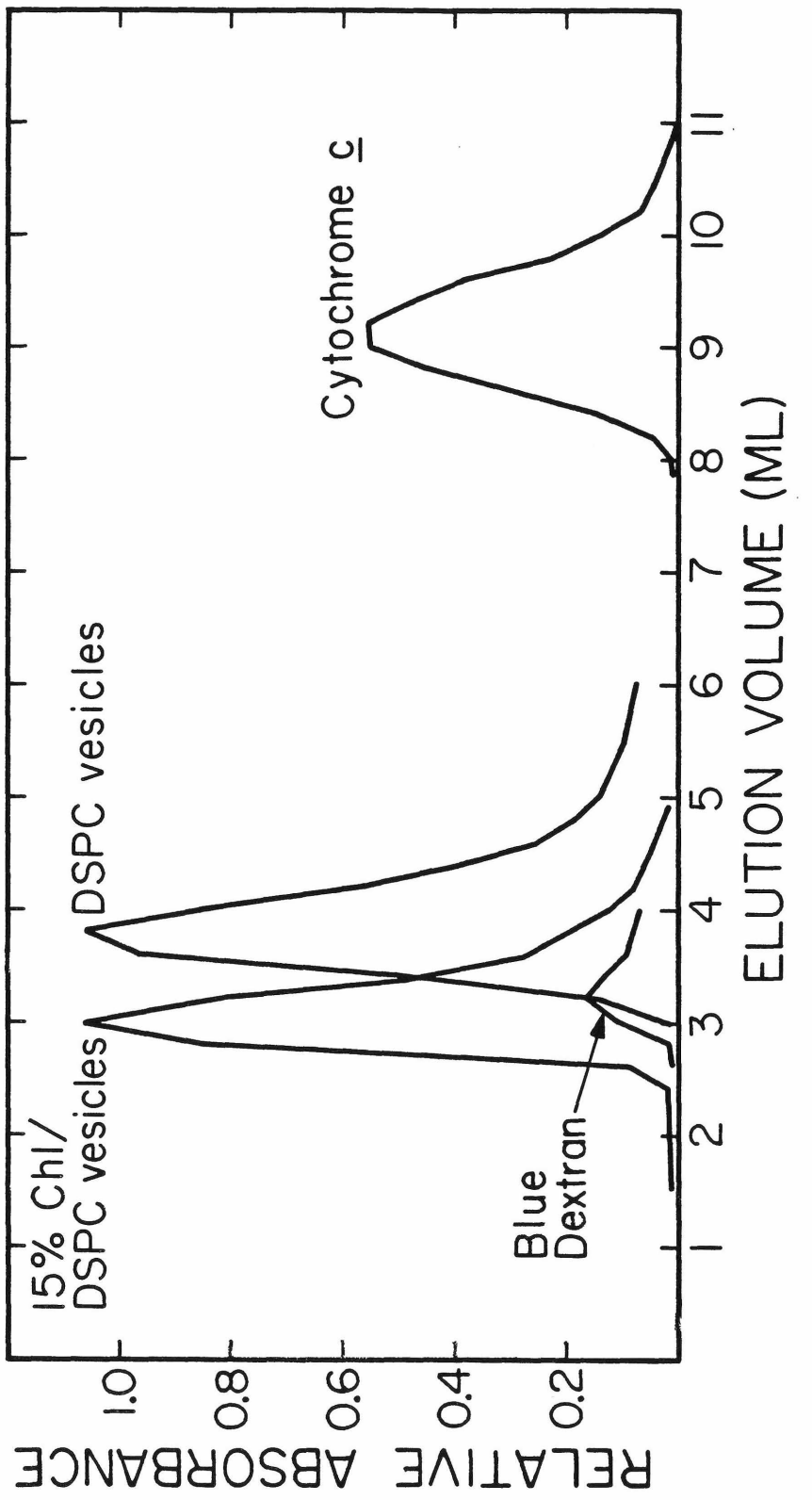
RELATIVE ABSORBANCE
1.0
0.8
0.6
0.4
0.2
15% Chl/
DSPC vesicles
DSPC vesicles
Cytochrome c
Blue
Dextran
1
2
3
4
5
6
7
8
9
10
11
ELUTION VOLUME (ML)

FIGURE II-7 (next page). Absorbance at 670 nm of chlorophyll a in 20% chlorophyll a/DSPC sonicated vesicles following the addition of a 500-fold molar excess of the membrane-impermeable oxidant $K_2S_2O_8$.

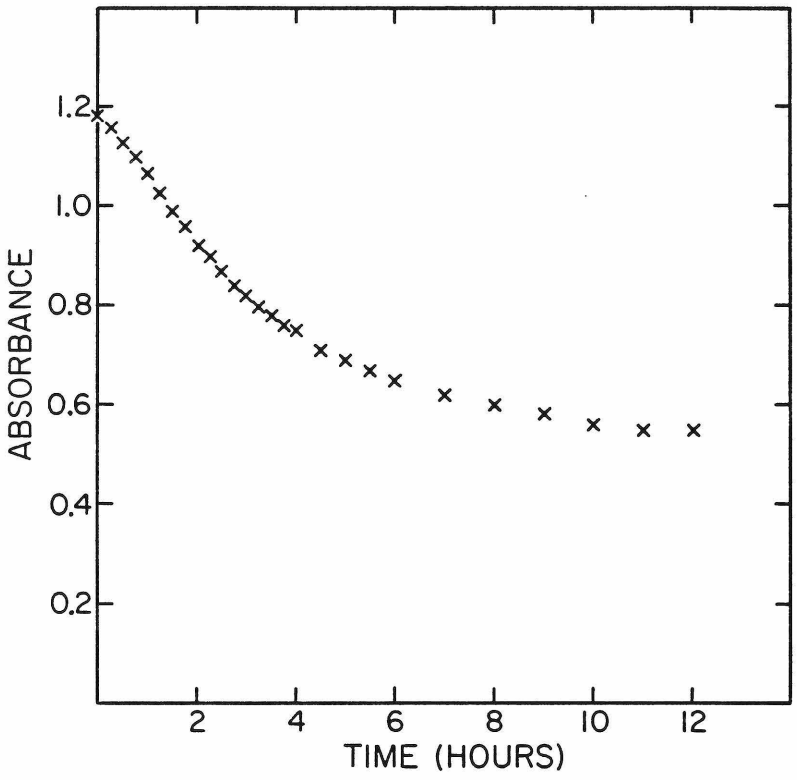
ABSORBANCE
1.2
1.0
0.8
0.6
0.4
0.2
2
4
6
8
10
12
TIME (HOURS)

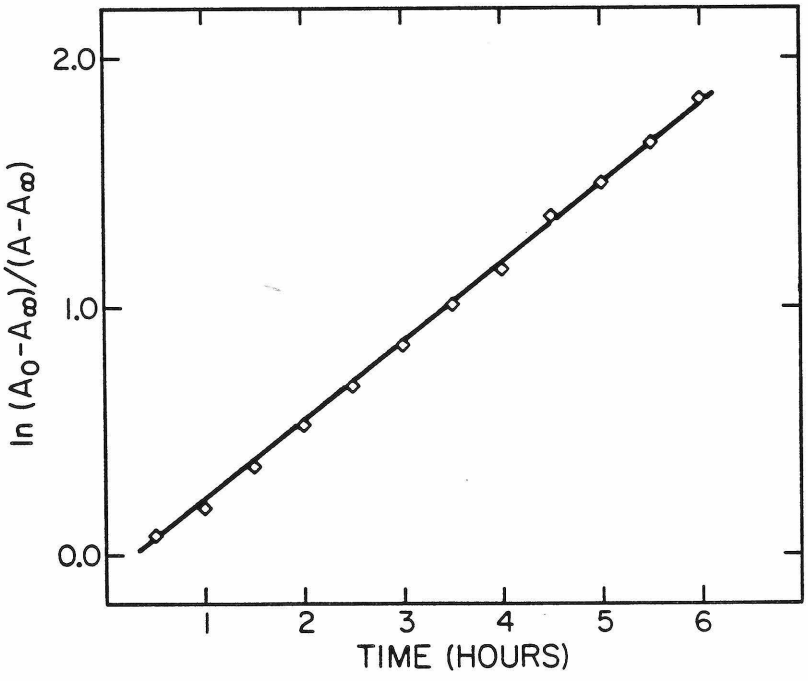
ln (A0-A∞)/(A-A∞)
2.0
1.0
0.0
1
2
3
4
5
6
TIME (HOURS)

shown in Figure II-8. Such analyses are only approximate because of a small amount of vesicle light scattering, typically 5% of the peak absorbance at 670 nm. Thus the results slightly underestimate the fraction of chlorophyll in the outer layer.

A number of conclusions can be reached from the previous results. First, the outer diameter of chlorophyll-containing vesicles is consistently larger than the 250 angstrom outer diameter of pure DSPC vesicles. It cannot be determined from the data whether their size changes with chlorophyll compositions. Second, the vesicle structure is intact over the 5-40 mole percent chlorophyll composition range. If this were not so, then all chlorophyll would be accessible to the oxidant. Third, we can infer that the transbilayer distribution of chlorophyll a is uniform beyond 15 mole percent. Below 15 mole percent there is a clear preference for the outer layer, most likely because the expansion at the outer layer better accommodates the large chlorophyll a headgroup.

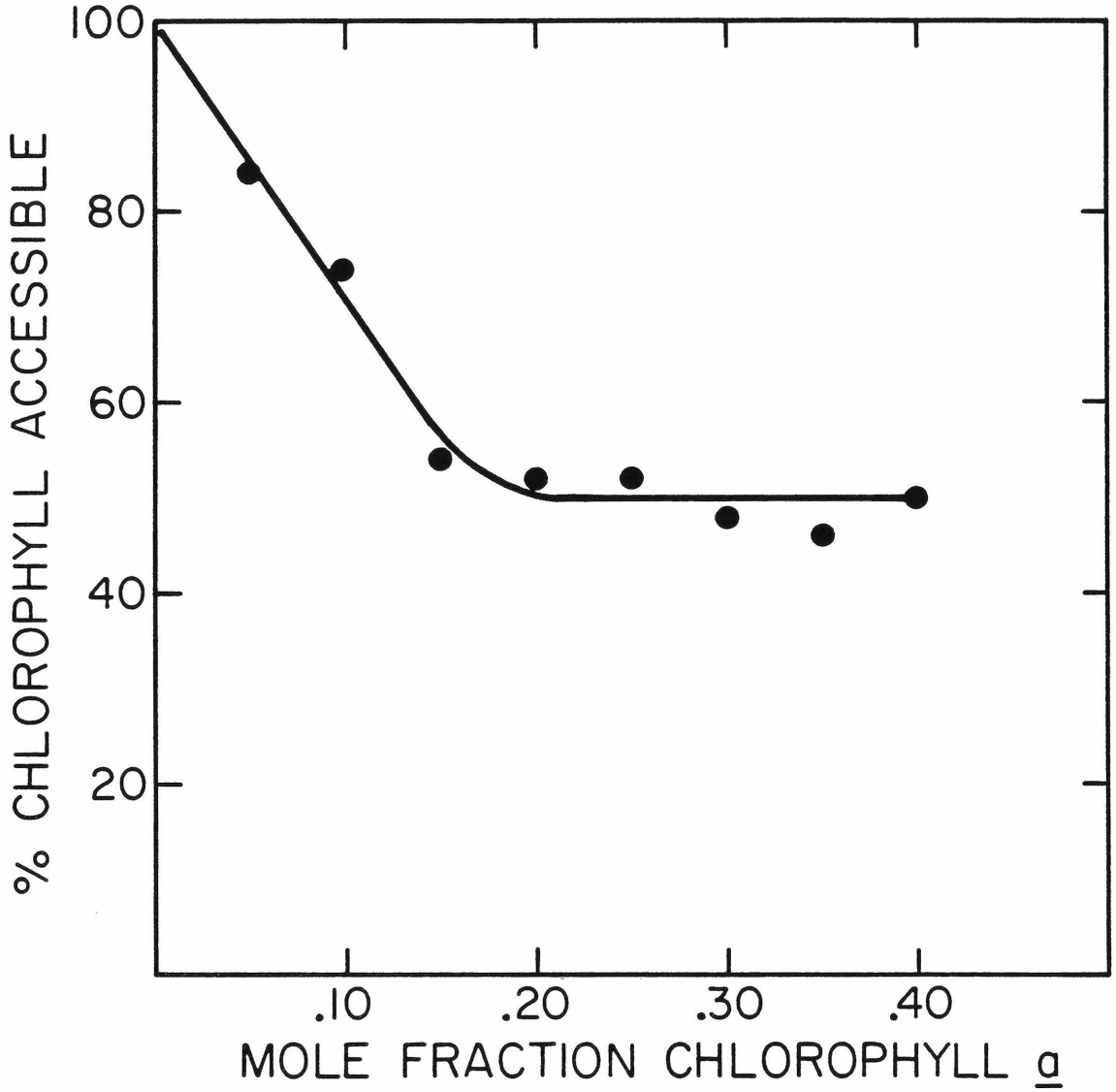

FIGURE II-8. The percentage of chlorophyll a in the accessible outer bilayer half for chlorophyll a/DSPC vesicles of various compositions as estimated by the reduction in absorbance due to bleaching by externally added $K_2S_2O_8$.

REFERENCES - CHAPTER II

1. H. H. Strain and W. A. Svec, in The Chlorophylls (L. P. Vernon and G. R. Seely, eds.), Academic Press, New York, 1966, pp. 22-66.
2. G. R. Seely, in The Chlorophylls (L. P. Vernon and G. R. Seely, eds.), Academic Press, New York, 1966, pp. 67-110.
3. G. R. Seely, in Primary Processes of Photosynthesis (J. Barber, ed.), Elsevier, Amsterdam, 1977, pp. 1-53.
4. K. Iriyama, N. Ogura, and A. Takamiya, J. Biochem., 76, 901-904 (1974).
5. H. H. Strain, M. R. Thomas, H. L. Crespi, M. I. Blake, and J. J. Katz, Ann. New York Acad. Sci., 84, 617-666 (1960).
6. H. H. Strain, M. R. Thomas, and J. J. Katz, Biochim. Biophys. Acta, 75, 306-311 (1963).
7. G. R. Seely and R. G. Jensen, Spectrochimica Acta, 21, 1835-1845 (1965).
8. H. Hashimoto and S. Murakami, Plant Cell Physiol., 16, 895-902 (1975).
9. S. Murakami and L. Packer, Arch. Biochem. Biophys., 146, 337-347 (1971).
10. M. Fragata, Experientia, 33, 177-178 (1977).
11. H. Dijkmans, R. M. Leblanc, F. Cogniaux, and J. Aghion, Photochem. Photobiol., 29, 367-372 (1979).

CHAPTER III

Interactions of Chlorophyll a with Phospholipids in Bilayer Membranes - Studies of the Thermal Phase Diagram by Differential Thermal Analysis

A. INTRODUCTION

Several groups have reported the inclusion of small amounts of chlorophyll a into artificial multilamellar and vesicular bilayer membrane systems[1-12] to develop useful models for studying energy transfer[1,2] and photo-induced electron transfer,[3-5] and to model the photosynthetic membrane itself.[4-8] As a result of these efforts it has been adequately demonstrated that chlorophylls are integrally incorporated into the bilayer with the porphyrin headgroup in the polar region of the membrane[9,10] and the non-polar phytol group inserted in the hydrophobic core of the membrane[6] along with the lipid fatty acyl chains. Conflicting interpretations have been offered, however, regarding the precise lateral membrane organization of chlorophyll and its concomitant intermolecular interactions. A clear understanding of the organization of chlorophyll in these model systems is essential if they are to be used to their full advantage.

Tomkiewicz and Corker[3] concluded from absorption, circular dichroism and electron paramagnetic resonance studies that chlorophyll a in egg lecithin vesicles (0.02-0.10 mole fraction chlorophyll a) is present in monomeric form, in other words with no direct chlorophyll-chlorophyll interactions, at room temperature (above the mem-

brane phase transition) and at lower temperatures. Oettmeier et al.[5,9] reached a similar conclusion for chlorophyll a/DPPC sonicated vesicles (0.033 mole fraction chlorophyll a) which should be below the phase transition at and below room temperature. Lee,[11] however, interpreted the decrease in chlorophyll a fluorescence at temperatures below the thermal phase transition of chlorophyll a/DPPC multilayers as being due to the segregation of chlorophyll a into non-fluorescent oligomers. This change is reversible with temperature, and both Lee[11] and Colbow[7] have used this to monitor the phase transition of various membrane systems although it is noted that the measured transition temperature is altered by changes in chlorophyll concentration. Podo et al.,[6] studying bacteriochlorophyll/DPPC vesicles (0.09 mole fraction bacteriochlorophyll, 20° C) concluded from X-ray diffraction and absorption polarization that bacteriochlorophyll inserts into the membrane without lateral phase separation of the two components. This observation would seem to be inconsistent with the findings of Lee regarding the segregation of chlorophyll a into oligomers although it is not clear to what extent these results are applicable to other chlorophylls.

In the present study we wish to show that the lateral organization of chlorophyll a within a host phospholipid bilayer membrane depends on both temperature and composition, and can in fact be much different depending upon the particular set of conditions chosen. This result suggests that in using chlorophyll a/phospholipid bilayers it is essential to assess the phase state of the membrane and to consider its effects on

the properties of the system in question.

B. MATERIALS AND METHODS

Synthetic β-γ-distearoyl-L-α-phosphatidylcholine (DSPC) was obtained from Calbiochem. Its purity was checked by thin layer chromatography on Whatman LK5DF analytical plates developed with chloroform/methanol/water (65:25:4). Since no impurities were found the DSPC was used without further purification.

Chlorophyll a was isolated from spinach extracts by the dioxane precipitation procedure of Iriyama[3] and purified by chromatography on powdered sugar according to Strain et al.[14,15] Particular care was taken in the chromatographic separation to exclude bands due to chlorophyll a alteration products which elute slightly ahead of authentic chlorophyll a. The final purity of the isolated product was determined from the optical absorption spectrum in diethyl ether. Molar extinction coefficients were determined from the absorption of a solution of chlorophyll a (approx. 1 milligram weighed to 0.1 microgram) in 100 ml of fresh diethyl ether. Molar extinction coefficients found (literature values[15] in parentheses): $\epsilon^{M}_{660} = 11.0 \times 10^4$ (11.2×10^4), $\epsilon^{M}_{428} = 8.56 \times 10^4$ (8.63×10^4) indicate that the purity is $>98\%$. The ratios of the absorption bands correspond well with previously determined values (literature[16] in parentheses): $\epsilon^{M}_{428}/\epsilon^{M}_{660} = 1.29$ (1.31), $\epsilon^{M}_{428}/\epsilon^{M}_{410} = 1.59$ (1.57).

Stock solutions of chlorophyll a and DSPC were prepared in fresh chloroform and mixed in the appropriate amounts to obtain the neces-

sary mole fraction of the two components. The solution was evaporated to dryness under N_2 and the solid mixture dried overnight under vacuum. To prepare samples for thermal analysis, 2 milligrams of the chlorophyll a/DSPC mixtures was finely divided and placed in 2 mm glass capillary tubes. Dionized water (5 microliters) was added and the capillary sealed. The samples were then allowed to hydrate for at least 2 hours at 70° C in order to form a multilamellar dispersion.

Differential thermal analysis was carried out on a DuPont 900 Differential Thermal Analyzer. The calibration of the instrument was checked by determining the transition temperature of pure DSPC multilayers prepared in exactly the same manner as the chlorophyll a/DSPC multilayers. The sample thermocouple was placed in the approximate center of the sample and referenced against a matched amount of water in an identical reference capillary. Both sample and reference were heated at a uniform rate of 6°/min. from 30-70° C. Following its return to 30° the sample was allowed to equilibrate for at least 30 min. to eliminate possible hysteresis effects. The measured transition temperatures were taken as the peak of the exotherm. According to the analysis of Smyth[17] this procedure is correct for the previously described conditions of a thermocouple measuring the temperature at the center of a cylindrical sample heated from the outside.

C. RESULTS AND ANALYSIS

1. Differential thermal analysis data

Differential thermal analysis (DTA) was performed on hydrated chlorophyll a/DSPC multilayers in order to determine the two-component thermal phase diagram of the bilayer system. DTA thermograms from 30-70° C were obtained in triplicate at 2 mole percent intervals over the composition range of 0-50 mole percent chlorophyll a. Peak positions for each composition were measured at the temperature of maximum exothermicity and the triplicate values were averaged. The average standard deviation in the values was approximately 0.20° C.

Some typical thermograms at selected compositions are shown in Figure III-1. The changes in the number and positions of the observed exothermic peaks indicate significant phase behavior for the system over the temperature and composition ranges studied. Briefly, thermograms of compositions up to 6 mole percent chlorophyll a show only a single unresolved peak that becomes broader with increased chlorophyll a composition. At 6 mole percent a small exotherm is partly resolved as a shoulder on the low temperature side of the main peak. From 8 mole percent to 30 mole percent chlorophyll a, two distinct exotherms are observed. The upper of these two decreases in temperature regularly with increasing chlorophyll a composition, while the lower maintains an average temperature of about 50° C. Near 32 mole percent chlorophyll a, the previous two exotherms coalesce into what is apparently an eutectic point. Beyond 32 mole percent two peaks again reappear, the lower remaining near 50° and the upper now increasing

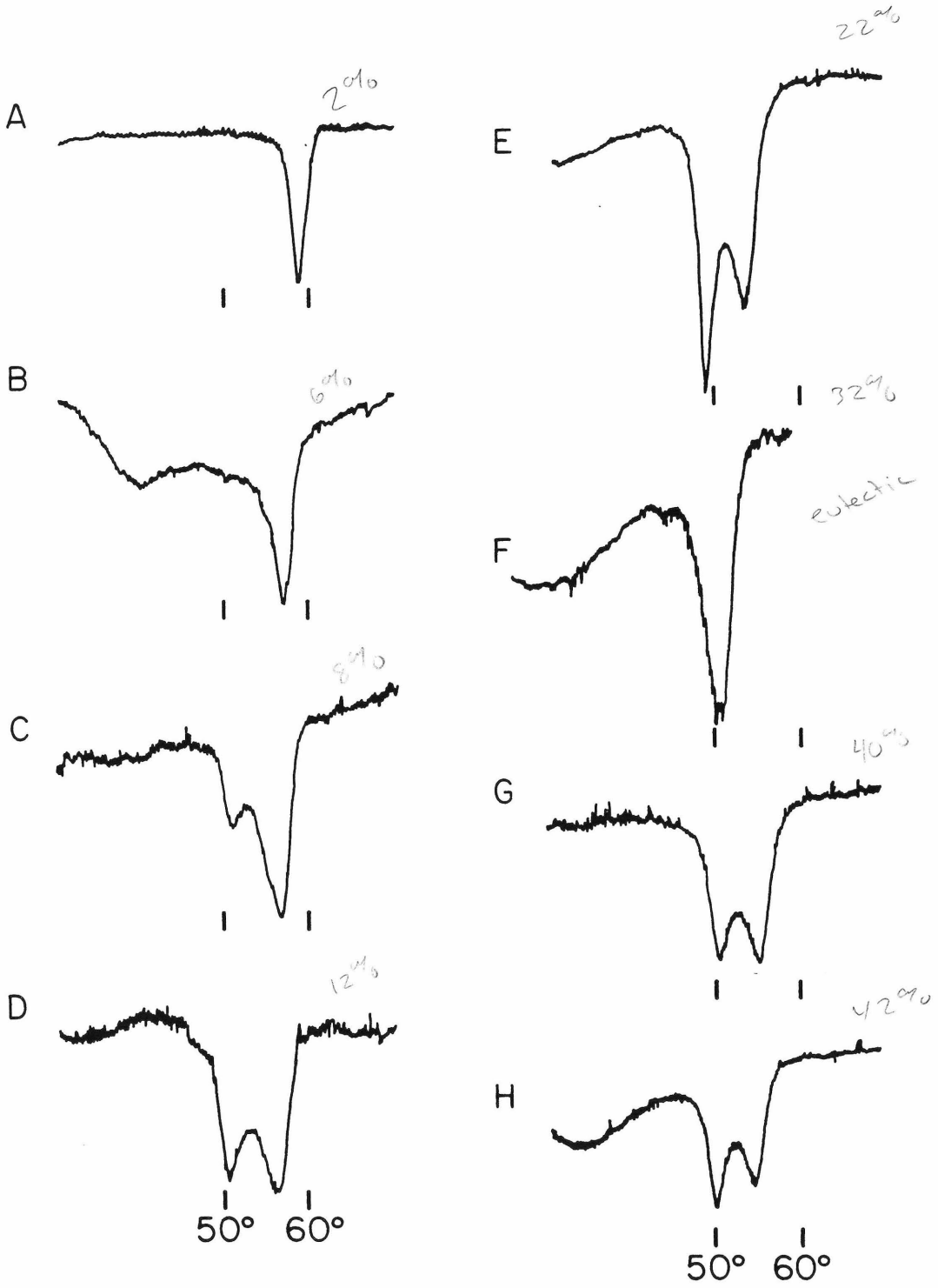

FIGURE III-1. Selected DTA heating thermograms of hydrated chlorophyll a/DSPC multilayers (5 mg H_2O per 2 mg total lipid). Compositions: A, 2%; B, 6%; C, 8%; D, 12%; E, 22%; F, 32%; G, 40%; H, 42%.

with chlorophyll a content. At 42 mole percent there is a slight but significant decrease in the temperature of the upper exotherm. Beyond 42 mole percent the temperatures of the peaks no longer change and the sensitivity of the thermograms decreases, most likely indicating that the bilayer is saturated with chlorophyll a at 42 mole percent.

The transition temperatures for each composition are plotted in the form of a two-component phase diagram in Figure III-2. The third component of the system, water, is present in large excess and we assume that its mole fraction in the system does not essentially change.

2. Interpretation of the phase diagram

The pattern of the data in Figure III-2 readily suggest a particular form of phase diagram characteristic of compound formation between chlorophyll a and the phospholipid DSPC. The location and nomenclature of the various phases consistent with this interpretation of the phase diagram are shown in Figure III-3. Additional support for this interpretation of the phase diagram as well as further characterization of some of the important phases is included in the following chapter. At this point it would be useful to consider some of the rationale behind our interpretation of the results.

Seen as in Figure III-2, the data clearly delineate various phase regions. The task at hand in interpreting the phase diagram is to assign the phases present in each region of the temperature-composition space. Several rules[18] aid in this construction of the phase diagram: 1) A two-component phase diagram must consist of unique one-phase and two-phase regions separated by lines of three-phase equilibria.

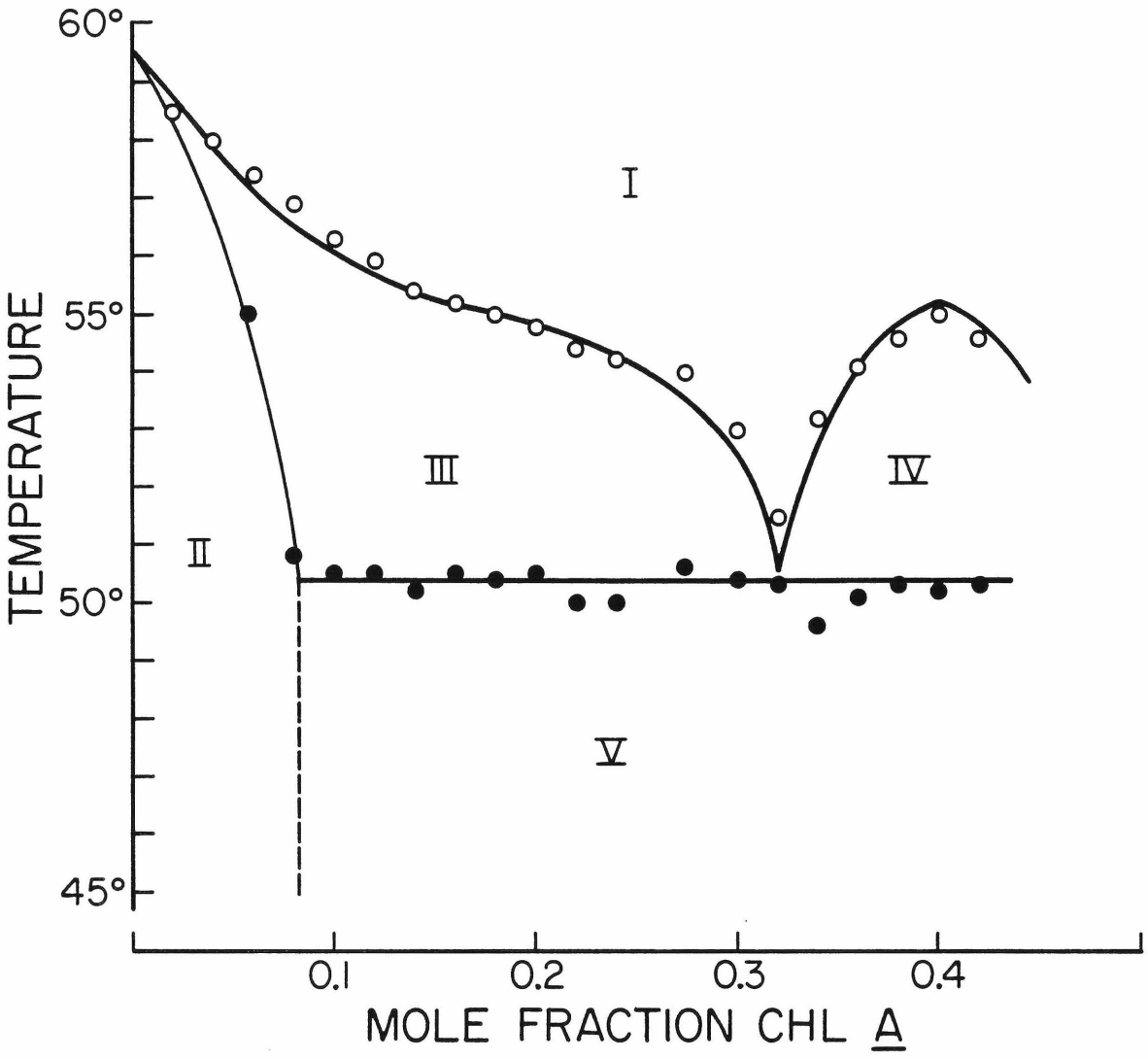

FIGURE III-2. Differential thermal analysis phase diagram of the chlorophyll a/DSPC bilayer membrane system prepared as an aqueous multilamellar suspension in excess water. Open and closed circles represent points of maximum exothermicity of the observed DTA peaks. The liquidi between regions I and II, and between I and IV were calculated to fit the data as described in the text.

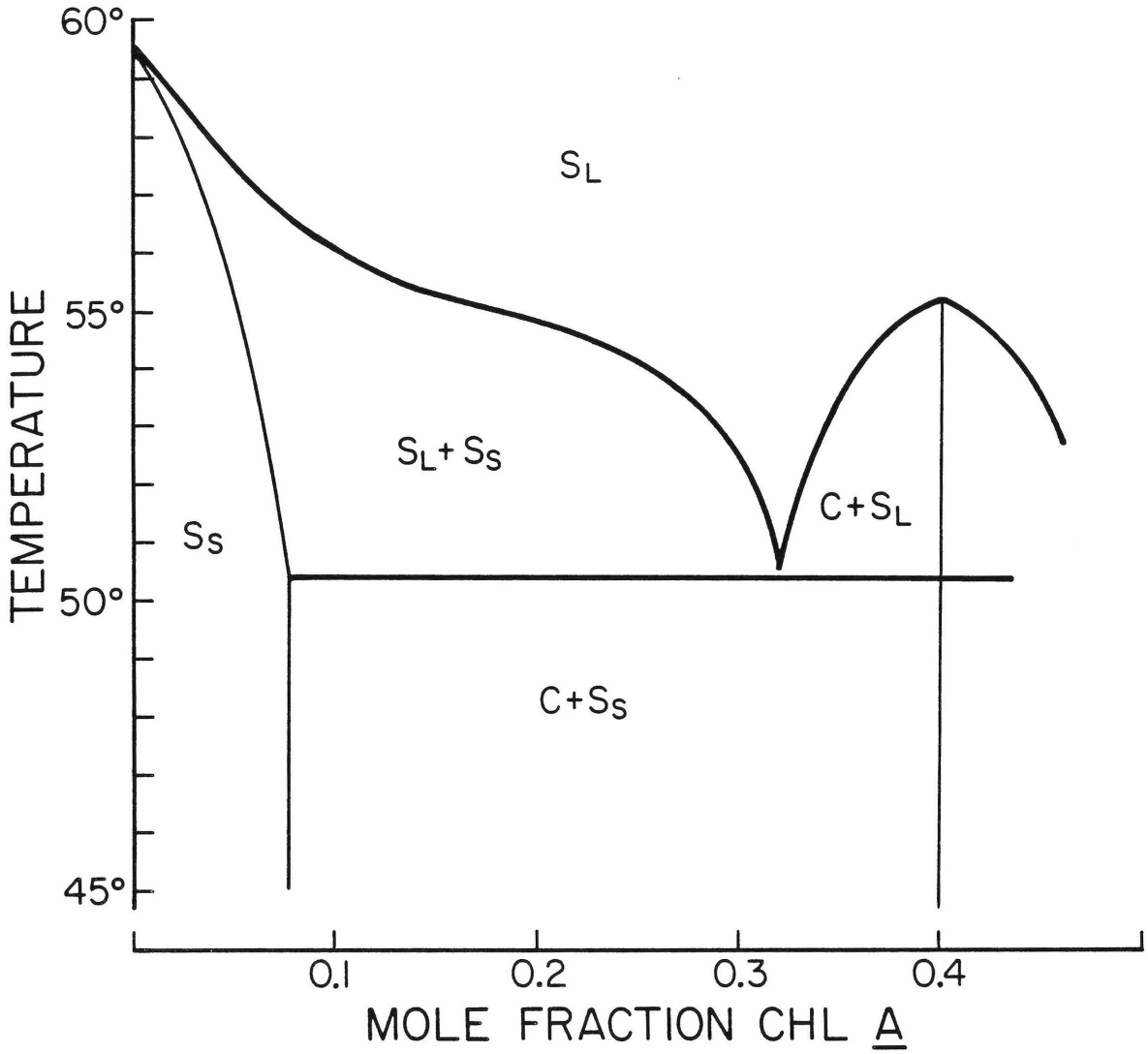

FIGURE III-3. Phase diagram of chlorophyll a/DSPC bilayers interpreted as a compound type of phase diagram with double side-by-side eutectics. Note that only a portion of the double eutectic phase diagram is observed in this system because of limited bilayer stability beyond about 42 mole percent chlorophyll a. Abbreviations: S_L, liquid-crystalline bilayer solution; S_S, solid solution or limited miscibility region; C, compound phase - 0.40 mole fraction chlorophyll a.

2) These regions must be arranged such that a horizontal isotherm alternately traverses one and two-phase regions. 3) a eutectic line is a line of three-phase equilibrium and must be a boundary for three two-phase regions, two above and one below it. The horizontal line in Figure III-2 at 50.4° C is clearly an eutectic line. Thus, rule 3) implies that regions III, IV and V should be two-phase regions. Rule 2) then requires that regions I and II be one-phase regions. Since the eutectic line characterizes a three-phase equilibrium and separates two two-phase regions, III and IV must share a common phase. Likewise, IV and V must share a common phase.

We are assisted further in the interpretation in that the phase behavior of one composition, namely pure DSPC or 0% chlorophyll is well characterized. Above the main transition temperature of 59° C DSPC multilayers are in a fluid-like liquid crystalline phase. At lower temperatures DSPC multilayers exist in a more solid-like and ordered gel phase. Since regions I and II are continuous with these pure-component phase regions, it is expected that they should share similar features. Thus region I, which is a one-phase region, should consist of a fluid-like solution of chlorophyll a in the host DSPC bilayer. Similarly region II, also a homogeneous one-phase region, should consist of a solid solution of chlorophyll a in a gel phase with DSPC. To be sure, these are not solutions in the usual sense but must be considered as two-dimensional solutions within the bilayer plane. Region III, in equilibrium with the phases of regions I and II, must then consist of these two phases in relative amounts governed by the appropriate tie-line.

These preliminary conclusions are sufficient to suggest two possible types of phase diagrams: A) a two-component single-eutectic with partial solid-state miscibility, or B) compound formation with side-by-side eutectics. The actual phase diagram of the system must of course consist of only part of the complete phase diagram because the bilayer system breaks down at higher chlorophyll compositions. In the case of phase diagram A, the two-phase region IV would consist of a chlorophyll a/DSPC solution in equilibrium with a phase consisting of mostly chlorophyll a with a limited solubility of DSPC. The possibility of such a phase seems quite unlikely since chlorophyll does not form stable bilayers. Furthermore, the decrease in transition temperature at 42 mole percent is inconsistent with a liquidus which should increase towards the right end composition. This decrease is, in fact, suggestive of the compound type of phase diagram which is shown in Figure III-3.

3. Simulation of the phase diagram

The experimental phase diagram of the chlorophyll a/DSPC bilayer system can be simulated to yield useful and otherwise unobtainable thermal parameters. For this simulation we mostly use the analysis of Lee[19, 20] for binary lipid mixtures which takes into account non-ideal mixing of the components. In the chlorophyll a/DSPC system, mixing is expected to be markedly non-ideal because of the very different chemical structures and because of the definite chemical interaction between chlorophyll a and the phospholipid necessary to form the compound.

In the case of an ideal binary solution, the chemical potential of the two components A and B is related to their relative mole fractions in the solution as:

$$\mu_A = \mu_A^\circ + RT\,\ell n X_A \qquad \text{(III-1)}$$

$$\mu_B = \mu_B^\circ + RT\,\ell n(1 - X_A) \qquad \text{(III-2)}$$

where μ_A° and μ_B° are the standard-state chemical potentials of components A and B and X_A and $X_B (= 1 - X_A)$ their mole fractions. The total free energy of the mixture is

$$G = X_A \mu_A^\circ + (1 - X_A)\mu_B^\circ + RT[X_A \ell n X_A + (1 - X_A)\ell n(1 - X_A)] \qquad \text{(III-3)}$$

Subtraction of the standard state chemical potential of the mixture, $X_A \mu_A^\circ + X_B \mu_B^\circ$, from the total Gibb's free energy expressed in (III-3) gives the change in free energy due to mixing:

$$\Delta G_{mix} = -RT[X_A \ell n X_A + (1 - X_A)\ell n(1 - X_A)]. \qquad \text{(III-4)}$$

This expression (III-4) can be used to calculated ΔS_{mix},

$$\Delta S_{mix} = \frac{\partial G_{mix}}{\partial T} = R[X_A \ell n X_A + (1 - X_A)\ell n(1 - X_A)]. \qquad \text{(III-5)}$$

Furthermore, since $G \equiv H - TS$ we can calculate the enthalpy of mixing from (III-4) and (III-5):

$$\Delta H_{mix} = 0. \qquad \text{(III-6)}$$

The assumption of an ideal solution is therefore synonymous with a zero enthalpy of mixing. This requirement is rarely met by mixtures of lipid molecules because of intermolecular interactions. In addition, different molecular volumes can produce an additional entropy of mixing in excess of that given by (III-5).

These deviations from ideal behavior can be taken into account by the activity coefficient j_A:

$$\mu_A = \mu_A^\circ + RT \ell n X_A j_A . \qquad \text{(III-7)}$$

The activity coefficient modifies the ideal chemical potential by a quantity $RT \ell n j_A$ which can be defined as the excess chemical potential μ_A^e:

$$\mu_A^e = RT \ell n j_A = \mu_A - \mu_A^\circ - RT \ell n X_A . \qquad \text{(III-8)}$$

For a binary mixture of components A and B, the total excess molar Gibbs free energy is

$$G^e = X_A \mu_A^e + X_B \mu_B^e . \qquad \text{(III-9)}$$

The excess Gibbs free energy for binary lipid mixtures has been modeled with success[19, 20] by the approximate expression:[21]

$$G^e = X_A X_B \rho_0 \qquad \text{(III-10)}$$

where ρ_0 is a so-called non-ideality parameter characteristic of differences in pair-wise interaction energies between nearest neighbors

in the solution. The parameter ρ_0 therefore contains information on the interaction energies between two lipid species. We make use of this in a later discussion.

For ideal binary solutions with complete immiscibility in the solid phase, the liquidus should be given by the freezing point depression curve which also describes the solubility of the solid component A in the solution:

$$\ell n X_A^{liq} = \frac{\Delta H_A}{R} \left(\frac{1}{T_A} - \frac{1}{T_{ideal}} \right) \qquad \text{(III-11)}$$

where T_A and ΔH_A are the melting temperature and heat of melting of the pure component A. The inclusion of the non-ideality parameter ρ_0 modifies[19] the liquidus according to

$$\frac{\rho_0 (1 - X_A)^2}{\Delta H_A} = \frac{T}{T_{ideal}} - 1. \qquad \text{(III-12)}$$

Treating X_A^{liq} as the independent variable, we may calculate the expected transition temperature T as a function of the variables ΔH_A, T_A, and ρ_0. Rearranging (III-11) to solve for T_{ideal} we obtain the relation

$$T_{ideal} = \left[\frac{1}{T_A} - \frac{R}{\Delta H_A} \ell n X_A^{liq} \right]^{-1}. \qquad \text{(III-13)}$$

The transition temperature T of a non-ideal mixture is then obtained from (III-12) and (III-13) as

$$\left[\frac{\rho_0 (1 - X_A^{liq})^2}{\Delta H_A} + 1\right] T_{ideal} = T . \qquad \text{(III-14)}$$

Equations (III-11) through (III-14) form the basis for calculating the liquidus curve of binary mixtures with complete solid phase immiscibility. Figures III-4 and III-5 illustrate the effects of ΔH_A and ρ_0 on calculated liquidus curves.

In the case of the chlorophyll a/DSPC system we will consider the solid solution phase to have thermodynamic properties identical to a pure DSPC solid phase. Since the amount of chlorophyll a in this phase is small, its effect on the transition enthalpy and transition temperature is likely to be of moderately small significance. This assumption is supported later by the agreement of the final results with the experimental data.

For a compound type of phase diagram, the end compositions are properly considered as those of the end phases. In the present case these are pure DSPC or 0.0 mole fraction chlorophyll a, and the compound phase or 0.40 mole fraction chlorophyll a. Thus X_A^{liq} varies between 1.00 and 0.00 as the chlorophyll a composition varies between 0.00 and 0.40. To account for this fact, the value of X_A^{liq} must be scaled by 2.5. When calculating the left-hand liquidus, $X_A^{liq} = 2.5(X_{chlorophyll})$. The liquidus right of the eutectic can also be calculated, but in this case $X_A^{liq} = 2.5(0.40 - X_{chlorophyll})$.

The parameters ΔH_A, T_A, and ρ_0 in (III-13) and (III-14) were varied systematically to obtain the best agreement of the calculated liquidus to the experimental data. Both the left and right liquidus curves

FIGURE III-4 (next page, top). Effect of ΔH_A on the theoretical liquidus calculated according to equation (III-11) assuming ideal solution phase mixing and a T_A of 58°.

FIGURE III-5 (next page, bottom). Liquidus curves in the case of non-ideal solution phase mixing calculated from equations (III-11) through (III-14). Parameters: ΔH_A = 10,840 cal/mole, T_A = 58° C, ρ_0 as indicated.

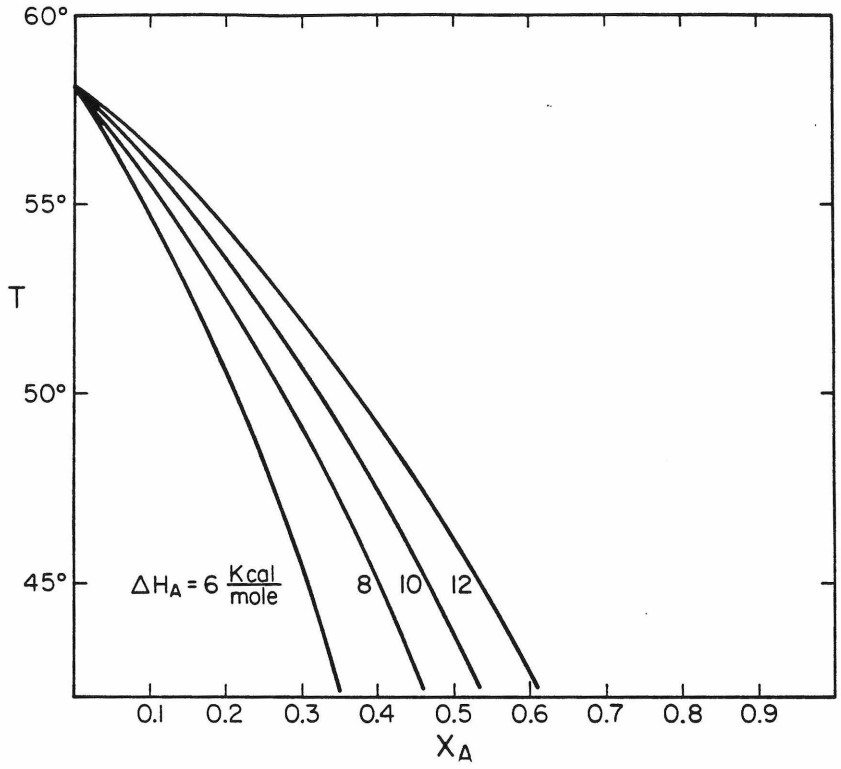
60°
55°
50°
45°
T
$\Delta H_A = 6 \frac{Kcal}{mole}$
8
10
12
0.1
0.2
0.3
0.4
0.5
0.6
0.7
0.8
0.9
X_A

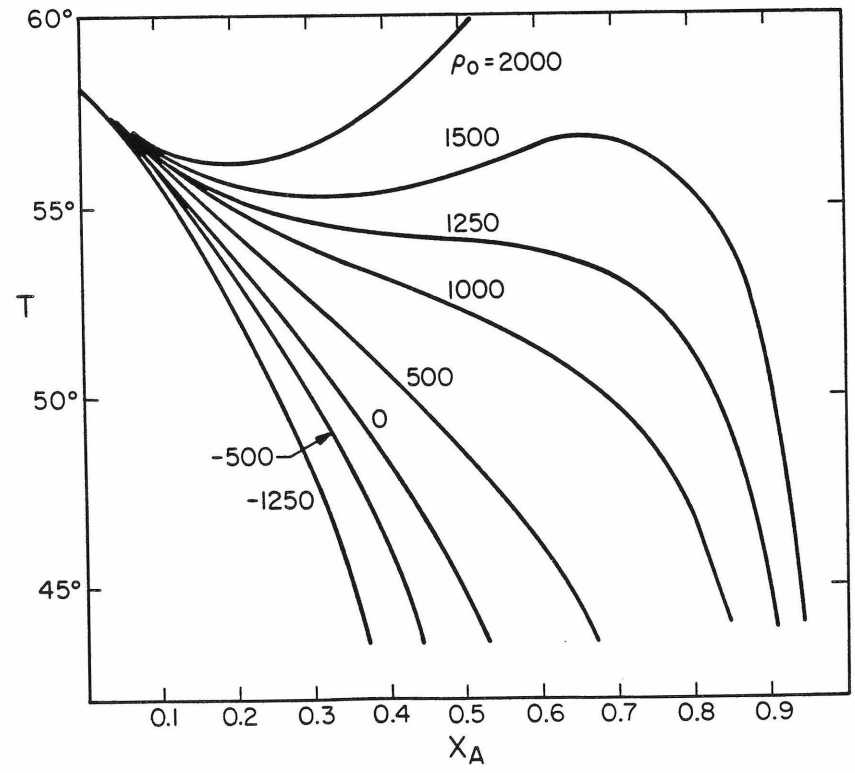
60°
55°
50°
45°
T
$\rho_0 = 2000$
1500
1250
1000
500
0
-500
-1250
0.1
0.2
0.3
0.4
0.5
0.6
0.7
0.8
0.9
X_A

were calculated with the best set of parameters determined independently for each. Figure III-6 gives these parameters and Figure III-3 shows the simulated phase diagram along with the DTA data.

It should be noted that an acceptable fit of the data can only be obtained with the compound composition as the end-phase. Under no circumstances could the data be simulated using 100% chlorophyll a as the composition of the end phase. This is taken as further support for the choice of the compound phase diagram interpretation.

D. DISCUSSION

1. Significance of the simulated phase diagram parameters

The liquidus left of the eutectic represents the solubility curve of DSPC in the chlorophyll a/DSPC solution. The value of the transition enthalpy for the formation of solid DSPC from chlorophyll a/DSPC solution agrees with corresponding values for pure DSPC multilayers[22,23] indicating that the phase transition is not influenced by the presence of chlorophyll a. The value obtained for the transition temperature for the pure component A or DSPC is slightly higher than published values[22, 23] for pure DSPC, possibly reflecting a systematic error which is perhaps due to using the peak rather than the onset of the exotherm as the measured transition temperature. The value determined for ρ_0, the non-ideality parameter, indicates that mixing of DSPC and chlorophyll a in the solution phase is non-ideal although not substantially different than for mixtures of other lipids.[20]

The liquidus to the right of the eutectic represents the solubility

FIGURE III-6. Table of thermodynamic values obtained by simulation of the phase diagram liquidus curves. Units: ΔH_A (cal./mole), T_A (°C), ρ_0 (cal./mole).

	ΔH_A	T_A	ρ_0
liquidus left of eutectic (X_A= 0.00 to X_A= 0.32)	10,840	59.5	1180
liquidus right of eutectic (X_A= 0.32 to X_A= 0.40)	45,000	55.2	-10,000

of the compound phase in the chlorophyll a/DSPC solution. The values of T_A, ΔH_A and ρ_0 obtained in this case are therefore characteristic of the compound phase. T_A, the melting temperature (or dissociation temperature) of the pure compound phase is 55.2°. ΔH_A, the corresponding transition enthalpy is about 45 kcal per mole of compound or about 4 times the transition enthalpy of pure DSPC. The larger heat is possibly a reflection of the molecularity of the compound phase and could indicate that there are on the order of 4 molecules of DSPC per mole of compound.

It is worthwhile to consider the significance of ρ_0. According to (III-10) a positive value of ρ_0 corresponds to a positive excess free energy of mixing and signifies that mixing between unlike components is energetically unfavorable. A negative value of ρ_0 implies the reverse. Thus the large negative value of ρ_0 for the mixing of chlorophyll a and DSPC in the compound phase indicates the mixing is extremely favorable, most likely as a result of a specific chemical interaction between them. It is tempting to extract the strength of this interaction from the values of ρ_0 obtained for the solution and compound phases, although the necessary assumptions for such an analysis make it a useful approximation only. The Wilson equation[24] relates the excess free energy to the pair-wise interaction energies (g_{AB}, g_{AA} and g_{BB}) according to

$$\frac{G^e}{RT} = X_A \ln(1 - A_{BA} X_B) - X_B \ln(1 - A_{AB} X_A) \qquad \text{(III-15)}$$

where

$$A_{BA} = 1 - \frac{\bar{V}_B}{\bar{V}_A} \exp -\left[\frac{(g_{AB} - g_{BB})}{kT} \right] \qquad \text{(III-15a)}$$

$$A_{AB} = 1 - \frac{\bar{V}_A}{\bar{V}_B} \exp -\left[\frac{(g_{AB} - g_{AA})}{kT} \right] . \qquad \text{(III-15b)}$$

If we make the assumption that the molecular volumes of chlorophyll a and DSPC in the bilayer are the same (equivalent to a regular solution approximation), then for $X_A = X_B = 0.5$ (corresponding to 20 mole percent chlorophyll a) equation (III-15) reduces to

$$\frac{G^e}{RT} = \frac{g_{AB} - \frac{1}{2}(g_{AA} + g_{BB})}{RT} . \qquad \text{(III-16)}$$

Since we previously expressed the excess free energy as $X_A X_B \rho_0$, we obtain

$$\frac{\rho_0}{4} = g_{AB} - \tfrac{1}{2}(g_{AA} + g_{BB}) . \qquad \text{(III-17)}$$

The quantity $\frac{1}{2}(g_{AA} + g_{BB})$ cannot be determined explicitly, but if we assume that it is independent of the phase state then it can be treated as a reference state energy. We could then determine the net interaction energy of the compound by comparing the values of g_{AB} obtained for the solution and compound phases. This results in a value of -2.8 kcal/mole for the interaction energy between a chlorophyll a and DSPC molecule in the compound phase. This must indicate that the

compound is fairly stable with a dissociation constant at 50° of about 10^{-2} mole-liter^{-1}.

2. Phase separation

The phase diagram predicts that under certain conditions there is phase separation, that is to say there are thermodynamically distinct phases in equilibrium. The phase diagram cannot, however, provide information about the spatial separation of the two phases within the plane of the membrane. The width of the DTA transitions provides evidence that the degree of intermixing is not great.

The width of the DTA transition is related to the size of a cooperative unit which is influenced by the presence of impurities. In the present case we consider the presence of one phase in another to be analogous to an impurity. The width of a transition can be related to the mole fraction of impurities X_2 according to

$$\Delta T_{\frac{1}{2}} = (9.5) \frac{RT_A^2}{\Delta H_A} X_2 \qquad \text{(III-18)}$$

where $\Delta T_{\frac{1}{2}}$ is the measured width of the transition peak at half-height, T_A and ΔH_A are the transition temperature and enthalpy. (Equation (III-18) is derived from an analogous expression[25] which assumes ideal mixing between phases.) Using values for ΔH_A and T_A from Figure III-6 and $\Delta T_{\frac{1}{2}}$ from Figure III-2, we obtain for 20 mole% chlorophyll a: $X_2 = 0.024$ for the upper transition, $X_2 = 0.057$ for the lower transition. These values indicate very little interprenetation of the phases, particularly if chlorophyll a in the DSPC solid solution is also

considered as an impurity.

Alternatively, the van 't Hoff enthalpy can be obtained from the measured transition width:

$$\Delta H_{vH} = 6.9 \frac{T_A^2}{\Delta T_{\frac{1}{2}}} \qquad \text{(III-19)}$$

and this in turn related to the cooperative unit size N by

$$\frac{\Delta H_{vH}}{\Delta H_{cal}} = N, \qquad \text{(III-20)}$$

where ΔH_{cal} is the measured calorimetric enthalpy and ΔH_{vH} is determined from (III-19). This yields the results N = 15.2 for the upper transition and N = 6.4 for the lower. Assuming that one impurity provides the nucleation site for each cooperative unit, the mole fraction of impurities is equal to 1/N and the two analyses agree within reason.

The thermodynamic and spatial separation of phases containing chlorophyll a implies that the distribution of chlorophyll a molecules within the membrane is not homogeneous. Therefore any property or process which depends on the separation between chlorophylls (e.g., energy transfer) will be affected.

E. CONCLUSIONS

The phase diagram obtained for the chlorophyll a/DSPC multilamellar system suggests a number of significant conclusions regarding the properties of chlorophyll a in a phospholipid bilayer matrix:

1) Its phase behavior, or in other words its organization and intermolecular interactions, can be much different depending on the temperature and composition of the system. 2) Phase separation can occur within the membrane over certain temperature ranges resulting in an inhomogeneous system. 3) Chlorophyll a can interact with phospholipids to give a compound phase of defined stoichiometry. We believe these results are applicable as well to other membrane systems containing chlorophyll a.

From the previous studies we see that the normal phase behavior of a membrane can be altered by the inclusion of chlorophyll a. This effect can be pronounced at higher chlorophyll compositions, although for very low chlorophyll concentrations the bulk phases are not substantially different from those of the pure-lipid membrane. Thus chlorophyll a can be used as a non-perturbing probe of the properties of the membrane as, for example, in the fluorescence studies of Lee, but only when used in very small amounts. At chlorophyll a compositions of more than a few mole percent, the membrane begins to acquire a character which reflects the influence of chlorophyll a. Depending on temperature and composition, the phase state of the membrane and the organization of chlorophyll a can vary substantially. Consider the phase changes with temperature of three different compositions as an illustration. At low chlorophyll a concentrations, say 4 mole percent, chlorophyll a is in a liquid solution phase of DSPC above 58°, phase separated into liquid solution and solid solution DSPC/chlorophyll a phases between 56-58°, and in a solid solution exclusively below 56°.

At medium chlorophyll a concentrations, say 20 mole percent, chlorophyll a is again in a solution phase above 55° and phase separated into liquid solution and solid solution phases between 50-55°, but forms a compound phase below 50°. At even higher chlorophyll a compositions, above about 32 mole percent, compound is formed at all temperatures below the liquidus and is the predominant chlorophyll containing phase below 50°.

In interpreting the physical and spectroscopic properties of chlorophyll a in a bilayer membrane, it is essential to consider the phase state of the membrane and the organization and environment of chlorophyll in the particular phase. Subsequent studies of the chlorophyll a/DSPC system will be devoted to considering the properties of chlorophyll a in the various phases and to assessing the relative importance of environment, ligation and ordering of chlorophyll in determining these properties.

REFERENCES - CHAPTER III

1. A. Mehreteab and G. Strauss, Photochem. Photobiol., 28, 369-375 (1978).
2. K. Colbow, Biochim. Biophys. Acta, 314, 320-327 (1973).
3. M. Tomkiewicz and G. A. Corker, Photochem. Photobiol., 22, 249-256 (1975).
4. P. Nicholls, J. West, and A. D. Bangham, Biochim. Biophys. Acta, 363, 190-201 (1974).
5. W. Oettmeier, J. R. Norris, and J. J. Katz, Z. Naturforsch., 31c, 163-168 (1976).
6. F. Podo, J. E. Cain, and J. K. Blasie, Biochim. Biophys. Acta, 419, 19-41 (1976).
7. K. Colbow, Biochim. Biophys. Acta, 318, 4-9 (1973).
8. H. Dijkmans, R. M. LeBlanc, F. Cogniaux, and J. Aghion, Photochem. Photobiol., 29, 367-372 (1979).
9. W. Oettmeier, J. R. Norris, and J. J. Katz, Biochem. Biophys. Res. Comm., 71, 445-451 (1976).
10. A. Steinemann, G. Stark, and P. Läuger, J. Membrane Biol., 9, 177-194 (1972).
11. A. G. Lee, Biochemistry, 14, 4397-4402 (1975).
12. E. Ritt and D. Walz, J. Membrane Biol., 27, 41-54 (1976).
13. K. Iriyama, N. Ogura, and A. Takamiya, J. Biochem., 76, 901-904 (1974).
14. H. H. Strain, M. R. Thomas, H. L. Crespi, M. I. Blake, and J. J. Katz, Ann. New York Acad. Sci., 84, 617-666 (1960).

REFERENCES (continued)

15. H. H. Strain, M. R. Thomas, and J. J. Katz, Biochim. Biophys. Acta, 75, 306-311 (1963).

16. G. R. Seely and R. G. Jensen, Spectrochimica Acta, 21, 1835-1845 (1965).

17. H. T. Smyth, J. Am. Ceram. Soc., 34, 221-224 (1951).

18. P. Gordon, Principles of Phase Diagrams in Materials Systems, McGraw-Hill, New York, 1968, pp. 186-191.

19. A. G. Lee, Biochim. Biophys. Acta, 507, 433-444 (1978).

20. A. G. Lee, Biochim. Biophys. Acta, 472, 285-344 (1977).

21. C. A. Eckert, in Solutions and Solubilities, (M. R. J. Dack, ed.), Part II, Wiley, New York, 1976.

22. H. J. Hinz and J. M. Sturtevant, J. Biol. Chem., 247, 6071-6075 (1972).

23. M. C. Phillips, R. M. Williams, and D. Chapman, Chem. Phys. Lipids, 3, 234-244 (1969).

24. G. M. Wilson, J. Am. Chem. Soc., 86, 127-130 (1964).

25. N. Albon and J. M. Sturtevant, Proc. Natl. Acad. Sci. USA, 75, 2258-2260 (1978).

CHAPTER IV

Interactions of Chlorophyll a with Phospholipids in Bilayer Membranes - Studies of the Intermolecular Interactions by Nuclear Magnetic Resonance

A. INTRODUCTION

Compared to the considerable amount of available information concerning the interactions of chlorophylls with other molecules in three-dimensional solutions, relatively little is known about the intermolecular interactions of chlorophyll within surface films and bilayer membranes. Such interactions are significant since to a large degree they determine the properties of chlorophyll which is confined to a lamellar matrix as it may be in model and *in vivo* photosynthetic membranes. Previously we considered the thermodynamic properties and phase diagram of chlorophyll *a*/DSPC bilayer membranes. Now we will consider in more detail the organization of chlorophyll *a* within the various regions of the phase diagram with the goal of ascertaining the molecular basis behind this interesting and unusual phase behavior. In particular, we wish to verify the thermodynamic phase separation within the predicted two-phase regions, and to determine the intermolecular interactions responsible for the observed compound formation between chlorophyll *a* and lipid.

The studies described here rely on nuclear magnetic resonance (NMR) techniques which can provide information on both membrane

structure and dynamics. Chlorophyll a is particularly suited to NMR studies by virtue of its ring current effect on the chemical shifts of nearby nuclei. In addition to the ring current effect, which provides structural and orientational information, linewidth and relaxation measurements can be used to study changes in the dynamics of the host membrane through the various phase transitions.

1. Structural aspects of chlorophyll-lipid interactions

Based on structural and chemical considerations, one might initially expect chlorophyll a to be surface-active and to associate with lipid membranes. Figure IV-1 compares the structures and relative dimensions of chlorophyll a and DSPC, a typical phospholipid with two saturated 18-carbon fatty acyl chains similar in length to the phytol chains of chlorophyll a. In both molecules, an interface between hydrophobic chains and hydrophilic headgroups imparts an amphiphilic character which causes them to be surface active and to form aggregates in aqueous solution by virtue of the so-called hydrophobic effect.[1] The tendency of pure phospholipids such as DSPC to self-associate into aggregated lipid bilayers is well known and has been extensively studied. Although chlorophyll a can form monolayers at an air-water interface,[2,3] it cannot by itself form bilayer membranes. However, it has previously been established that in conjunction with other lipids chlorophyll a can form black lipid films,[4,5] multilayers and small unilamellar vesciles.[6-10] In a manner of speaking, the chlorophyll phytol group can apparently serve as a lipophilic anchor binding chlorophyll to the host membrane.

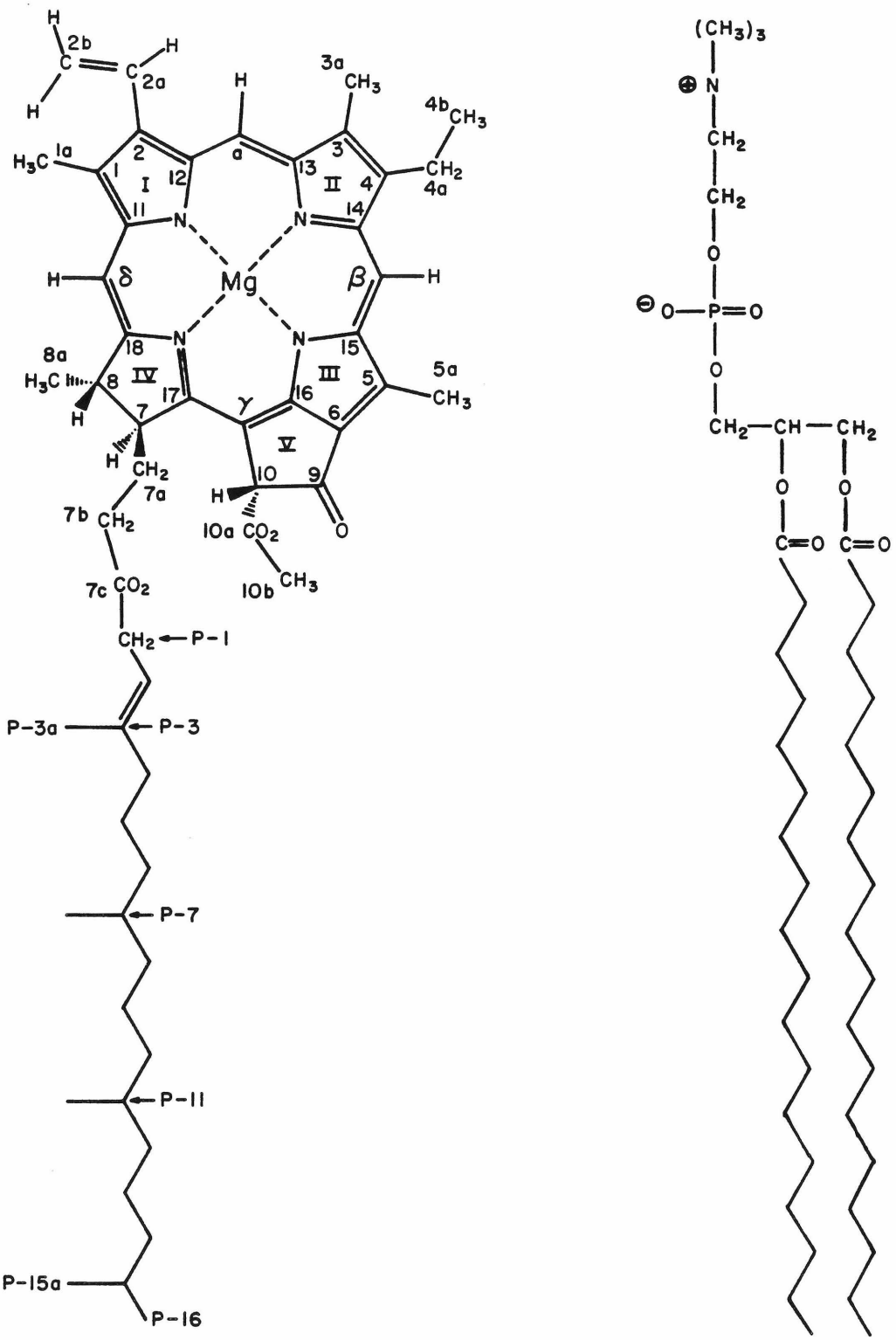

FIGURE IV-1. Chemical structures of chlorophyll a (left) and DSPC, distearoyl phosphatidylcholine (right).

In addition to the phytol chain there are two other features of chlorophyll a which are potentially important in determining its interactions with other lipid molecules. First, the central magnesium atom of chlorophyll is coordinatively unsaturated in the porphyrin tetrapyrrole system[11-14] and has always been observed to be complexed to one and sometimes two nucleophilic axial ligands. This coordination requirement must also be satisfied in the bilayer. Second, the β-keto ester of ring V could provide a means of hydrogen bonding via intervening water molecules between chlorophyll a and similar acyl carbonyls on nearby lipid molecules.[15]

2. Chlorophyll ring current effects

When chlorophyll is placed in a magnetic field, the induced current in the aromatic π-system of electrons produces a large anisotropy in magnetic shielding about the porphyrin macrocyle. This ring current effect causes the resonance positions of nearby nuclei to be shifted upfield or downfield depending on the distance and azimuthal angle with respect to the porphyrin plane. Exact solutions for the magnitude of ring current shifts are difficult because of the complexity of the current loops in the porphyrin macrocycle. We have chosen to use the approximate empirical expression of Shulman et al.[16] which is nearly accurate for distances greater than 3 angstroms. Figure IV-2 illustrates the chlorophyll shift map calculated according to this formula.

The ring current shift effect has been used to good advantage in studies of the interaction between chlorophyll a and other molecules

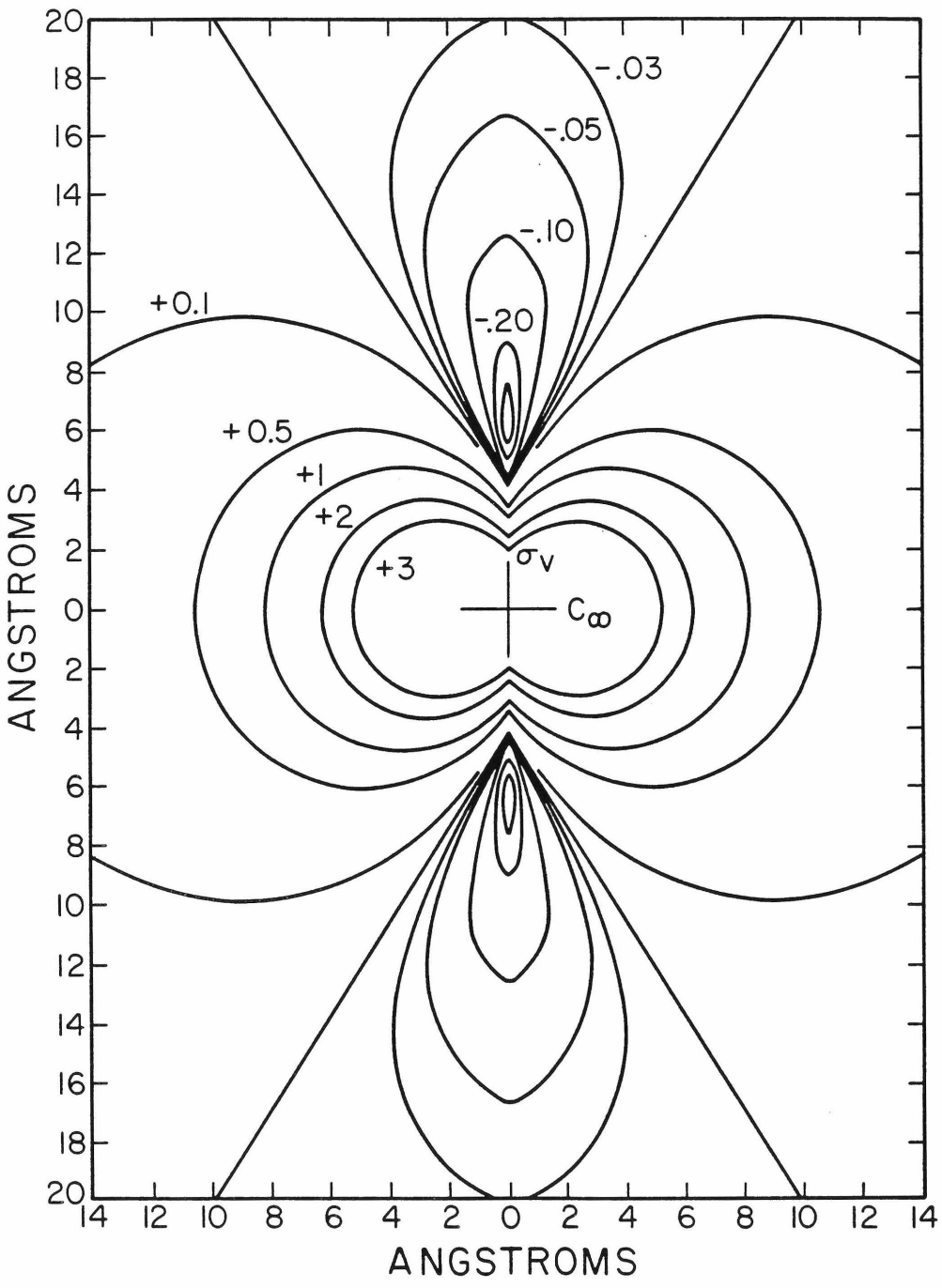

FIGURE IV-2. Ring current shift map of chlorophyll a calculated according to the empirical expression of Shulman et al.[16] (iso-shielding lines labeled in parts per million). The porphyrin plane lies on a vertical plane perpendicular to the page (σ_v) and is assumed to have rotational symmetry about C_∞ and reflection symmetry through σ_v.

in solution.[11,12,14] In these studies the measured ring current shifts are used to deduce the orientation of interacting molecules with respect to the porphyrin plane. Since the magnitude of the observed ring current shift decreases as the cube of the distance to the center of the porphyrin plane, only molecules immediately adjacent to chlorophyll are affected. Inasmuch as solution molecules spend only a small fraction of time near the porphyrin they experience only a small net upfield shift. Thus only molecules actually bound to chlorophyll as long-lived complexes will exhibit significant ring current shifts.

The interactions of chlorophyll with molecules in a bilayer phase can also be studied using the ring current effect. Figure IV-3 shows qualitatively how the upfield and downfield shift regions are distributed about a chlorophyll a molecule and suggests how the orientations of neighboring lipid molecules could be determined. We have exploited such ring current shift effects in the following experiments.

B. MATERIALS AND METHODS

Chlorophyll a was isolated from spinach by techniques cited in the previous paper. Molar extinction coefficients at 660 nm and 428 nm were measured in diethyl ether and indicate that the purified chlorophyll a is substantially free of impurities. Synthetic β-γ-distearoyl-L-α-phosphatidylcholine (DSPC) was purchased from Calbiochem, checked for impurities by thin layer chromatography, and used without further purification.

Small unilamellar vesicles were prepared by sonication. Weighed

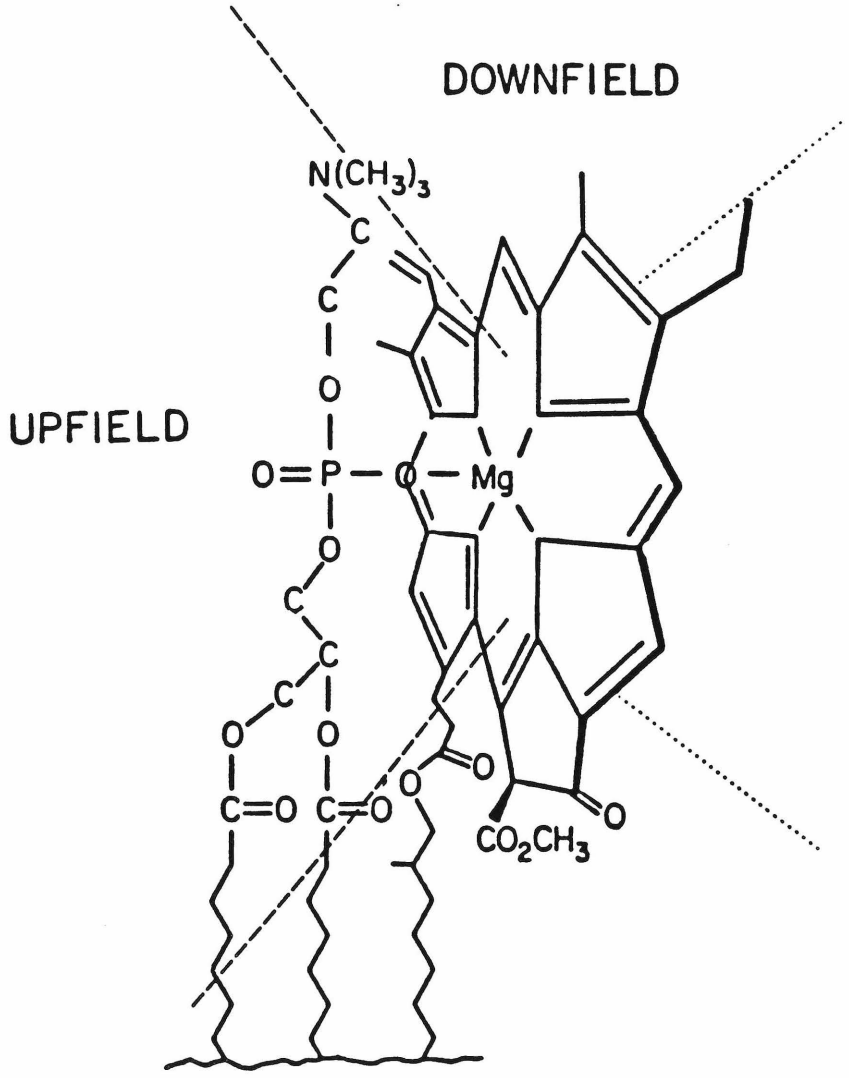

FIGURE IV-3. The effect of the chlorophyll a ring current diamagnetic anisotropy on the chemical shifts of a neighboring lipid molecule. Resonance positions of nuclei positioned above the face of the porphyrin macrocycle are shifted upfield by an amount (given in Figure IV-3) which depends on the distance from, and angle with respect to, the porphyrin plane. Nuclei positioned about the peripheral edge of the porphyrin would be shifted downfield.

amounts of chlorophyll a and DSPC were dissolved together in fresh chloroform in order to assure their complete mixing. The chloroform solutions of chlorophyll a and DSPC were evaporated by a stream of nitrogen gas and residual solvent was completely removed under vacuum. The dried chlorophyll a/DSPC film was then suspended in an appropriate volume of 99.8%-d $^{2}H_{2}O$ by a vortex mixer. The resulting multilayer suspension was transferred to a centrifuge cone and sonicated with a Heat Systems-Ultrasonics, Inc. model W-225R cell disruptor using a stepped microtip and the highest possible power setting in order to minimize the sonication time. Best results were obtained by continuous sonication for 3 minutes in a cool glycerol bath followed by 10 minutes of sonication on a 50% duty cycle with the glycerol bath removed so as to allow the temperature to rise slightly above the bilayer phase transition of about 55° C. The solution was then centrifuged to remove titanium particles eroded from the sonicator tip and also small, usually negligible, amounts of large bilayer structures. We have found that the foregoing procedure produces a uniform population of small vesicles whose average size, determined by gel permeation chromatography on Sepharose 4B, does not change with further sonication.

NMR experiments were performed on vesicle solutions which had been hydrated and sonicated just prior to their use. The solution concentrations were 30 milligrams of lipid (chlorophyll a + DSPC) per milliliter for ^{31}P experiments, and 10 mg/ml for the ^{1}H experiments. We are confident that the vesicle suspensions were stable during the

course of our experiments for the following reasons: 1) the solutions remain optically clear at the end of experiments, 2) vesicle spectra are easily distinguished from multilayer spectra which give noticeably broadened bulk-methylene resonances, and 3) all spectral changes are fully reversible.

^{31}P spectra at 40.5 MHz and ^{1}H-NMR spectra at 100 MHz were obtained on Varian XL-100 spectrometers using standard Fourier transform techniques. Sample temperatures were regulated by Varian temperature controllers which had been previously calibrated with a thermocouple. ^{31}P spectra were proton-decoupled by continuous broadband irradiation over the range of proton frequencies. 360 MHz ^{1}H-NMR spectra were obtained at the Stanford Magnetic Resonance Laboratory on a Bruker HXS-360 spectrometer. The Bruker temperature controller was calibrated prior to each set of experiments by measuring the frequency difference between the resonances of ethylene glycol at several temperatures. Temperatures quoted within the results section can be considered to be accurate to within about one degree centrigrade.

C. RESULTS AND DISCUSSION

The results of the present NMR studies on the chlorophyll a/DSPC bilayer system are best interpreted in terms of the phase diagram. The thermal phase diagram which was previously obtained (see Figure III-3) suggests a number of interesting conclusions regarding the differences in intermolecular interactions between chlorophyll a

and phospholipid at high and low temperatures. At high temperatures the phase diagram indicates that chlorophyll a and DSPC form a single-phase solution within the bilayer. However, below a thermal phase transition temperature of about 50° C, the phase diagram predicts that both chlorophyll a and DSPC are present in two distinct phases. One of these phases should consist of a solid solution while the other was thought to be an inter-lipid compound phase formed by some specific chemical interaction between chlorophyll a and DSPC. These conclusions are supported by the following NMR experiments. The results also provide some insight into the intermolecular interaction responsible for the formation of the compound.

1. ^{31}P-NMR

Figure IV-4 shows 40.5 MHz ^{31}P-NMR spectra of a 20% chlorophyll a/DSPC vesicle suspension at two different temperatures corresponding to the two different regions of the phase diagram. The spectrum at 57°, in the one-phase homogeneous solution region of the phase diagram, does indeed show a single phospholipid resonance. At 46°, corresponding to the two-phase compound region below the solidus, there are two phospholipid resonances observed. One of these two peaks has a chemical shift nearly the same as that of the single peak obtained in the higher temperature spectrum, whereas the second, additional peak is shifted 5.8 ppm upfield. The observation of two peaks in the 46° spectrum conclusively demonstrates that phase separation occurs at temperatures below the solidus of the phase diagram.

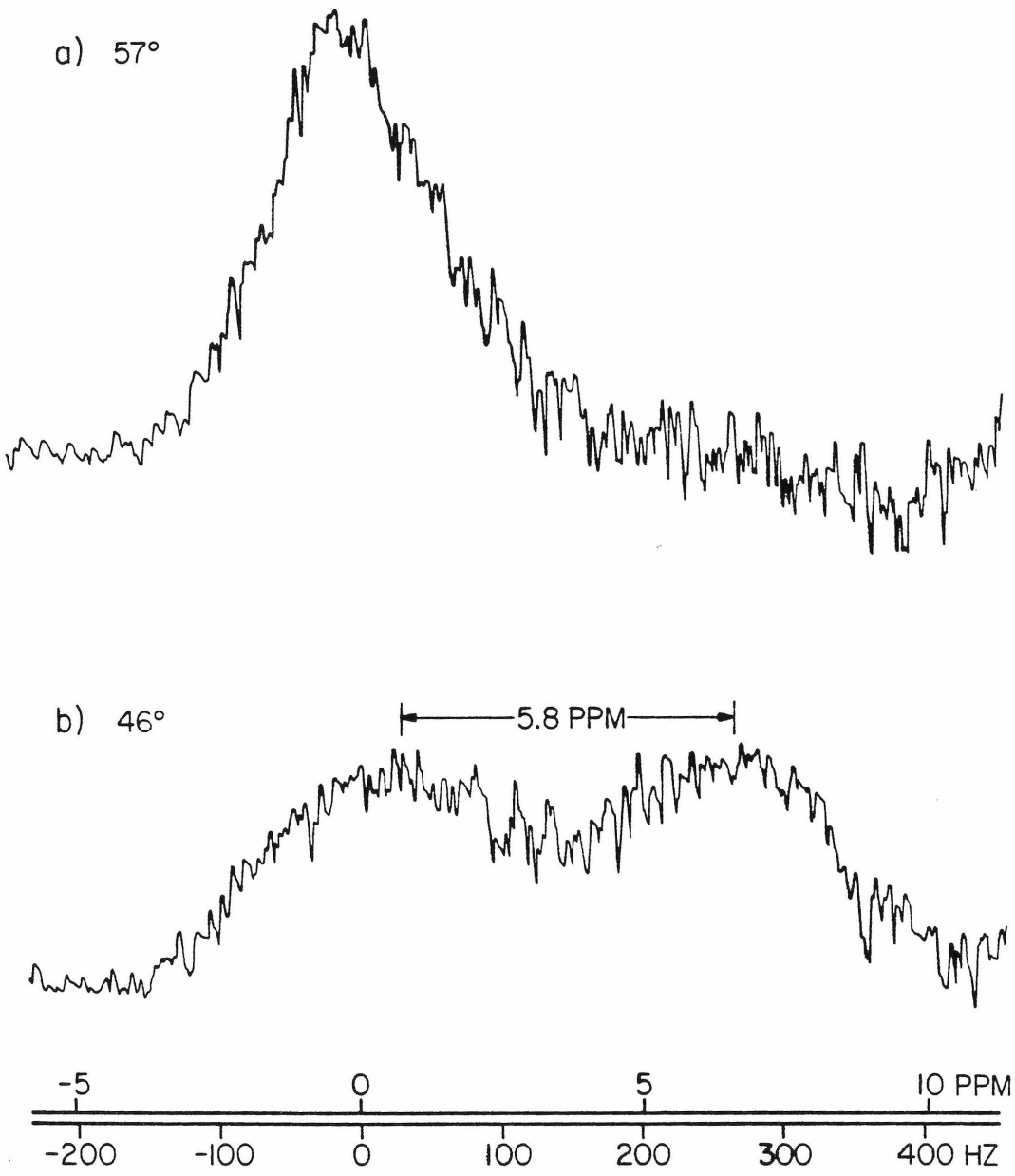

FIGURE IV-4. Proton decoupled ^{31}P-NMR spectra at 40.5 MHz of sonicated 20% chlorophyll a/DSPC single-walled bilayer vesicles at 57° (top) and 46° (bottom). At 57° the membranes are in the solution region of the phase diagram. At 46° the phase diagram predicts phase separation into solid DSPC and compound phases.

The additional resonance in the 46° spectrum must presumably correspond to phospholipid of the compound phase shifted upfield by the ring current effect of an adjacent chlorophyll molecule. An upfield shift of this magnitude would require the phosphate moiety of the DSPC molecule to be located close to and directly over the face of the chlorophyll a porphyrin macrocycle as in Figure IV-3. Assuming that the only source of shift is the ring current magnetic anisotropy of chlorophyll a, and presupposing that the phosphorus of DSPC is perpendicular to the central magnesium atom of chlorophyll, the observed 5.8 ppm upfield shift would correspond to a phosphorus to magnesium distance of 3.4 angstroms. A shift of the same magnitude could also be produced by a smaller angle and a correspondingly shorter distance, but a deviation of more than 30° from the perpendicular direction would necessitate an unreasonably small distance, less than the sum of the P, O and Mg covalent radii. Thus we conclude that the phosphorus atom of the compound phase DSPC molecule probably lies within 30° of a perpendicular to the central magnesium atom of chlorophyll a and is no more than 3.4 angstroms away.

The observation of two resonances in the 46° spectrum suggests that the rate of exchange of DSPC molecules between the compound-phase and solution-phase environments is slow. If the chemical exchange was faster than the timescale set by the static chemical shift differences between the two environments, then a single unresolved resonance would be observed. The condition for coalescence of two peaks in chemical exchange is given[17] by $K_{exchange} = 2\pi \Delta\nu/\sqrt{2}$,

from which we may calculate an upper bound for the exchange rate of DSPC between compound and solution phases of less than 1000 sec^{-1}.

The observed ^{31}P linewidths of about 150-200 Hz are substantially larger than the 50 Hz linewidth normally obtained in spectra of pure DSPC vesicles. This could be explained by exchange broadening in the 46° spectrum, although the resonance linewidth of the single peak in the 57° solution spectrum is nearly as large. A more likely explanation is that the inclusion of chlorophyll a into the bilayer disrupts the normal intermolecular headgroup interactions of pure DSPC bilayers.

2. ^{1}H-NMR

Proton spectra of chlorophyll a/DSPC vesicles at several compositions were obtained as a function of temperature at 100 MHz and 360 MHz. The spectra shown in Figure IV-5 are typical. These and all other proton spectra are prosaic by contrast with the ^{31}P spectra at first sight, but upon closer scrutiny they reveal useful information. Because of the rigidity of the chlorophyll a porphyrin macrocycle and the additional motional restriction imposed by binding chlorophyll a to the membrane, no porphyrin resonances contribute to the high resolution spectra. Phytol methyl and methylene resonances do contribute to the spectrum however. This can be seen by comparing the methyl and methylene intensities in a series of spectra of different chlorophyll a compositions as shown in Figure IV-6. Since chlorophyll a has comparatively more methyl groups than does DSPC, increasing its content relative to DSPC increases the methyl to methylene ratio. Other than this difference and some subtle changes in linewidths,

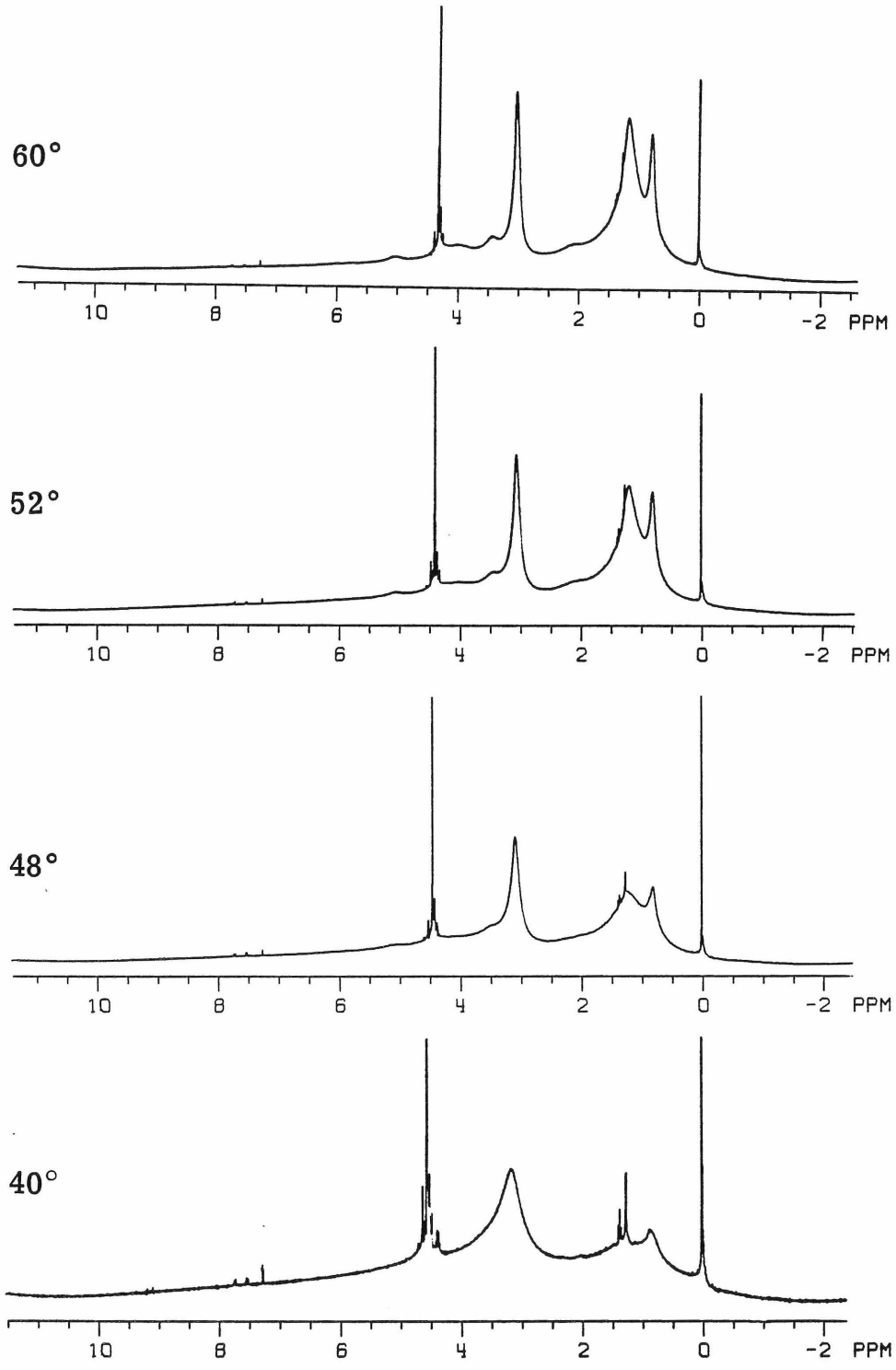

FIGURE IV-5. Proton NMR spectra of 15% chlorophyll a/DSPC vesicles at selected temperatures. The sharp resonance at 0 ppm (TMS) and other low intensity sharp resonances are from the reference capillary.

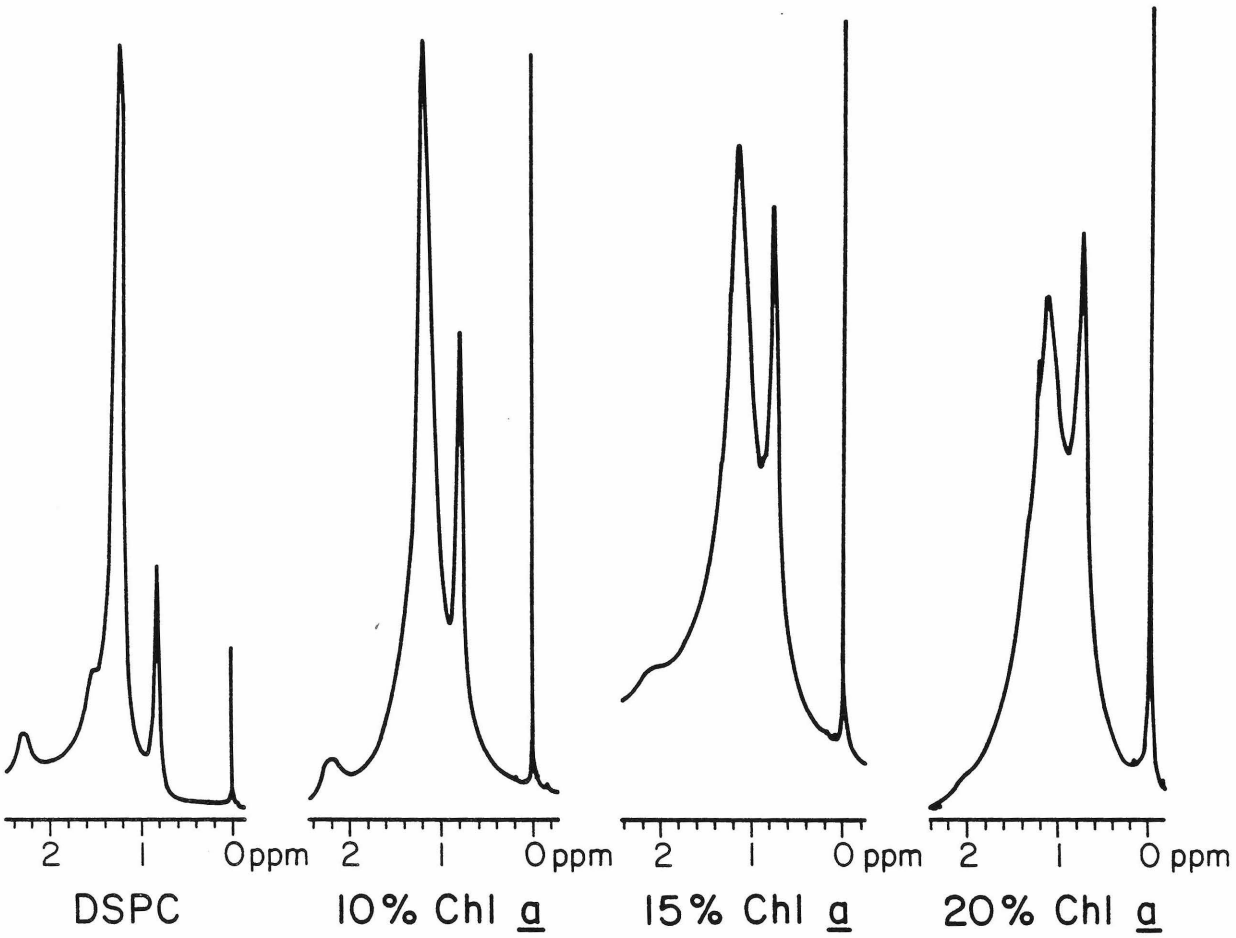

FIGURE IV-6. Proton NMR spectra of chlorophyll a/DSPC sonicated vesicles at 0, 10, 15, and 20 mole percent chlorophyll a in the methyl and methylene region.

the spectra are virtually indistinguishable from pure phospholipid vesicle spectra.

In contrast to the ^{31}P spectra, which show clear evidence of two classes of phospholipid below the solidus, the ^{1}H spectra show only a single choline N-methyl resonance over a temperature range encompassing all regions of the phase diagram. It cannot be determined whether other proton resonances are split at lower temperatures since they become obscured by broadened choline N-methyl and chain methylene resonances. The observation of a single choline peak implies that the difference in the chemical shifts of the choline N-methyl resonances of lipids in the compound and solution phases is small. The manifestation of this chemical shift difference will actually depend on the rate of exchange between the two environments. If exchange is slow on the NMR timescale then the single observed resonance must be a superposition of two lines separated by less than the resonance linewidth, about 100 Hz or less than 0.3 ppm. On the other hand, if exchange is fast, i.e., $K_{exchange} > 2\pi \Delta\nu/\sqrt{2}$, then the observed resonance represents a dynamic exchange-averaged resonance intermediate between two static resonances separated by no more than $\sqrt{2}/2\pi$ times the exchange rate. From the upper bound for the exchange rate of 1000 sec^{-1} obtained from the ^{31}P spectrum, we can estimate that the chemical shift difference could be no greater than 230 Hz, or about 0.6 ppm.

The chemical shift of the choline N-methyl resonance is temperature dependent and can be correlated with the predicted phase changes.

Figure IV-7 shows these resonance positions referenced to external TMS in C^2HCl_3 at 100 MHz and 360 MHz. Inasmuch as the shifts in Figure IV-7 are referenced to an external standard, corrections must be made for changes in bulk susceptibility with temperature. This is easily accomplished by making use of the fact that the change in bulk susceptibility is approximately linear over small temperature ranges,[18] and is opposite in sign and twice the magnitude for solenoid versus electromagnet field/sample geometries.[19] Making the necessary corrections, we obtain the corrected data of Figure IV-8. These data show a small shift in the peak position of the choline N-methyl resonance as the temperature is raised and a complete bilayer solution is formed between chlorophyll a and the lipid. This upfield shift is analogous to an aromatic solvent shift[20] resulting from the dissolution of a molecule into an aromatic solvent capable of producing a ring current shift which does not spatially average to zero.

The proton linewidths are also correlated with the predicted phase changes. Figure IV-9 shows the measured linewidths of two lipid resonances from 20% chlorophyll a/DSPC vesicles. There is an abrupt change in the linewidth of the choline N-methyl resonance at about 49°, corresponding approximately to the solidus of the phase diagram where compound is formed from the solution phase. The methylene resonance begins to broaden at a somewhat higher temperature, corresponding to the liquidus of the phase diagram, with a further break at the solidus. These changes all occur upon formation or elimination of a phase at a boundary of the phase diagram and

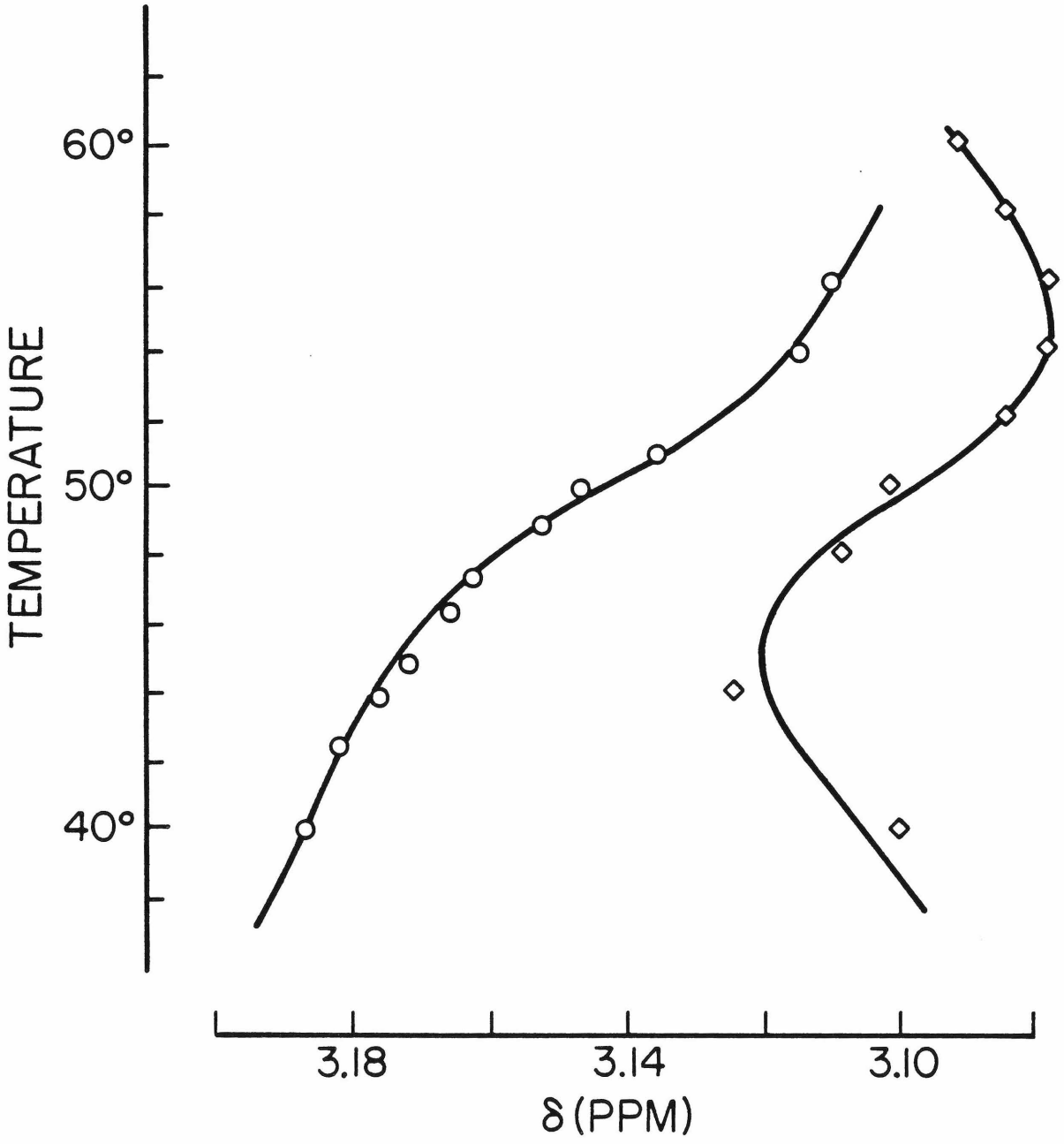

FIGURE IV-7. Chemical shift of the DSPC choline N-methyl proton resonance (referenced to TMS) from 20% chlorophyll a/DSPC sonicated vesicles as a function of temperature. Open circles: 360 MHz superconducting solenoid spectrometer. Open squares: 100 MHz electromagnet spectrometer.

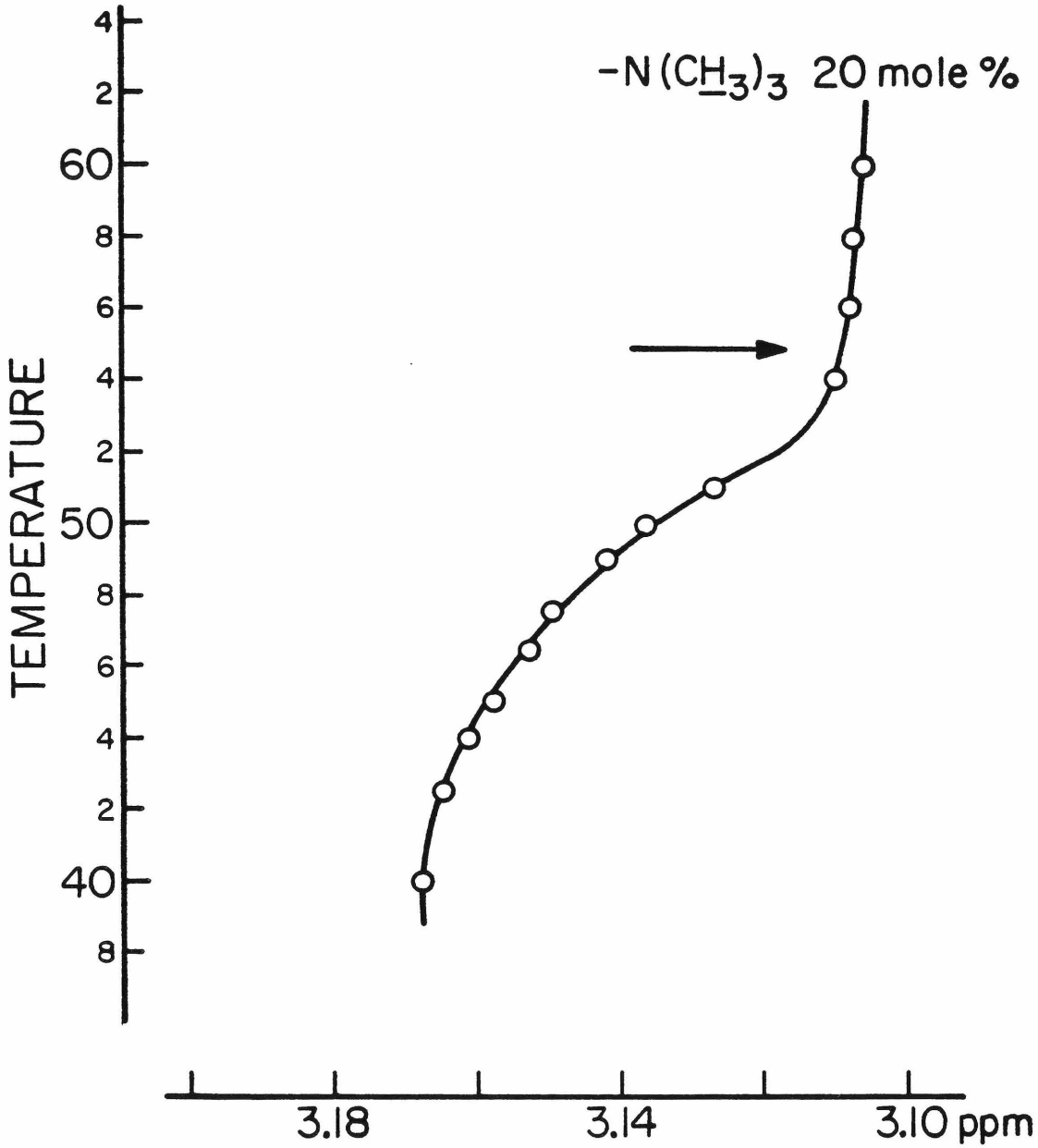

FIGURE IV-8. Data of Figure IV-7 corrected for changes in the solvent bulk magnetic susceptibility with temperature. The arrow indicates the liquidus phase transition temperature.

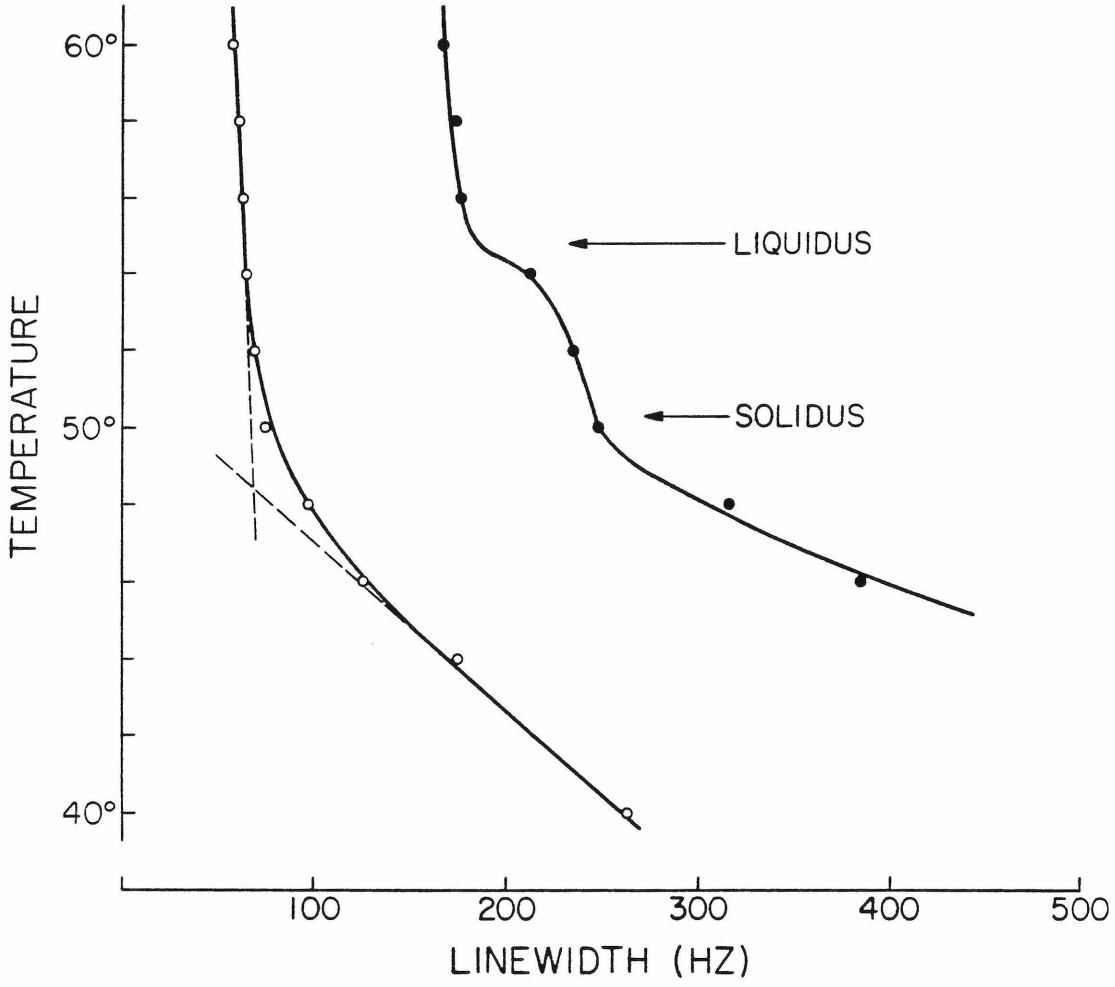

FIGURE IV-9. Linewidths at half height of the choline methyl (open circles, left) and bulk fatty acid methylene (closed circles, right) lipid resonances from 20% chlorophyll a/DSPC vesicles as a function of temperature. The liquidus and solidus temperatures at this composition are indicated by arrows. These data were obtained from spectra at 360 MHz.

correspond to changes in the motional state of the lipids. The linewidth of the methylene resonance changes at points where lipid is transformed from gel to liquid crystalline forms which influences the motional state of the hydrocarbon chains. The break in the choline N-methyl resonance linewidth at the solidus implicates the lipid headgroup in the transformation between compound and solution phases. This is significant in deducing the nature of the compound phase.

Such a conclusion can also be reached by examining the spin-lattice relaxation times of pure DSPC vesicles and chlorophyll a/DSPC vesicles. Values of T_1 obtained at 360 MHz by the inversion recovery technique are given in Figure IV-10. These data indicate that T_1 of the choline N-methyl proton resonance is unaffected by increasing amounts of chlorophyll a when the temperature is 60°. This is consistent with the phase diagram in that at 60° all compositions are in a similar solution phase. In contrast to the situation at 60°, the T_1 data at 48° show a substantial increase with increasing chlorophyll a content. This too is consistent with the phase diagram. Below 50° the phase diagram predicts that the 15% chlorophyll a composition should contain 90% of the DSPC in the solution phase and only 10% in the compound phase. Thus the T_1 value for 15% chlorophyll a, which is only slightly higher than for pure DSPC, indicates that the relaxation rate in the solution phase is similar to that of DSPC. On the other hand, the 32% chlorophyll a composition should consist of 65% compound phase DSPC, and the larger T_1 value indicates that T_1 for the compound phase is much longer. Simultaneous equations can be solved

FIGURE IV-10. Table of T_1 relaxation times (in seconds) of the choline N-methyl protons.

COMPOSITION	48°	60°
DSPC	0.36 (± 0.13)	0.41 (± 0.02)
15% Chlorophyll *a*	0.49 (± 0.21)	0.51 (± 0.10)
32% Chlorophyll *a*	0.91 (± 0.07)	0.44 (± 0.15)

to determine that a pure compound phase should have T_1 = 1.2 seconds. This must indicate that the lipid headgroup is relatively restricted in the compound.

D. CONCLUSIONS

The NMR studies presented here support the basic interpretation of the phase diagram for the chlorophyll a/DSPC bilayer system which was advanced in the preceding report. They confirm that there is a homogeneous population of phospholipid in the solution region of the phase diagram, whereas below the solidus there is clear evidence of the predicted phase separation. In addition they provide strong evidence for an interaction between the DSPC headgroup and chlorophyll a in the compound phase, which in all likelihood involves a coordination interaction between the DSPC phosphate and central magnesium atom of chlorophyll.

Evidence for a specific interaction between chlorophyll a and DSPC comes in two parts: first, the magnitude of the ^{31}P ring current shift, and second, linewidth and relaxation rate measurements of the choline N-methyl resonance. The linewidth change at the solidus temperature and the longer T_1 for the choline N-methyl resonance indicate that the headgroups of DSPC molecules involved in the compound phase are motionally restricted. This conclusion is also supported by the ^{31}P results which suggest that in the compound the phosphate of DSPC is situated sufficiently close to chlorophyll a, and remains there on a long enough timescale to produce a slow-

exchange spectrum and yield a substantial upfield shift. The magnitude of this shift indicates that the phosphorus nucleus of the DSPC molecule is probably no more than 3.4 angstroms away from the central magnesium atom of chlorophyll a. The presence of this phosphate group would necessarily preclude any other axial ligand to chlorophyll a, and indeed it is likely that the nucleophilic phosphate is itself the axial ligand. Subtracting from 3.4 angstroms the phosphate P-O bond distance of 1.5 angstroms leaves about 2.0 angstroms for the distance between oxygen and magnesium. This is considerably less than the sum of their van der Waals radii and is more on the order of the sum of their ionic radii. Hence we conclude that in the compound phase the obligatory requirement of chlorophyll a for a nucleophilic axial ligand is satisfied by the phosphate of an adjacent lipid molecule.

Interactions between lipid molecules and chlorophyll a in solution have been inferred from optical spectra,[21,22] but to our knowledge the present studies are the first conclusive evidence that such interactions can occur within a lipid bilayer membrane. The observation of a compound formed between chlorophyll a and a lipid molecule lends considerable support to the proposal of Beddard and Porter[23] that chlorophyll molecules in the chloroplast antenna are physically separated from each other by strongly coordinating lipid molecules. This separation is necessary to prevent the formation of excitation traps from orbital overlap of two chlorophyll molecules. While phospholipids are only a minor constituent of chloroplast membranes, other lipid molecules could provide similar nucleophilic ligands.

For example, the strong interaction of chlorophyll with alcohols suggests that galactolipids could coordinate with chlorophyll perhaps even more strongly than with phospholipids. In addition to serving as a means of separation, the interaction of chlorophyll a with lipid molecules could provide a means of ordering chlorophyll within the membrane. It is therefore interesting to note that a large portion of in vivo chlorophyll a is oriented with respect to the thylakoid membrane in a way which is consistent with its known orientation in model membranes. The ordering of chlorophyll within the membrane has important consequences with respect to its optical properties. This effect will be discussed in a future communication. There is as yet no conclusive proof as to whether or not chlorophyll a - lipid interactions such as we have observed actually occur in vivo, although we have recently found (manuscript in preparation) that there is a population of chlorophyll in thylakoids with a motional state quite similar to that of the lipids.

REFERENCES - CHAPTER IV

1. C. Tanford, The Hydrophobic Effect, Wiley, New York, 1973
2. G. L. Gaines, W. D. Bellamy, and A. G. Tweet, J. Chem. Phys., 41, 538-552 (1964).
3. B. Ke, in The Chlorophylls, (L. P. Vernon and G. R. Seely, eds.), Academic Press, New York, 1966, pp. 253-279.
4. A. Steinemann, G. Stark, and P. Läuger, J. Membrane Biol., 9, 177-194 (1972).
5. H. P. Ting, W. A. Huemueller, S. Lalitha, A. L. Diana, and H. T. Tien, Biochim. Biophys. Acta, 163, 439-450 (1968).
6. H. Dijkmans, R. M. LeBlanc, F. Cogniaux, and J. Aghion, Photochem. Photobiol., 29, 367-372 (1979).
7. F. Podo, J. E. Cain, and J. K. Blasie, Biochim. Biophys. Acta, 419, 19-41 (1976).
8. W. Oettmeier, J. R. Norris, and J. J. Katz, Biochem. Biophys. Res. Comm., 71, 445-451 (1976).
9. A. G. Lee, Biochemistry, 14, 4397-4402 (1975).
10. K. Colbow, Biochim. Biophys. Acta, 318, 4-9 (1973).
11. J. J. Katz, Dev. Appl. Spectrosc., 6, 201-218 (1968).
12. J. J. Katz, Inorg. Biochem., 2, 1022-1066 (1973).
13. J. J. Katz, G. L. Closs, F. C. Pennington, M. R. Thomas, and H. H. Strain, J. Am. Chem. Soc., 85, 3801-3809 (1963).
14. G. L. Closs, J. J. Katz, F. C. Pennington, M. R. Thomas, and H. H. Strain, J. Am. Chem. Soc., 85, 3809-3821 (1963).

REFERENCES (continued)

15. L. L. Shipman, T. R. Janson, G. J. Ray, and J. J. Katz, Proc. Natl. Acad. Sci. USA, 72, 2873-2876 (1975).

16. R. G. Shulman, K. Wüthrich, T. Yamane, D. J. Patel, and W. E. Blumberg, J. Mol. Biol., 53, 143-157 (1970).

17. T. L. James, Nuclear Magnetic Resonance in Biochemistry, Academic Press, New York, 1975, pp. 58-60.

18. C. J. Jameson, A. K. Jameson, and S. M. Cohen, J. Magn. Reson., 19, 385-392 (1975).

19. D. H. Live and S. I. Chan, Analyt. Chem., 42, 791-792 (1970).

20. J. A. Pople, W. G. Schneider, and H. J. Bernstein, High-Resolution Nuclear Magnetic Resonance, McGraw-Hill, New York, 1959, pp. 424-428.

21. S. Aronoff, Photosynthetica, 12, 298-303 (1978).

22. T. Trosper and K. Sauer, Biochim. Biophys. Acta, 162, 97-105 (1968).

23. G. S. Beddard and G. Porter, Nature, 260, 366-367 (1976).

CHAPTER V

Interactions of Chlorophyll a with Phospholipids in Bilayer Membranes - Effects of Phase Behavior on Optical Absorption Properties

A. INTRODUCTION

Electronic spectra of chlorophyll a/phospholipid bilayer membranes are similar in many ways to spectra of chlorophyll a in native photosynthetic membranes.[1-4] The spectra of both model and natural membranes are unusual in some respects and suggest an unique organization of chlorophyll a molecules. In the previous chapters we found that the organization of chlorophyll a in phospholipid bilayer membranes depends on the temperature and composition of the membrane. This behavior was interpreted in terms of the bilayer phase diagram, Figure III-3, for the chlorophyll a/DSPC model membrane system.

In this section we will describe how the optical properties of the model system change with temperature, show that these changes are consistent with the previously discussed interpretations of the phase diagram, and finally discuss the origins of the spectral changes. It is hoped that these investigations will lead to a clearer understanding of the optical properties of chlorophyll a in vivo.

B. MATERIALS AND METHODS

Chlorophyll a was obtained by the procedures described in Chapter II. DSPC was purchased from Calbiochem and used without further purification. Multilamellar membranes (multilayers) were prepared by dissolving the appropriate amounts of chlorophyll a and DSPC in chloroform, completely evaporating the solvent, and hydrating the dried film in deionized water. Dissolution in water was most easily accomplished by heating to above 60° and stirring with a vortex mixer. On some occasions chlorophyll a and DSPC were initially co-dissolved in methanol. This procedure gave a different set of results which we note in the text.

Absorption spectra were recorded on a Beckman Acta III visible absorption spectrometer with a Beckman TM temperature programmer accessory. Typically spectra were recorded over the complete spectral range at a scan rate of 1 nm/sec, and then the region of the Q_y transition was expanded and scanned at a much slower rate to accurately determine the peak position. Positions of the absorption maxima are generally reproducible to within 0.2 nm.

C. RESULTS

Optical absorption spectra from 350 to 750 nm of multilamellar chlorophyll a/DSPC membranes were obtained at 5° intervals over the temperature range 15-65°. Typical spectra of 4 mole percent and 20 mole percent chlorophyll a compositions at 15° and 65° are shown in Figure V-1 along with a solution spectrum of chlorophyll a in diethyl

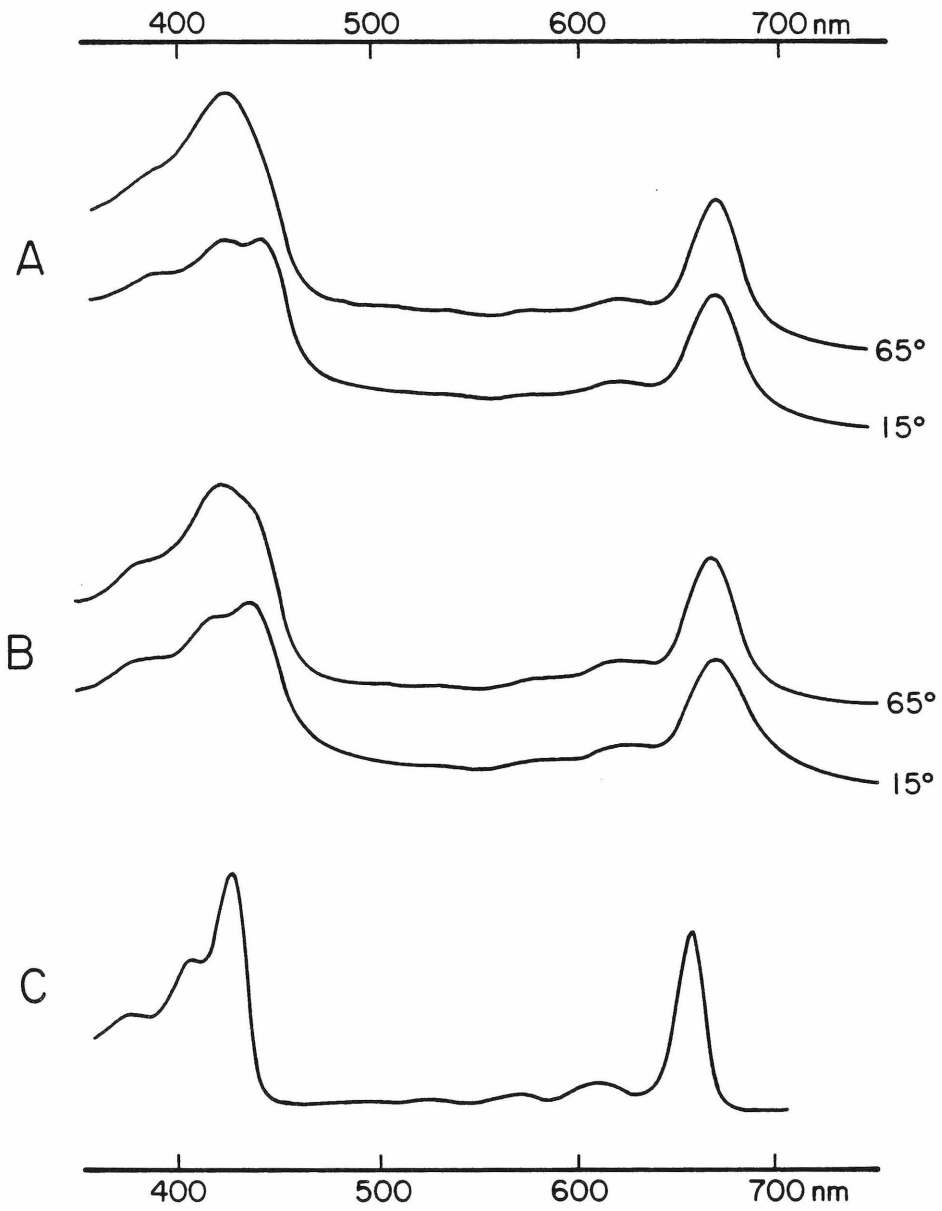

FIGURE V-1. Optical absorption spectra of chlorophyll a in: A, 4% chlorophyll a/DSPC multilayers; B, 20% chlorophyll a/DSPC multilayers; C, diethyl ether solution.

ether for comparison. The most obvious differences between the solution and bilayer spectra are: 1) the position of the red Q_y band is shifted to longer wavelengths in the bilayer spectra, 2) the bilayer spectra have generally broader features than the solution spectrum, and 3) the intensity of the η band, or soret satellite, at about 410 nm is greater in the bilayer spectra. There are also some obvious differences in the bilayer spectra themselves. At lower temperatures the Q_y absorption at about 670 nm is shifted to the red, is broader, and has a smaller extinction coefficient than at higher temperature. In addition, the widths and relative intensities of the soret and soret satellite bands change with temperature. It is observed that all of these spectral changes occur over about a 10° range near the thermal phase transition temperature of the membrane.

The turbidity of the multilamellar suspensions used in these experiments changes slightly from sample to sample and with temperature. These changes would complicate the quantitative measurement and comparison of relative extinction coefficients if uncorrected. Figure V-2 shows how the turbidity, measured as the absorbance at 550 nm (a region relatively free of other absorbances), changes with temperature. It can be seen from Figure V-2 that light scattering from the colloidal multilayer particles decreases above the thermal phase transition temperature. This effect has also been observed in pure phospholipid bilayers.[5] All subsequent data which we report have been corrected for light scattering by measuring the turbidity at 550 nm and allowing for the fourth power wavelength dependence of the

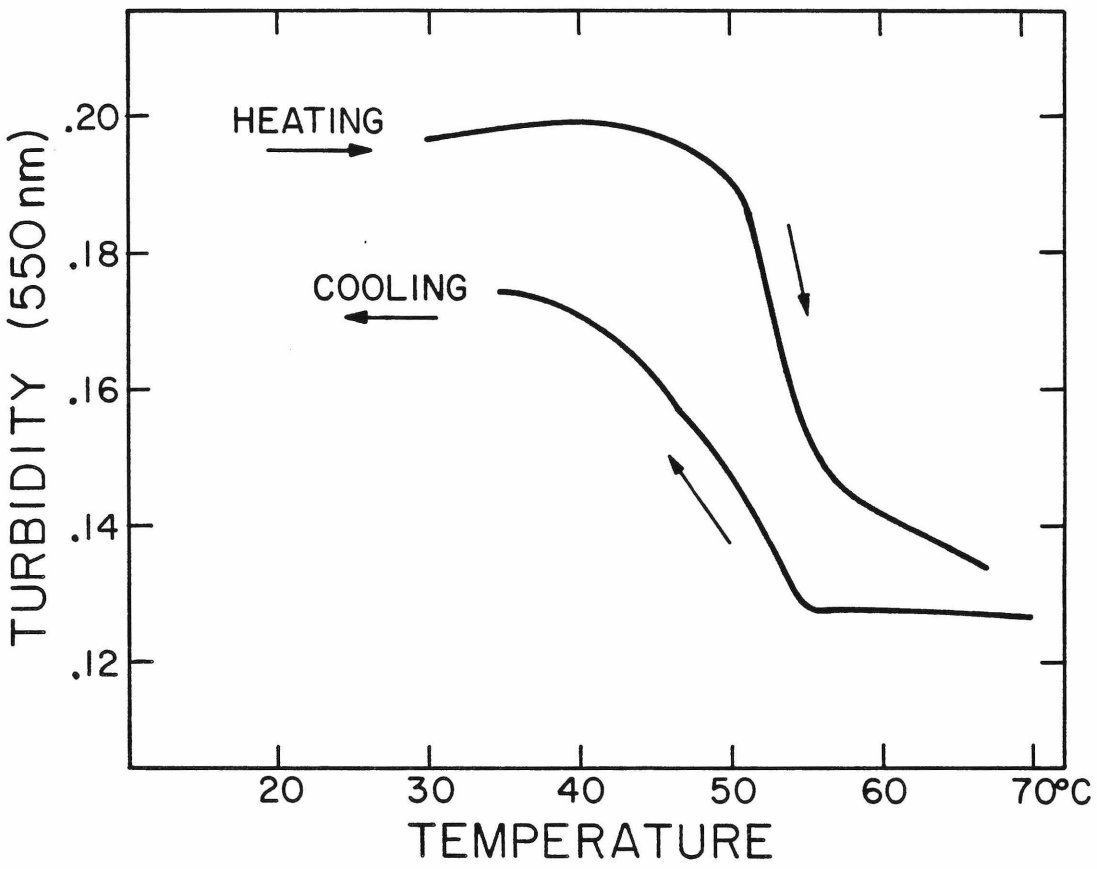

FIGURE V-2. Turbidity of 20% chlorophyll a/DSPC multilayers (measured as the absorbance of the sample at 550 nm).

scattering.

Figure V-3 tabulates the relative extinction coefficients (in arbitrary units) of the Q_y (ϵ), soret (ϵ_s) and soret satellite (ϵ'_s bands. The intensity of the soret band parallels that of the Q_y band throughout the entire temperature range, whereas the intensity of the soret satellite increases disproportionately above about 50°. This would be thought to be due to pheophytinization (removal of magnesium) or other chemical alterations of the chlorophyll a structure except that the observed changes were found to be fully reversible.

Particular data for the Q_y band of 20% chlorophyll a/DSPC multilayers are shown in Figure V-4 where a number of interesting changes with temperature can be observed. The absorption maximum, shifted about 10-15 nm to the red of the maximum in diethyl ether, is red-shifted farthest below 50°, from about 670 nm at 60° to over 673 nm at 15°. Concomitant with this shift, the relative extinction coefficient decreases as the peak broadens.

For other samples with different proportions of chlorophyll a the position of the Q_y band changes with temperature much the same as at 20% chlorophyll a, although in some instances the absorption maximum was found to increase to as much as 675.5 nm. However, the width and relative extinction coefficients were found to be dependent on the composition of chlorophyll a in the membrane. This is illustrated by Figure V-5 which shows the measured widths of the Q_y band as a function of temperature for 4, 8 and 20% chlorophyll a. We find that the width is independent of composition above about 50°, but increases

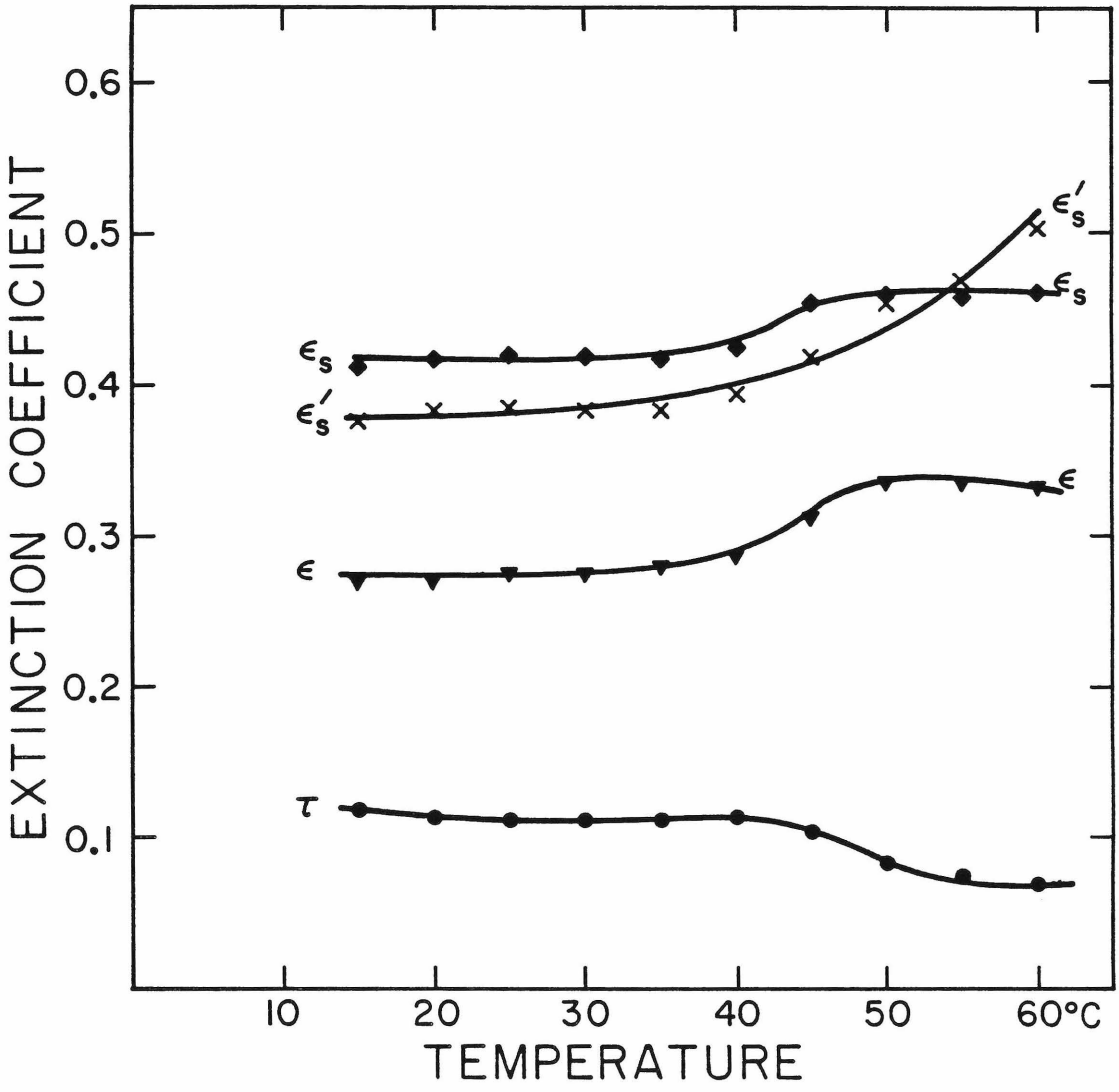

FIGURE V-3. Relative extinction coefficients (in arbitrary units) as a function of temperature of the soret (ϵ_s), soret satellite (ϵ_s'), Q_y (ϵ) absorption bands, and the turbidity at 550 nm (τ). Data from optical absorption spectra of 20% chlorophyll a/DSPC multilayers.

FIGURE V-4. (next page). Data for the width (δ), extinction coefficient (ϵ, arbitrary units), and position (λ_{max}) of the chlorophyll $\underline{a}$ $Q_y(0,0)$ visible absorption band in 20% chlorophyll $\underline{a}$/DSPC multilayers. The data shown are for increasing temperature (5° intervals every 10-15 minutes) and are fully reversible with decreasing temperature on this timescale.

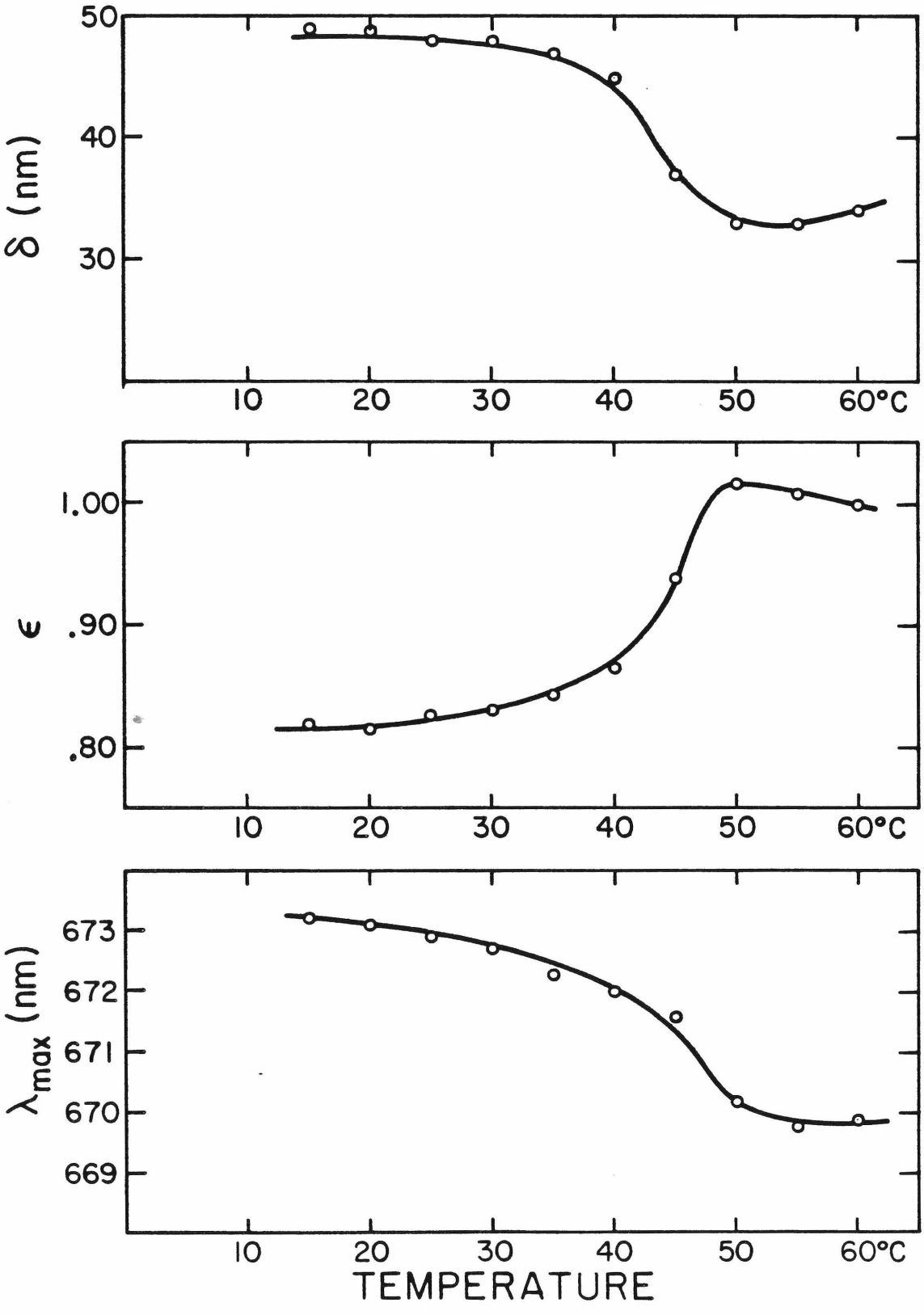
δ (nm)
50
40
30
10
20
30
40
50
60°C
ε
1.00
.90
.80
10
20
30
40
50
60°C
λmax (nm)
673
672
671
670
669
10
20
30
40
50
60°C
TEMPERATURE

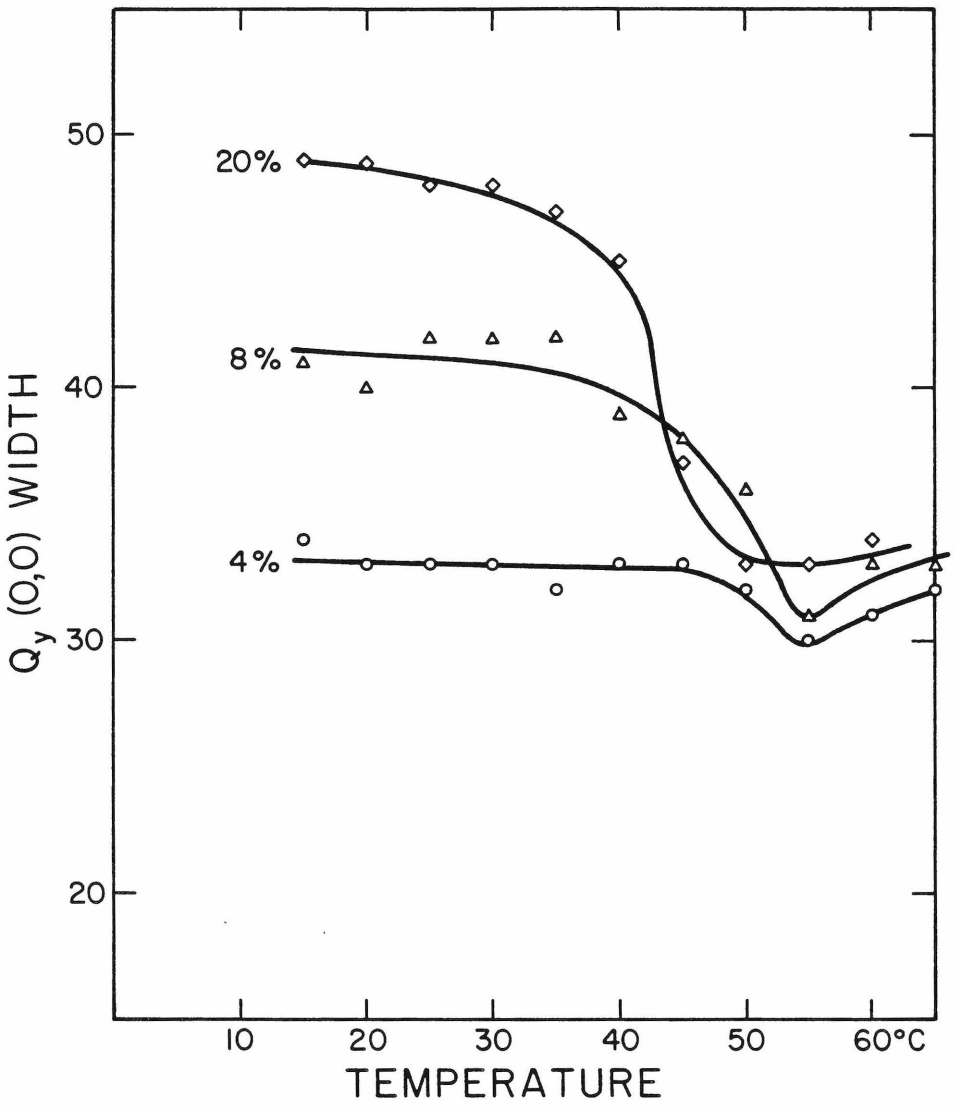

FIGURE V-5. Width of the $Q_y(0,0)$ absorption band as a function of temperature for 4, 8, and 20% chlorophyll a/DSPC multilayers.

with increasing chlorophyll a content below 50°. At 38% chlorophyll a, omitted for clarity, the width below 50° is about 42 nm or slightly less than for 20% chlorophyll a.

The product of the relative extinction coefficient and the width provides a measure of the integrated absorption intensity and therefore the oscillator strength of the transition. By this procedure we find that the oscillator strength of the Q_y band changes with temperature and furthermore that below 50° the 4% and 8% compositions have a lower oscillator strength than do the 20% and 38% compositions. At temperatures greater than 50° they are all nearly the same. Relative values of the estimated oscillator strength are shown in Figure V-6.

Finally we wish to give some results which may prove helpful in explaining a number of differences between previously reported studies of chlorophyll a/phospholipid bilayer membrane systems. In our preparations we initially dissolve chlorophyll a and DSPC together in chloroform and then remove the solvent in order to ensure complete mixing. If this initial dissolution is in methanol, which strongly coordinates to chlorophyll a,[6] then much different absorption maxima are obtained as shown in Figure V-7. The absorption maxima of chlorophyll a/DSPC bilayers which were previously dissolved in methanol have absorption maxima nearly the same as for chlorophyll a dissolved in methanol solution. This may indicate that in such samples the methanol remains as a strongly coordinating ligand to chlorophyll a.

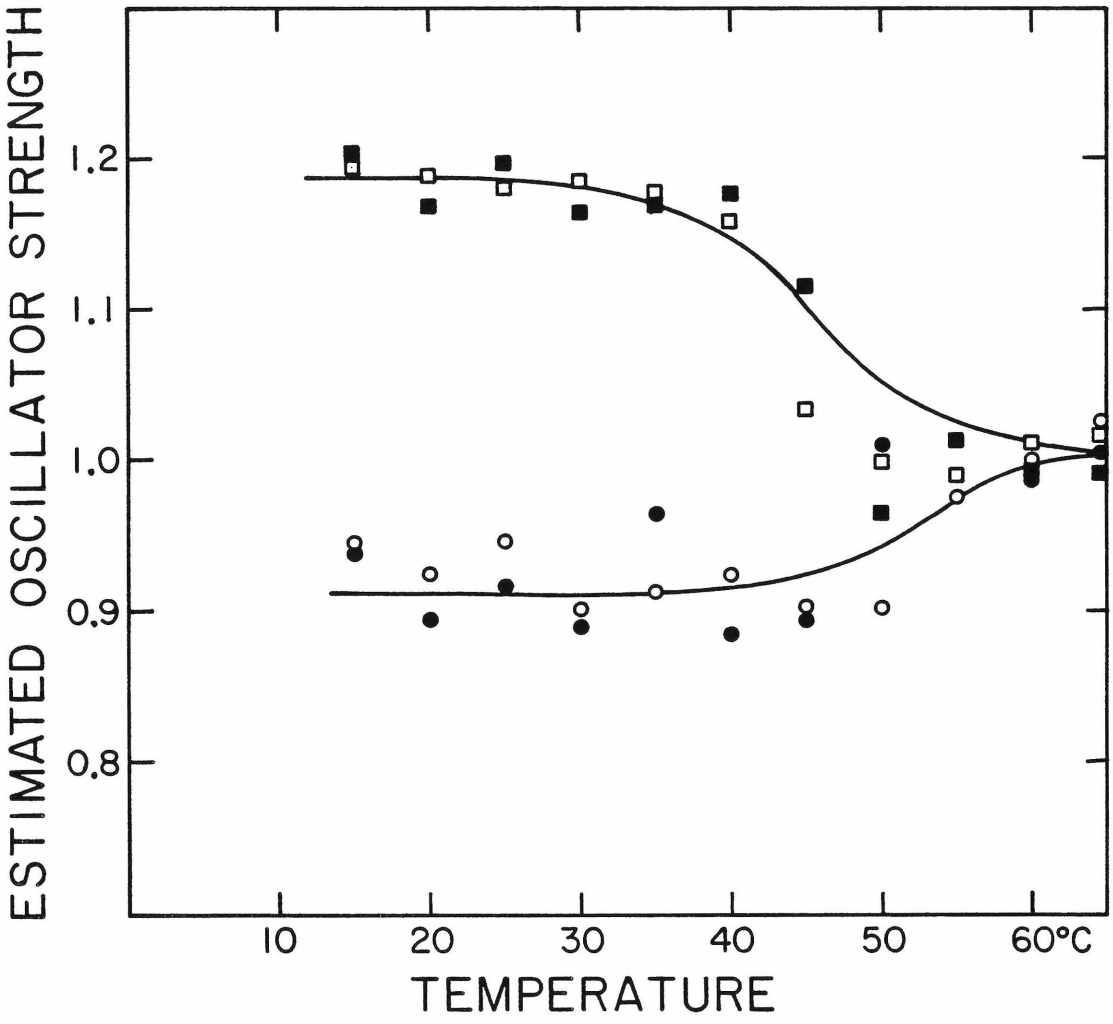

FIGURE V-6. Product of the width and relative extinction coefficient of the $Q_y(0,0)$ absorption band as a function of temperature for 4% (open circles), 8% (closed circles), 20% (open squares), and 38% (closed squares) chlorophyll a/DSPC multilayers. The actual numbers on the vertical axis are entirely arbitrary.

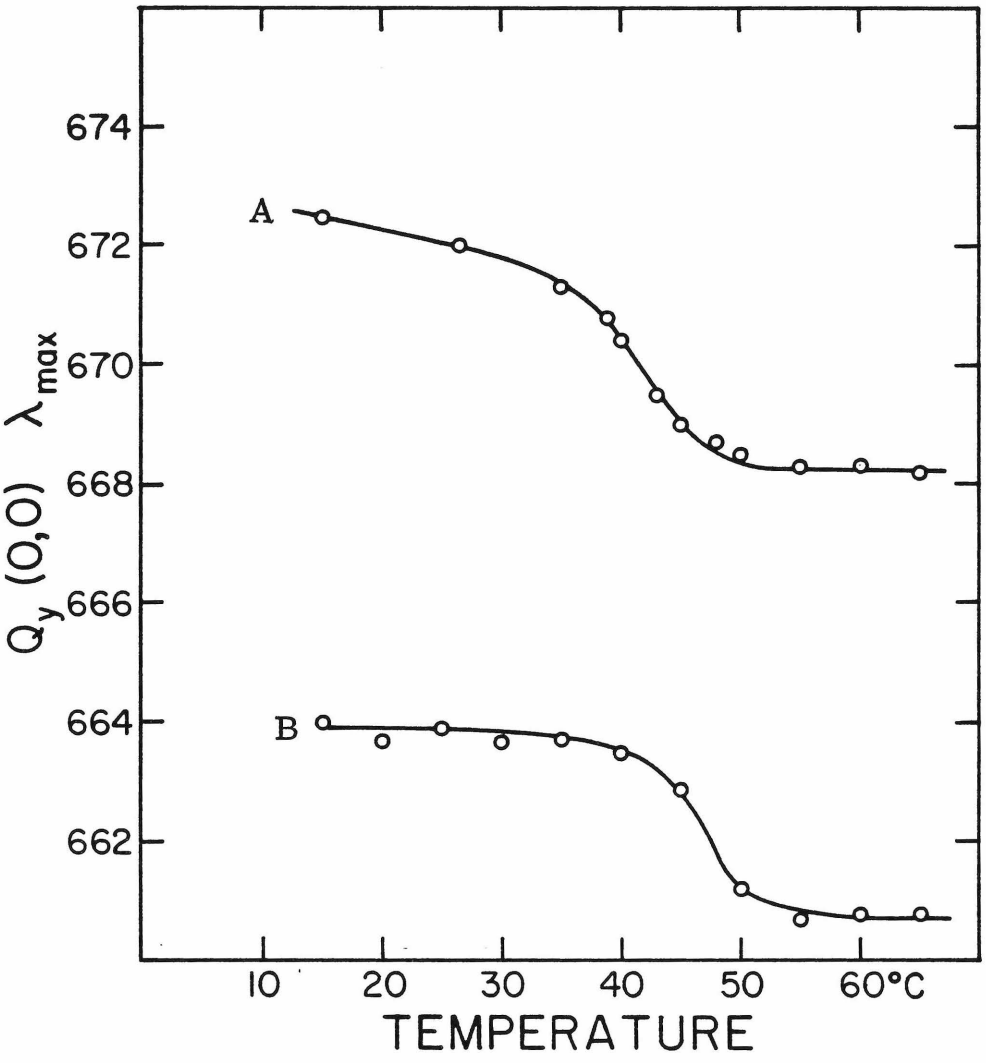

FIGURE V-7. Position of the Q_y (0, 0) absorption maximum versus temperature in chlorophyll a/DSPC multilayers initially dissolved in chloroform (A) and in methanol (B).

D. DISCUSSION

1. Agreement with the chlorophyll a/DSPC phase diagram

Most of the preceding results can be rationalized on the basis of the phase diagram discussed in chapters III and IV. For example all of the changes in the positions, widths, and relative extinction coefficients occur over a relatively narrow range of temperatures near the transition temperatures previously observed by thermal techniques. The apparent transition width is about 10° in agreement with the temperature course of the NMR results in chapter IV and the width of the DTA transitions in chapter III.

According to the phase diagram for the chlorophyll a/DSPC system, found in Figure III-3, all compositions are in a similar phase state above the liquidus temperature. This is consistent with the similar linewidths found for all compositions of chlorophyll a above about 50° (Figure V-5). Upon lowering the temperature from above to below the transition, a considerable amount of liquid crystalline lipid is converted into the gel-like phase. Thus we find (Figure V-2) that the light scattering increases as observed for similar transitions of pure DSPC bilayers.[5] In the low temperature region below about 50°, the phase diagram indicates that bilayers with a composition of less than 8 or 10% chlorophyll a should consist of a single solid solution phase, while compositions of 10% or greater must have solid-solution and compound phases coexisting in equilibrium. This is consistent with the observation that the oscillator strength of the Q_y transition is similar

for 4% and 8% chlorophyll a and for 20% and 38% chlorophyll a below the 50° transition temperature. At higher temperatures, where all four compositions should be in a similar phase state, the relative oscillator strengths are the same. The lower oscillator strength for the Q_y band in the 4% and 8% samples perhaps indicates that chlorophyll a in the solid solution phase is aggregated, as chlorophyll aggregates have lower Q_y intensities than monomeric chlorophyll.[7]

We have previously found in the NMR results of chapter IV that exchange of components between phases is slow on the NMR timescale; it must be extremely slow compared to optical standards. Hence when two phases are in equilibrium the composite of their individual absorption spectra must be observed. The following discussion will attempt to show how this can be used to explain a number of the experimental observations.

2. Analysis of composite absorption spectra

Consider a mixture of two different spectral forms of chlorophyll a in the proportions f_1 and f_2, with $f_1 + f_2 = 1$. Assume that each has a gaussian absorption profile, that they are centered at λ_1 and λ_2 with half-widths δ_1 and δ_2 and extinction coefficients ϵ_1 and ϵ_2. If $\lambda_2 - \lambda_1$ is less than the smallest δ, then these peaks will be merged into a single gaussian band with maximum extinction coefficient ϵ_m at λ_m with an observed half-width at half-height δ_m. The following conditions must then hold:[8]

$$f_1 \epsilon_1 \frac{(\lambda_1 - \lambda_m)}{\sigma_1^2} + f_2 \epsilon_2 \frac{(\lambda_2 - \lambda_m)}{\sigma_2^2} = 0 \qquad \text{(V-1)}$$

$$\epsilon_m = f_1 \epsilon_1 \left(1 - \frac{(\lambda_m - \lambda_1)^2}{2\sigma_1^2}\right) + f_2 \epsilon_2 \left(1 - \frac{(\lambda_m - \lambda_2)^2}{2\sigma_2^2}\right) \qquad \text{(V-2)}$$

$$\sum_{i=1}^{2} f_1 \epsilon_i \exp \frac{-(\delta_m + \lambda_m - \lambda_i)^2}{2\sigma_i^2} = \tfrac{1}{2} \sum_{i=1}^{2} f_i \epsilon_i \exp \frac{-(\lambda_m - \lambda_i)^2}{2\sigma_i^2} \qquad \text{(V-3)}$$

In (V-1) through (V-3) the variance σ is related to the half-width by

$$\delta_i^2 = 2 \ell n 2 \, \sigma_i^2 . \qquad \text{(V-4)}$$

Among the variables, the observables are λ_m, δ_m and ϵ_m; f_1 and f_2 can in principle be obtained from the phase diagram. This leaves six indeterminate variables and therefore some approximations must be made. Assume that the two pure absorptions 1 and 2 have equal extinction coefficients and widths, $\epsilon_1 = \epsilon_2$ and $\delta_1 = \delta_2$. Under these conditions equation (V-1) can be simplified and rearranged:

$$f_1(\lambda_m - \lambda_1) + f_2(\lambda_m - \lambda_2) = 0 \qquad \text{(V-5)}$$

$$(\lambda_m - \lambda_1) = f_2(\lambda_2 - \lambda_1) \qquad \text{(V-6a)}$$

$$(\lambda_m - \lambda_2) = f_1(\lambda_1 - \lambda_2) . \qquad \text{(V-6b)}$$

Also eqn. (V-3) can be reduced to the following approximate expression for the observed half-width δ_m:

$$\exp \frac{-\delta_m(\delta_m + 2(\lambda_m - \lambda_1))}{2\sigma_1^2} + \exp \frac{-\delta_m(\delta_m - 2(\lambda_m - \lambda_1))}{2\sigma_1^2} = 1 \qquad \text{(V-7)}$$

Substituting (V-6a) into the above gives a useful expression:

$$\exp\frac{-\delta_m(\delta_m + 2f_2(\lambda_2 - \lambda_1))}{2\sigma_1^2} + \exp\frac{-\delta_m(\delta_m - 2f_2(\lambda_2 - \lambda_1))}{2\sigma_1^2} = 1 \qquad \text{(V-8)}$$

We now require values for the half-widths of the components. Knowing that the 8% sample is very near the composition of the solid-solution phase and similarly that 38% chlorophyll a is close to the compound composition, we choose their linewidths to represent δ_1 and δ_2. (We will continue to use 1 and 2 to denote respectively the solid solution and compound phases.) Since both linewidths are 42 nm, the previous assumption of equal linewidths is justified and we calculate $2\sigma_1^2 = 2\sigma_2^2 = 636.8$. Figure V-8 shows how the observed half-width δ_m varies with the quantity $f_2(\lambda_2 - \lambda_1)$ according to eqn. (V-8). In the case of the 20% chlorophyll a composition, the observed half-width δ_m is about 24 nm. From Figure V-8 we find that this corresponds to a value of 90 nm for $f_2(\lambda_2 - \lambda_1)$. According to the phase diagram in Figure III-3, at 20% chlorophyll a there should be 38% of the compound phase with 0.40 mole fraction chlorophyll a and 62% of a solid-solution phase with 0.08 mole fraction chlorophyll a. Hence at this particular composition 76% of the chlorophyll is in the compound phase below 50°, or $f_2 = 0.76$. From this $(\lambda_2 - \lambda_1) = 11.8$ nm. Then using eqns. (V-6a) and (V-6b) and the observed λ_m of about 675 nm, we find the approximate positions of the constituent absorbance peaks, $\lambda_1 = 666$, $\lambda_2 = 678$ nm.

The point of the preceding analysis is that the changes in position and width of the observed absorbance peaks with temperature can be

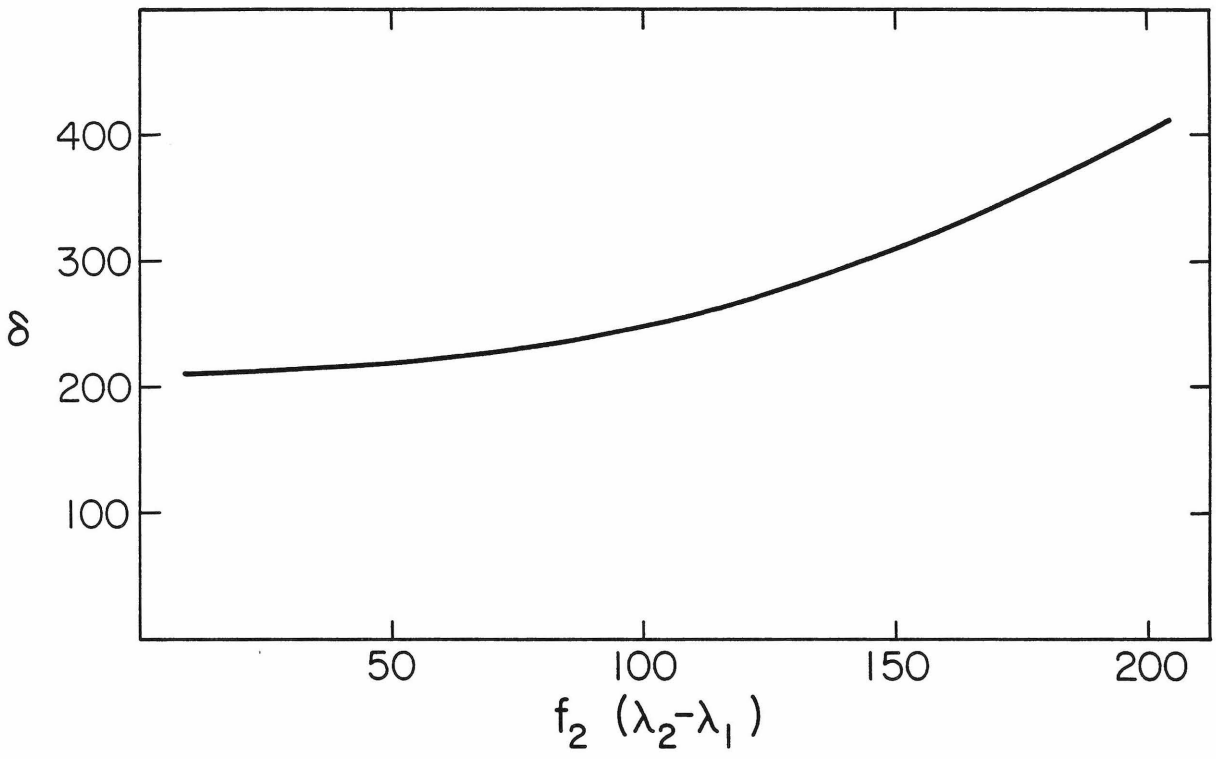

FIGURE V-8. The observed width δ for the superposition of two equivalent gaussian peaks separated by $(\lambda_2 - \lambda_1)$ and in the relative amounts f_2 and $1-f_2$.

explained by simply assuming that spectra in the two-phase regions of the phase diagram are composites of the individual spectra of each phase. Figure V-9 shows the values of position and width for the Q_y band of the individual phases as determined from the analysis of the spectra. Although the accuracy of the values is perhaps compromised by the required assumptions, some trends are apparent. The width seems to be related to the gel or liquid crystalline character of the phase, with the more solid-like phases broader. The position on the other hand seems to be determined by some other factor which we will consider next.

3. Origin of the red-shift in chlorophyll a bilayers

The position of the Q_y absorption band for chlorophyll a in bilayers is considerably red-shifted compared to its position in organic solvents. This is true of all phases listed in Figure V-9. Both of the solution phases have similar maxima near 666-668 nm; the compound phase absorbance is shifted to even longer wavelengths. This red-shift could be accounted for by any of a number of factors: a) a general solvent effect due to the polar headgroup environment of the lipid bilayer, b) dispersion interactions between neighboring chlorophyll molecules, c) charge polarization by ligands to chlorophyll, or d) exciton interactions between oriented and electronically coupled chlorophyll molecules.

a. Solvent shifts - environmental effects. The solvent effect is generally adequate to explain the spectra of chlorophyll a in solution. It arises from interactions between the electronic structure of chlorophyll a and the static and induced fields of the solvent. According to

FIGURE V-9. The estimated position and width of the $Q_y(0, 0)$ absorption band of chlorophyll a in the three constituent phases of the chlorophyll a/DSPC binary phase diagram.

PHASE	position (nm)	width (nm)
liquid-crystalline solution (S_L)	668	32
solid solution (S_s)	666	42
compound (C)	678	42

the formulation by Bakhshiev[9] and as discussed by Seely,[10] the solvent shift $\Delta\lambda$ is related to the solvent refractive index n and dipole moment D by

$$\Delta\lambda = \frac{e^2 f \lambda^3}{8\pi^2 mc^2 r^3} \left\{\frac{n^2-1}{2n^2+1}\right\} \qquad \text{(V-9)}$$

$$+ \frac{\lambda^2}{hcr^3} \left\{\frac{2n^2+1}{n^2+2}\right\} (\mu_e^2 - \mu_g^2) \left\{\frac{n^2-1}{n^2+2}\right\}$$

$$+ \frac{2\lambda}{hcr^3} \left\{\frac{2n^2+1}{n^2+2}\right\} \mu_g (\mu_e \cos\alpha - \mu_g) \left\{\frac{D-1}{D+2} - \frac{n^2-1}{n^2+2}\right\},$$

where e and m are the charge and mass of the electron, f is the oscillator strength of the transition, λ is the vapor phase absorption maximum, μ_g and μ_e are the ground and excited state dipole moments of chlorophyll a and α is the angle between them. The quantity r represents the radius of the cavity containing the solute molecule. Seely finds[10] that r is about 2.7 angstroms for chlorophyll a which implies that only immediately adjacent molecules determine the solvent shift. With reasonable values of n and D for the headgroup region of the bilayer,[5,11] shifts to almost 670 nm such as in the bilayer solution phases could be accounted for solely by the solvent effect. The Bakhshiev formulation assumes that solvent molecules are oriented randomly with respect to the solute, although such is not necessarily the case for lipid bilayer solutions which are considerably more ordered. It is conceivable that under favorable circumstances the dipole moments of the chlorophyll a solute and lipid solvent could be more strongly

coupled as a result of ordering. Thus an even larger shift than predicted by (V-9) could result. The extreme case of this circumstance, where chlorophyll a is ligated by a lipid molecule, is considered under effect c).

b. Dispersion interactions - aggregation effects. Dispersion interactions between chlorophyll a molecules extend the solvent effect to include other chlorophyll a molecules as part of the environment. Any shifts due to this effect should not be significant unless chlorophyll a molecules are extremely close as in an aggregate. The available evidence suggests that this does not occur in bilayers (see chapters III and IV).

c. Charge polarization - ligand effects. It was determined in chapter 5 that the compound phase is formed as a result of complexation between the central magnesium atom of chlorophyll a and a lone pair of electrons from the phosphate group of the phospholipid headgroup. Depending on the extent to which the magnesium group is conjugated into the pi-electron system, this ligation may have a significant effect on the electronic structure and absorption spectrum of chlorophyll a. This is what is meant by effect c). By analogy[12] consider a conjugated polyene I. Now form the trimolecular charge transfer complex II by interaction of the polyene system with an electron donor D and an electron acceptor A. The additional resonance structure III causes the absorption spectrum of II to be shifted to longer wavelengths than I.

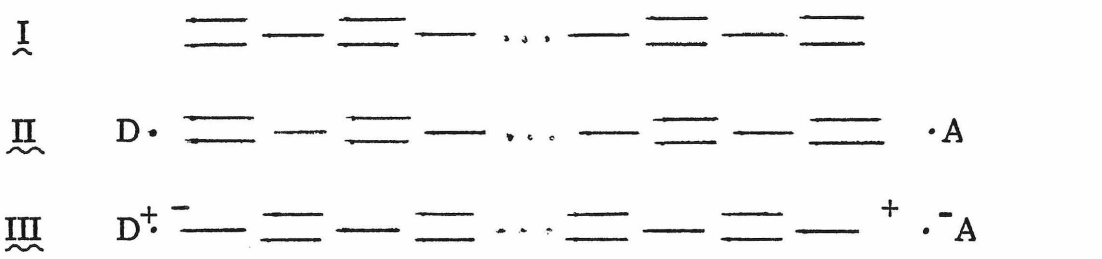

An example of this is the merocyanine dyes which have a structure like IV. A second dipolar structure V allows the absorption spectrum to shift according to the polarity of the environment.[13] The conjugated porphyrin macrocycle could mediate a similar donor-acceptor interaction between the electrophilic magnesium and the nucleophilic ketone of ring V. This charge redistribution would be facilitated by the ligand interactions with magnesium and by hydrogen-bonding to the ketone. As a result of such interactions, the absorption spectrum could be considerably shifted to the red.

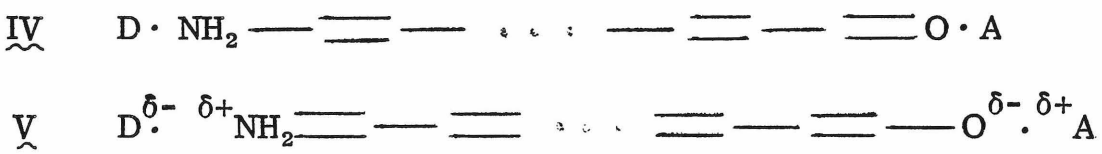

d. Exciton interactions - orientation effects. Because of the ordering of chlorophyll a molecules in the compound phase, the possibility of spectral shifts due to excitonic interactions among the chlorophylls should be considered. In the present situation the term 'exciton interaction' denotes[14] excited state resonance interactions among chromophores whose intermolecular interactions are strong

enough to couple the electronic states but sufficiently weak so as to preserve molecular individuality. This corresponds to the weak-coupling criterion of Simpson and Peterson,[15] or the localized exciton model of Davydov.[16] Both of these models predict a shift in absorption maximum with a concomitant broadening but retention of the general bandshape.[14] This in fact is the pattern of spectral changes which we observe for the transformation into the compound phase.

Hochstrasser and Kasha[17] have applied the molecular exciton model to lamellar systems to calculate the expected spectral changes for a number of orientational geometries. For an arbitrary square array of chromophores with lattice spacing a, the predicted shift in position, $\epsilon(o)$, and bandwidth are given by

$$\epsilon(o) = 8.4 \frac{e^2|d|^2}{a^3} (3\cos^2\theta - 1) \qquad \text{(V-10)}$$

$$\text{bandwidth} = 16.8 \frac{e^2|d|^2}{a^3} (3\cos^2\theta - 1) \qquad \text{(V-11)}$$

where $e|d|$ is the excited state dipole moment and θ is the angle between the transition dipole and a normal to the membrane plane. Shipman et al.[7] give 16.8 D^2 for the transition dipole strength $e^2|d|^2$ of the $Q_y(0,0)$ transition. Steinemann et al.[4] have determined from the dichroism of chlorophyll a in black lipid membranes that the Q_y transition dipole is at an angle of 34° to the membrane plane, hence $\theta = 56°$. Using these values, and the 11.8 nm difference between

absorption maxima of solution and compound phases (Figure V-8), we calculate from (V-10) a value of 10.2 angstroms for a, the distance between oriented chlorophyll a molecules. Space-filling (CPK) models show that this is precisely the expected distance for the closest approach of two molecules physically separated by a coordinated intervening phospholipid molecule.

As a further check on the consistency of this model with the observed data, consider the width of the transition. Equations (V-10) and (V-11) show that the increase in width due to exciton coupling should be twice the measured shift, independent of the values of $e|d|$, θ or a. The normal width of the Q_y transition in organic solvents[9] is 20 nm (± 10%) and the measured width in the present case is 42 nm. The difference between these is 22 nm, or 1.86 times the observed shift. Within the error this easily agrees with the value predicted by the exciton model.

While the previous analyses do not prove that excited state resonance interactions are responsible for the observed spectral changes, they do show a remarkable agreement with all the available data. Furthermore such interactions would explain the decrease in fluorescence observed by Lee[2] for bilayers below the thermal phase transition. Energy transfer between chromophores, if the exciton model is correct, should be extremely efficient and open another pathway for the electronic excitation with a corresponding reduction in the probability of fluorescence.

REFERENCES - CHAPTER V

1. H. Dijkmans, R. M. Leblanc, F. Cogniaux, and J. Aghion, Photochem. Photobiol., 29, 367-372 (1979).
2. A. G. Lee, Biochemistry, 14, 4397-4402 (1975).
3. K. Colbow, Biochim. Biophys. Acta, 318, 4-9 (1973).
4. A. Steinemann, G. Stark, and P. Läuger, J. Membrane Biol., 9, 177-194 (1972).
5. P. N. Yi and R. C. MacDonald, Chem. Phys. Lipids, 11, 114-134 (1973).
6. J. J. Katz, Dev. Appl. Spectroscopy, 6, 201-218 (1968).
7. L. L. Shipman, T. M. Cotton, J. R. Norris, and J. J. Katz, J. Am. Chem. Soc., 98, 8222-8230 (1976).
8. G. R. Seely, Spectrochimica Acta, 21, 1847-1856 (1965).
9. N. G. Bakhshiev, Optics and Spectroscopy, 10, 379-384 (1960).
10. G. R. Seely and R. G. Jensen, Spectrochimica Acta, 21, 1835-1845 (1965).
11. F. Bellemare and M. Fragata, J. Colloid Interface Sci., 77, 243-252 (1980).
12. J. R. Platt, Science, 129, 372-374 (1959).
13. L. G. S. Brooker and W. T. Simpson, Ann. Rev. Phys. Chem., 2, 121-150 (1951).
14. M. Kasha, Rad. Research, 20, 55-71 (1963).
15. W. T. Simpson and D. L. Peterson, J. Chem. Phys., 26, 588-593 (1956).

REFERENCES (continued)

16. A. S. Davydov, Theory of Molecular Excitons, (trans. by M. Kasha and M. Oppenheimer, Jr.), McGraw-Hill, New York, 1962.

17. R. M. Hochstrasser and M. Kasha, Photochem. Photobiol., 3, 317-331 (1964).

CHAPTER VI

Lipid-Associated Chlorophyll: Evidence from ^{13}C NMR of the Photosynthetic Spinach Thylakoid Membrane

A. INTRODUCTION

Understanding the molecular architecture of the photosynthetic membrane is an essential step toward unraveling the details of its function. Although the spectroscopic heterogeneity of chlorophyll a[1] suggests that nature has found it expedient to diversify the process of light absorption and transduction by structural means, the organization and distribution of chlorophyll in the membrane is still an issue which is not totally settled. Much of our knowledge regarding the location of chlorophyll in the photosynthetic membrane has been based on studies[2-4] wherein one attempts to dissect the membrane with various detergents. Such studies indicate that much of the chlorophyll is associated with membrane proteins although a significant fraction is usually obtained as a protein-free pigment band by gel chromatography.[5] While these studies are valuable, they suffer several disadvantages. Detergent solubilization must necessarily cause gross disruption of the membrane structure resulting in a loss of information concerning membrane organization. In addition, it is possible that membrane components became artifactually associated as a result of the detergent solubilization. Clearly, some of these difficulties can be alleviated by studying the organization of the photosynthetic membrane by in situ techniques. In particular, nuclear magnetic resonance allows one to

investigate the structure and dynamics of a biological system such as the photosynthetic membrane without structural perturbations. In this paper we report ^{13}C-NMR studies of intact thylakoid photosynthetic membranes. Our results show that well-resolved spectra can be obtained from whole thylakoid membranes, with resonances which can be assigned to specific membrane components. The linewidths and apparent intensities of these resonances have allowed us to draw some limited conclusions concerning the organization of chlorophyll in the thylakoid membrane.

B. MATERIALS AND METHODS

For these studies, thylakoid membranes from spinach were obtained by procedures[6] which do not alter their native structure. Whole chloroplasts were harvested from leaves of fresh spinach by homogenization in isotonic sucrose buffer and centrifugation to remove cell debris. Thylakoid membranes were isolated from the intact chloroplasts by osmotic lysis of the double outer envelope membrane in a hypotonic buffer medium. The thylakoids were pelleted by centrifugation and resuspended several times to effect separation of the thylakoid and envelope fractions. All buffer media contained cations (5 mM $MgCl_2$, 75 mM NaCl, 10 mM $Na_4P_2O_7$, pH 7.2) which prevent the dissociation and swelling of the thylakoid grana.[7] The optical spectrum of thylakoid membranes isolated in this manner was found to be essentially indistinguishable from that of whole chloroplasts.

Proton-decoupled Fourier transform ^{13}C spectra at 90.5 MHz of the resulting thylakoid preparation were obtained at 25° C on a Bruker

HXS-360 spectrometer at the Stanford Magnetic Resonance Laboratory[8] within 24 hours of sample preparation. Transients were accumulated every 2.5 seconds using 16K data points and a spectral width of 20 KHz.

C. RESULTS AND DISCUSSION

The resulting ^{13}C-NMR spectrum of isolated spinach thylakoids, depicted in Figure VI-1, shows a number of well-resolved resonances which may be identified by comparison with previous spectra of chlorophyll *a*[9,10] and other naturally occurring thylakoid lipids.[11-13] These assignments are indicated in Figure VI-2a, VI-2b and VI-2c. Virtually all of the observed resonances may be assigned either to galactolipids, which are the predominant lipid constituent of the membrane,[6] or to phytol chains of chlorophyll. The assignment of resonances is facilitated by the fact that polyunsaturated 16:3 and 18:3 fatty acids comprise about 90% of the esterified hydrocarbon chains of thylakoid lipids[14,15] and that resonances from the porphyrin headgroup of chlorophyll *a* are not observed because of the rigidity of the porphyrin macrocycle and the additional motional restriction imposed by association of the chlorophyll with the membrane. The relative intensities of the various galactolipid resonances are consistent with their known mole fractions in the membrane, although the intensities of the assigned chlorophyll resonances relative to those of the lipids are somewhat less than expected. Measurements of the absolute intensities of the chlorophyll phytol resonances indicate that not all of the chlorophyll is observable in the high resolution spectrum. By comparison of the spectral intensities of resonances in Figure VI-1 with those of chlorophyll *a*/phospholipid

FIGURE VI-1 (next page). Proton-decoupled natural abundance 90.5 MHz ^{13}C Fourier transform NMR spectrum of isolated spinach thylakoid membranes at 25° C. The sample is a loosely packed pellet of thylakoid membranes in D_2O in a 10 mm tube. A total of 26,875 transients were accumulated and Fourier transformed with a 15 Hz exponential window to yield the above spectrum. The chemical shift scale is in parts per million relative to tetramethylsilane.

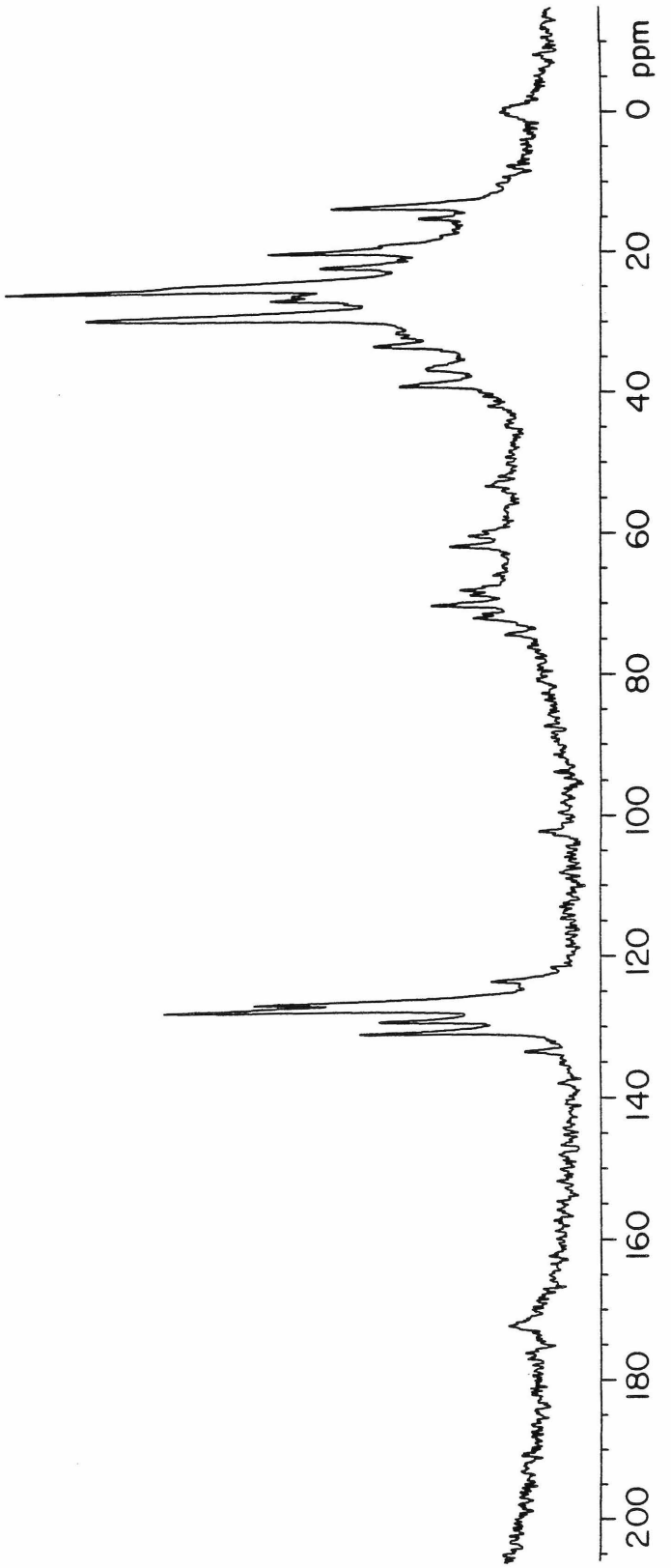
0 ppm
20
40
60
80
100
120
140
160
180
200

FIGURE VI-2 (next page). Assignments of the ^{13}C-NMR spectrum from spinach thylakoids. The selected regions of Figure 1 are expanded for ease of comparison. a) Saturated carbon region (10-45 ppm). Positions of phytol and linolenic fatty acid resonances taken from references 9 and 12 are indicated by vertical bars. b) Galactolipid headgroup and glycerol backbone region (50-85 ppm). Positions of MGD and DGD resonances from reference 12 are indicated by the bars. The letters S and C indicate peaks assignable to sulfolipid (S) and chlorophyll (C). c) Unsaturated carbon region (110-140 ppm). Positions of linolenic acid resonances from reference 12 are again indicated by bars. Resonances assigned but not shown: galactosyl C-1 of MGD (104.8 ppm), fatty acid carbonyls (172 ppm). Abbreviations: MGD, monogalactosyl diglyceride; DGD, digalactosyldiglyceride; linolenoyl, 9Z, 12Z, 15Z-Octadecatrienoate.

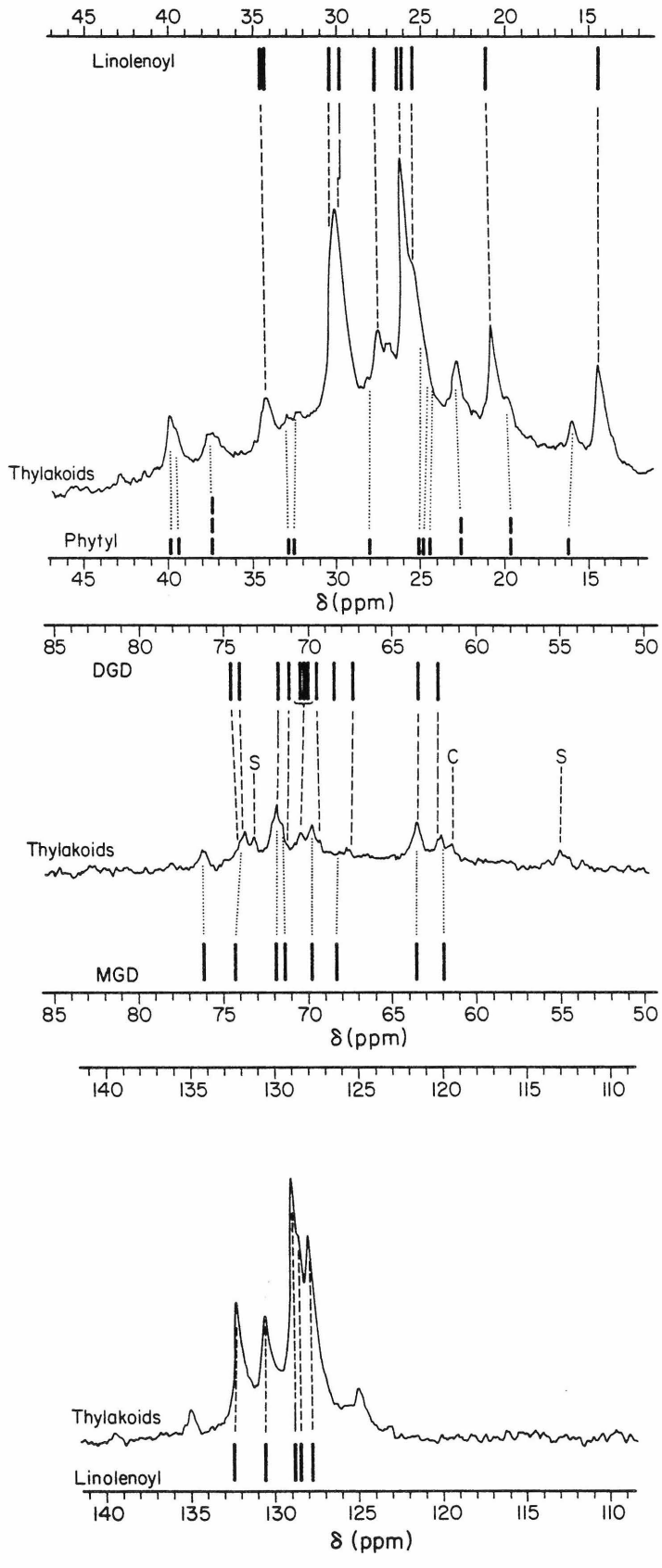
45 40 35 30 25 20 15
Linolenoyl
Thylakoids
Phytyl
45 40 35 30 25 20 15
δ(ppm)
85 80 75 70 65 60 55 50
DGD
S
C
S
Thylakoids
MGD
85 80 75 70 65 60 55 50
δ(ppm)
140 135 130 125 120 115 110
Thylakoids
Linolenoyl
140 135 130 125 120 115 110
δ (ppm)

model bilayer systems under equivalent instrumental conditions (after correction to equivalent concentrations and signal-to-noise ratios) it is estimated that a pool of 30 ± 10% of the total chlorophyll complement of the thylakoid is observed in the high resolution spectrum.

Notably absent are resonances from membrane proteins. This result is consistent with previous ^{13}C-NMR studies of biological membranes where the high resolution resonances arise from lipids rather than proteins.[16] Since lipid and protein are present in similar amounts this observation must be due to differences in the molecular motion of the two membrane fractions. ^{13}C relaxation mechanisms are predominantly intramolecular and therefore principally related to internal flexibility.[17] Thus protein resonances are not observed (i.e., are broad) because of incomplete motional averaging resulting from restricted internal motion or long motional correlation times. On the other hand, the relatively narrow phytol resonances of chlorophyll must indicate more complete motional averaging. It may therefore be concluded that the motional state of the pool of chlorophyll observed in the ^{13}C spectrum is much different than the motional state of the protein, and that indeed it more closely approximates that of the lipid fraction of the membrane. Since the manner in which chlorophyll is bound to the membrane will influence both its lateral mobility and internal flexibility and, therefore, its overall motional state, the present observations may have some bearing on the question of how chlorophyll is distributed within the membrane.

Assume for the purpose of discussion that the observed chlorophyll is contained within membrane protein. This being the case, the

chlorophyll must be bound in such a way that the motional state of the phytol chain is not affected by the surrounding protein shell. If the chlorophyll were contained within a hydrophobic core which is sufficiently spacious to allow this type of motion, then aliphatic protein side-chains should have equally free motion. However, the lack of resonances from such groups in the ^{13}C spectrum suggests that this is not the case. Furthermore, in the case of the only chlorophyll containing protein for which the crystal structure has been determined, the authors concluded that both the porphyrin and phytol portions of the chlorophyll are held firmly in position with little or no freedom of movement.[18]

Since the motional state of the chlorophyll phytol chains observed here more closely resembles that of the lipid portion of the membrane, it is more reasonable to assume that this pool of chlorophyll is not embedded in protein, but rather is contained in the bilayer portion of the membrane or, perhaps bound at the periphery of membrane protein with the phytol chains essentially free.[19] Such a conclusion is consistent with the observation of a free pigment band found in gel chromatography of detergent solubilized membrane and is further supported by evidence for the close association of galactolipids with chlorophyll in vivo.[20-23] The biological significance of this pool of chlorophyll is not certain, although studies of model systems of chlorophyll in lipid bilayers suggest that it can be involved as, or be a part of, a photosynthetic antenna.

REFERENCES AND NOTES - CHAPTER VI

1. L. L. Shipman, T. M. Cotton, J. R. Norris, J. J. Katz, J. Am. Chem. Soc., 98, 8222-8230 (1976).
2. J. P. Thornber, J. P. Markwell, S. Reinman, Photochem. Photobiol., 29, 1205-1216 (1979).
3. J. M. Anderson, J. C. Waldron, S. W. Thorne, FEBS Lett., 92, 227-233 (1978).
4. J. P. Markwell, J. P. Thornber, R. T. Boggs, Proc. Natl. Acad. Sci. U.S.A., 76, 1233-1235 (1979).
5. Some recent studies[4] purport that all chlorophyll is associated within protein complexes. However, it has not been adequately demonstrated that the detergent solubilization procedures used in these studies do not artificially associate non-protein bilayer components.
6. H. Hashimoto and S. Murakami, Plant Cell Physiol., 16, 895-902 (1975).
7. S. Murakami and L. Packer, Arch. Biochem. Biophys., 146, 337-347 (1971).
8. The Stanford Magnetic Resonance Laboratory is supported by NSF Grant GP-23633 and NIH Grant RR-00711. We are grateful to the SMRL staff, in particularly Anthony Ribeiro, for able assistance.
9. R. A. Goodman, E. Oldfield, A. Allerhand, J. Am. Chem. Soc., 95, 7553-7559 (1973).
10. S. G. Boxer, G. L. Closs, J. J. Katz, J. Am. Chem. Soc., 96, 7058-7066 (1974).

REFERENCES (continued)

11. S. R. Johns, D. R. Leslie, R. J. Willing, D. G. Bishop, Aust. J. Chem., 30, 813-822 (1977).

12. S. R. Johns, D. R. Leslie, R. J. Willing, D. G. Bishop, Aust. J. Chem., 30, 823-834 (1977).

13. S. R. Johns, D. R. Leslie, R. J. Willing, D. G. Bishop, Aust. J. Chem., 31, 65-72 (1978).

14. A. T. James and B. W. Nichols, Nature, 210, 372-375 (1966).

15. C. F. Allen and P. Good, Methods Enz., 23, 523-547 (1971).

16. K. M. Keough, E. Oldfield, D. Chapman, P. Beynon, Chem. Phys. Lipids, 10, 37-50 (1973).

17. A. Allerhand, D. Doddrell, R. Komoroski, J. Chem. Phys., 55, 189-198 (1971).

18. R. E. Fenna and B. W. Matthews, Brookhaven Symp. 28th, 170-182 (1976).

19. J. M. Anderson, Nature, 253, 536-537 (1975).

20. A. Rosenberg, Science, 157, 1191-1196 (1967).

21. E. S. Bamberger and R. B. Park, Plant Physiol., 41, 1591-1600 (1966).

22. Z. Krupa and T. Baszynski, Biochim. Biophys. Acta, 408, 26-34 (1975).

23. L. K. Ostrovskaya, S. M. Kochubei, T. M. Shadchina, Biokhimiya, 40, 169-174 (1975).

24. This work is supported by United States Public Health Service Grant GM-22432 from the National Institute of General Medical

REFERENCES (continued)

Sciences. KEE and WRC were supported by NIH National Research Service Awards GM-07616 and GM-01262 from the National Institute of General Medical Sciences. This is contribution No. 6192 from the Division of Chemistry and Chemical Engineering, California Institute of Technology.

APPENDIX A

Analysis of ^{1}H-NMR Linewidths in Chlorophyll a/DSPC Bilayer Vesicles-Contribution of Anisotropic Chemical Shifts to Nuclear Spin Relaxation

In Chapter IV it was noted that the resonance linewidth of the choline N-methyl protons in NMR spectra of chlorophyll a/DSPC vesicles was a sensitive indicator of the solidus phase transition. An analysis of the dependence of these linewidths on the static magnetic field strength reveals that this phenomenon is a consequence of an unusual relaxation mechanism heretofore unobserved for protons. Although the following information does not contribute substantially to the theme of the organization of chlorophyll a in membranes, it is sufficiently interesting to warrant further discussion.

Linewidth Data

The full width at half-maximum (FWHM) of the choline N-methyl proton resonance was measured from spectra of chlorophyll a/DSPC vesicles obtained according to the procedures described in chapter IV. Figure A-1 shows the measured FWHM linewidths in Hertz for 10, 15 and 20 mole percent chlorophyll a as a function of temperature at 100 MHz and 360 MHz. (These frequencies correspond respectively to the Larmor frequencies of protons in magnetic fields of 23.4 and 84.6 kilogauss.) The linewidths are markedly dependent on field strength, particularly at increased chlorophyll a composition. At a given field the linewidths depend on chlorophyll a content as well. It can be recognized at once that the increase in linewidth with field is

FIGURE A-1. Table of linewidths for the DSPC choline N-methyl protons in 10, 15, and 20 mole percent chlorophyll a/DSPC vesicles as a function of temperature and observation frequency.

	10 mole%		15 mole %		20 mole%	
°C	100 MHz	360 MHz	100 MHz	360 MHz	100 MHz	360 MHz
60°	11.2 Hz	21 Hz	--	37 Hz	13.8 Hz	57 Hz
58	11.6	22	--	39	14.2	61
56	12.2	22	--	41	14.6	63
54	12.6	22	--	42	15.0	65
52	12.8	22	--	47	15.2	69
50	13.4	22	--	51	15.6	75
48	14.0	27	--	59	18.0	97
46	16.0	33	--	78	25.6	126
44	24.0	41	--	102	48.0	175
40	36.0	57	--	155	58.0	248

not due to an unresolved chemical shift distribution since the linewidths are not constant in parts per million relative to the observational frequency. This suggests that the measured linewidth is under the control of relaxation effects.

Analysis of the Field Dependence of Linewidths

The only relaxation mechanism which is dependent on the strength of the applied field is relaxation via anisotropic electronic shielding, also called chemical shift anisotropy (CSA). The relaxation rate due to this CSA mechanism is proportional to the square of the static magnetic field H_0^2. Other relaxation mechanisms that do not depend on an applied field should also contribute to the overall relaxation rate. Since the FWHM linewidth $W_{\frac{1}{2}}$ is related to the spin-spin relaxation rate T_2^{-1},

$$W_{\frac{1}{2}} = 1/\pi T_2 \qquad \text{(A-1)}$$

and since the individual contributions to the overall relaxation rate are additive as

$$1/T_2 = \sum_i (1/T_2)_i \qquad \text{(A-2)}$$

we can deconvolute the observed linewidth into a sum of field-independent and field-squared-dependent terms. Let these contributions to the linewidth be called x and y respectively. We can then express the FWHM linewidth at 100 MHz as

$$W_{\frac{1}{2}}^{100} = x + y \qquad \text{(A-3)}$$

and the linewidth at 360 MHz as

$$W_{\frac{1}{2}}^{360} = x + (3.6)^2 y. \qquad \text{(A-4)}$$

Solving (A-3) and (A-4) simultaneously for x and y, we obtain the results of Figure A-2 for the 10% and 20% chlorophyll a compositions. Since there is linewidth data for 15% chlorophyll a at only 360 MHz, that data could not be analyzed by this procedure.

The contribution of CSA relaxation is relatively unimportant at 100 MHz, adding only a few percent to the resonance linewidth, whereas at 360 MHz it dominates the observed linewidth. The deconvoluted linewidth data tabulated in Figure A-2 are plotted in a more easily interpreted format in Figures A-3a and A-3b. These figures illustrate the interesting result that the field-independent contribution to the linewidth is also independent of the chlorophyll a content. Hence it is apparent that all of the dependence of the linewidth on chlorophyll a content occurs through the field-dependent relaxation mechanism. By averaging the values of x for 10% and 20% chlorophyll a and subtracting this from the linewidth data for 15% chlorophyll a at 360 MHz, we can obtain a reasonably accurate estimate of the field-dependent component of the linewidth for this set of data. These data for 15% chlorophyll a, along with the values for 10% and 20% data, are plotted in Figure A-4 to show the regular increase in linewidth with increasing chlorophyll a content.

Relaxation via Chemical Shift Anisotropy

The magnetic field which a given nucleus experiences depends on

FIGURE A-2. Results of the deconvolution of the data in Figure A-2 into field-dependent (y) and field-independent (x) contributions. The columns y/w and x/w are the fractional contributions of each to the total linewidth.

100 MHz

	10% chlorophyll *a*				20% chlorophyll *a*			
°C	y	x	y/w	x/w	y	x	y/w	x/w
60	0.8	10.4	0.07	0.93	3.6	10.2	0.26	0.74
58	0.9	10.7	0.07	0.93	3.9	10.3	0.27	0.73
56	0.8	11.3	0.07	0.93	4.0	10.6	0.27	0.73
54	0.8	11.8	0.06	0.94	4.2	10.8	0.28	0.72
52	0.8	12.0	0.06	0.94	4.5	10.7	0.30	0.70
50	0.7	12.7	0.05	0.95	4.9	10.7	0.31	0.69
48	1.1	12.9	0.08	0.92	6.6	11.4	0.37	0.63
46	1.4	14.6	0.09	0.91	8.4	17.2	0.33	0.67
44	1.4	22.6	0.06	0.94	10.6	37.4	0.22	0.78
40	1.7	34.2	0.05	0.95	15.8	42.2	0.27	0.73

360 MHz

	10% chlorophyll *a*				20% chlorophyll *a*			
°C	y	x	y/w	x/w	y	x	y/w	x/w
60	10.6	10.4	0.51	0.49	46.8	10.2	0.82	0.18
58	11.3	10.7	0.51	0.49	50.7	10.3	0.83	0.17
56	10.6	11.3	0.48	0.52	52.0	10.6	0.83	0.17
54	10.1	11.8	0.46	0.54	54.6	10.8	0.83	0.17
52	10.0	12.0	045	0.55	58.5	10.7	0.84	0.16
50	9.3	12.7	0.43	0.57	63.7	10.7	0.85	0.15
48	14.0	12.9	0.52	0.48	85.8	11.4	0.88	0.12
46	18.5	14.6	0.56	0.44	109.2	17.2	0.86	0.14
44	18.5	22.6	0.45	0.55	137.8	37.4	0.79	0.21
40	22.8	34.2	0.40	0.60	205.4	42.2	0.83	0.17

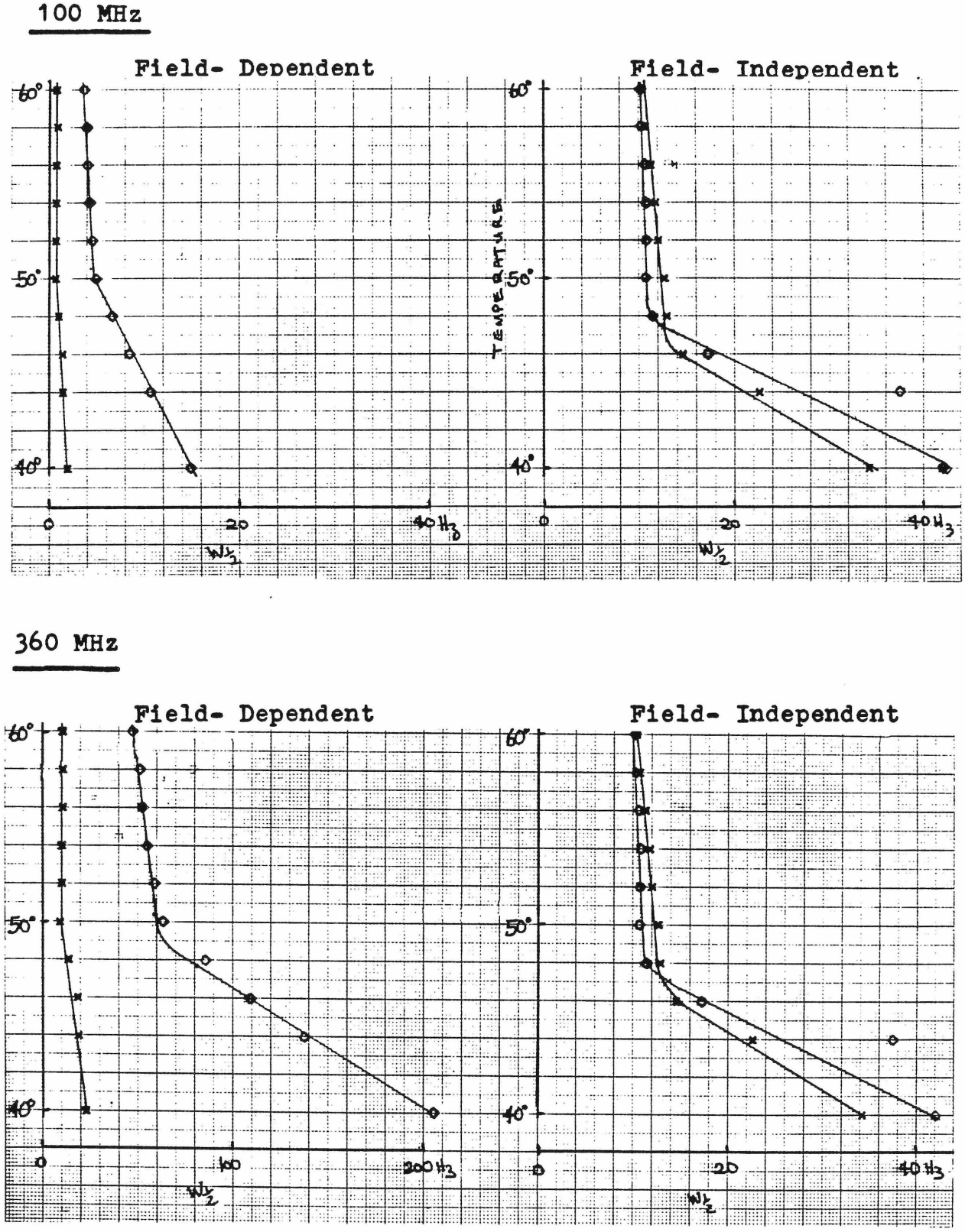

FIGURE A-3. Field-dependent and field-independent contributions to the linewidth versus temperature for 10% (×) and 20% (open squares) chlorophyll a/DSPC vesicles.

FIGURE A-4 (next page). The field-dependent component of the choline N-methyl linewidth in 10%, 15%, and 20% chlorophyll a/DSPC vesicles.

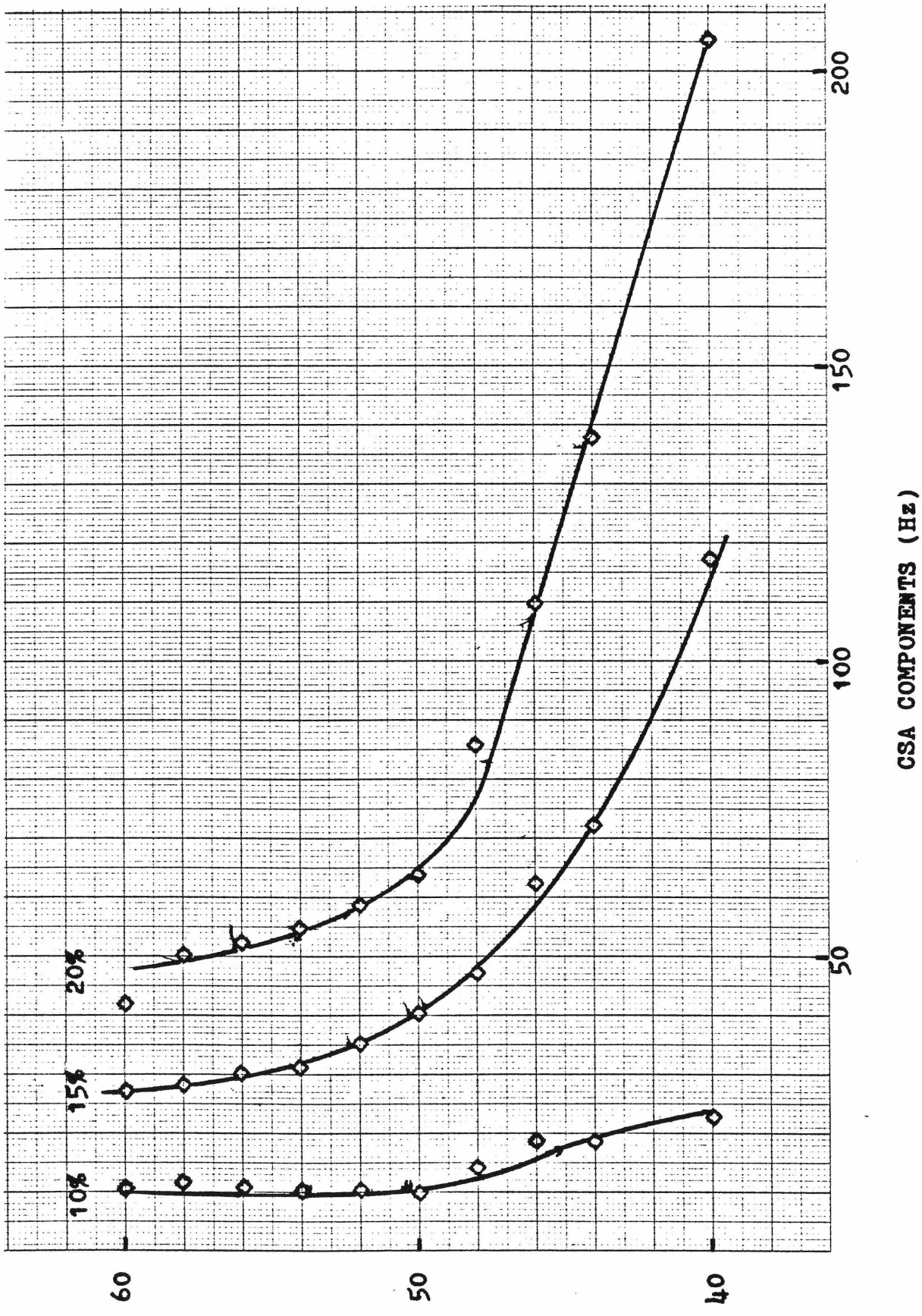
60
50
40
TEMPERATURE
10%
15%
20%
50
100
150
200
CSA COMPONENTS (Hz)

the electronic shielding about the nucleus. If this shielding varies with the direction of the applied field, then there is said to be a chemical shift anisotropy about the nucleus. As the system rotates with respect to the static applied field, the anisotropy can produce a secondary fluctuating field which contributes to the relaxation of the nuclear spin system. Fluctuations with Fourier transform components near the Larmor frequency contribute to both spin-lattice and spin-spin relaxation; those at lower frequencies contribute to spin-spin relaxation only. The contribution to the nuclear relaxation from chemical shift anisotropy is given by[1]

$$\frac{1}{T_1} = \frac{6}{40} \gamma^2 H_0^2 \Delta\sigma^2 \left(1 + \frac{\eta^2}{3}\right) J(\omega_0) \qquad \text{(A-5)}$$

$$\frac{1}{T_2} = \frac{1}{40} \gamma^2 H_0^2 \Delta\sigma^2 \left(1 + \frac{\eta^2}{3}\right) \{3 J(\omega_0) + 4 J(0)\} \qquad \text{(A-6)}$$

Where T_1 and T_2 are the spin-lattice and spin-spin relaxation times, γ is the magnetogyric ratio, H_0 the applied field, $\Delta\sigma$ is the difference between the shielding constants with the field parallel and perpendicular, $J(\omega_0)$ and $J(0)$ are the spectral densities at ω_0 and zero frequency.

Figure A-5 shows two ways in which a fluctuating field can be produced by chlorophyll a molecules in lipid bilayer vesicles, the first due to vesicle rotation, the second due to lateral diffusion within the membrane. When a given chlorophyll a molecule is oriented perpendicular to the applied field, the ring current effect produces either a shielding or a deshielding (σ) on nearby nuclei. As the vesicle tumbles

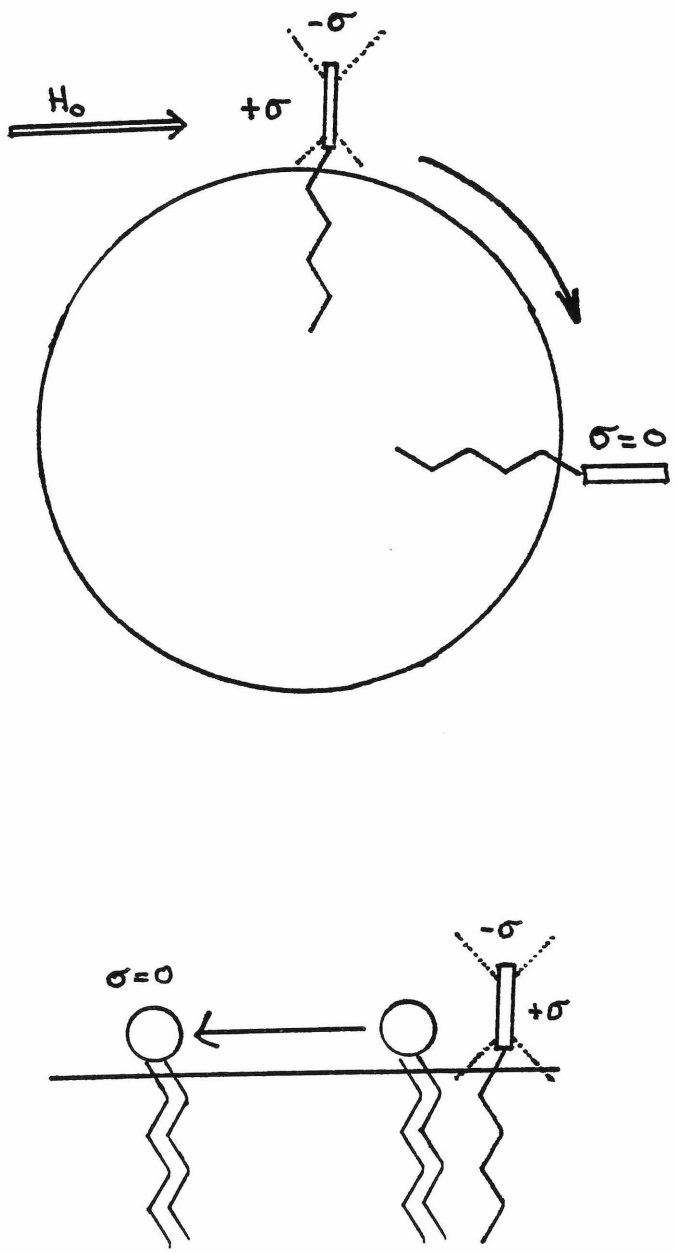

FIGURE A-5. Modulation of the ring current chemical shift anisotropy by rotation of the vesicle (top) and by lateral diffusion of a lipid molecule within the vicinity of a chlorophyll a molecule (bottom).

by 90°, the applied magnetic field is parallel to the chlorophyll a macrocycle and is ineffectural in producing a ring current within the porphyrin pi-system. Thus there is a field $\Delta\sigma$ fluctuating at the timescale of vesicle tumbling τ_R. A second effect, which is independent of vesicle tumbling, occurs as a bilayer lipid molecule diffuses past a chlorophyll a molecule with a timescale determined by the lateral diffusion coefficient. Both of these processes occur at frequencies at least three orders of magnitude slower than ω_0, hence $J(\omega_0) \approx 0$. Thus we see that CSA contributes only to T_2 relaxation. Equation (A-6) can then be expressed as $(1 + \eta^2/3 \approx 1)$:

$$\frac{1}{T_2} = \frac{1}{10} \gamma^2 H_0^2 (\Delta\sigma)^2 \tau_R \qquad \text{(A-7)}$$

where it is assumed that the correlation time of vesicle tumbling predominates over that of lateral diffusion. Since $\gamma H_0 = 2\pi\nu_0$, the linewidth $1/\pi T_2$ is given by

$$\frac{1}{\pi T_2} = \frac{4\pi}{10} \nu_0^2 (\Delta\sigma)^2 \tau_R \quad . \qquad \text{(A-8)}$$

This equation is graphed for reasonable values of τ_R in Figure A-6. The vesicle rotational correlation time τ_R can be obtained from Debye-Stokes theory. If the vesicle is treated as a sphere of radius a, in a medium of viscosity η (not the same η as before) with average molecular radius a_s, then τ_R is[2]

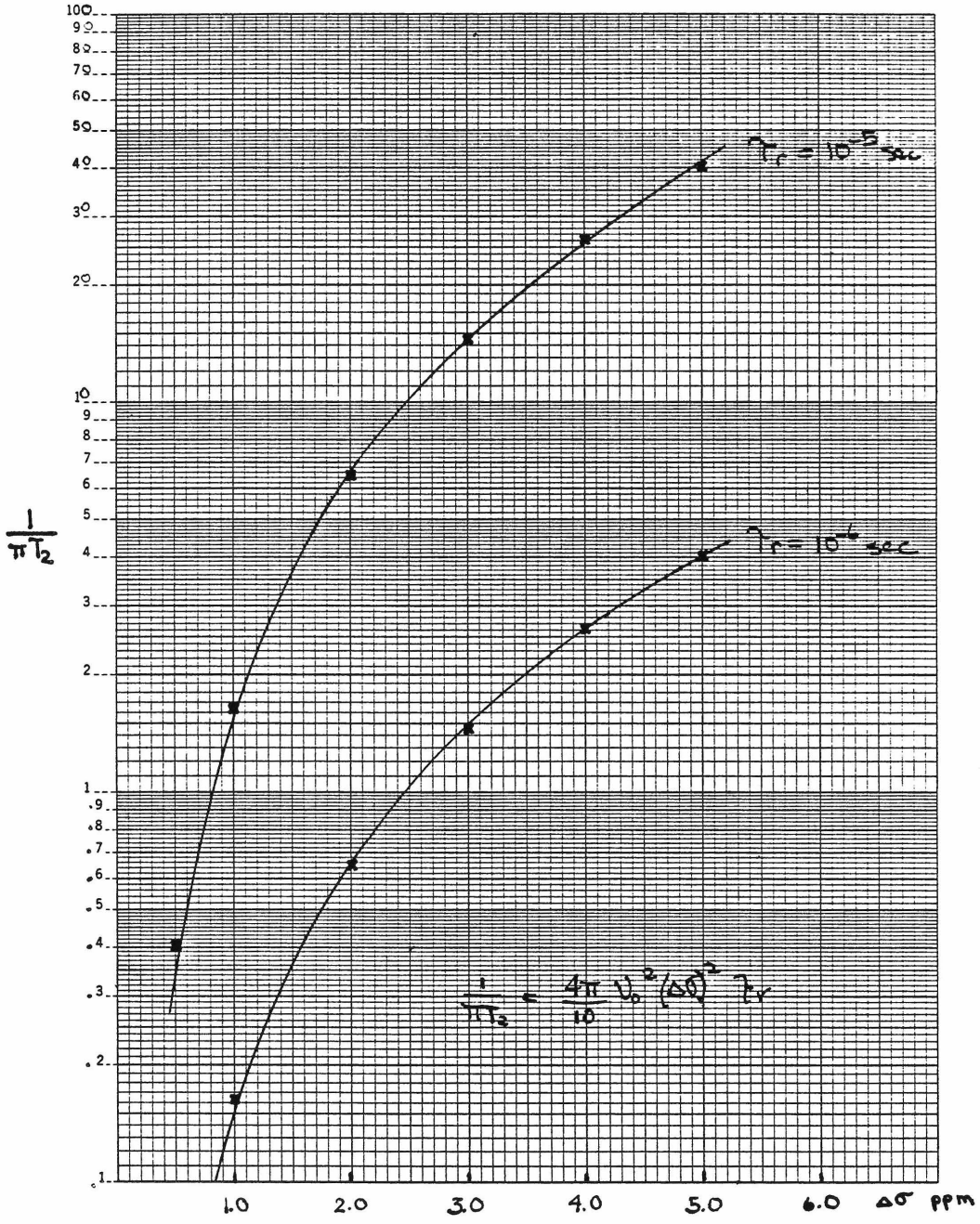

FIGURE A-6. Graph of equation (A-8).

$$\tau_R = \frac{4\pi a^3 \eta}{3kT} \left[6 \frac{a_s}{a} + \left(1 + \frac{a_s}{a}\right)^{-3} \right]^{-1}. \qquad \text{(A-9)}$$

The vesicle radius a is much larger than a_s, hence the microviscosity factor (the bracketed term) is nearly 1. The linewidth can then be expressed in a more determinable form:

$$\frac{1}{\pi T_2} \approx \frac{4\pi}{10} \nu_0^2 (\Delta\sigma)^2 \frac{4\pi a^3 \eta}{3kT} . \qquad \text{(A-10)}$$

Equation (A-10) is graphed in Figure A-7 for various vesicle radii. Figure A-7 shows that the observed linewidths are adequately accounted for by reasonable values of the vesicle radius and shielding asymmetry.

The functional form of the data can be checked to see if it follows (A-10). Rearranging (A-10) to collect terms which are independent of temperature, it is seen that the linewidth should be a simple function of viscosity and temperature:

$$\frac{1}{\pi T_2} = \frac{16\pi^2 \nu_0^2}{30k} (\Delta\sigma)^2 a^3 \left(\frac{\eta}{T}\right) \qquad \text{(A-11)}$$

A plot of linewidth versus η/T should then result in a straight line of slope $16\pi^2 \nu_0^2 (\Delta\sigma)^2 a^3/30\,k$. Figure A-8 shows that this is indeed the case. The change in slope at the bilayer phase transition is undoubtedly a result of a change in $\Delta\sigma$ between the solution and compound phases. The vesicle radius a cannot change more than a few percent as a result of the phase transition and can be regarded as essentially

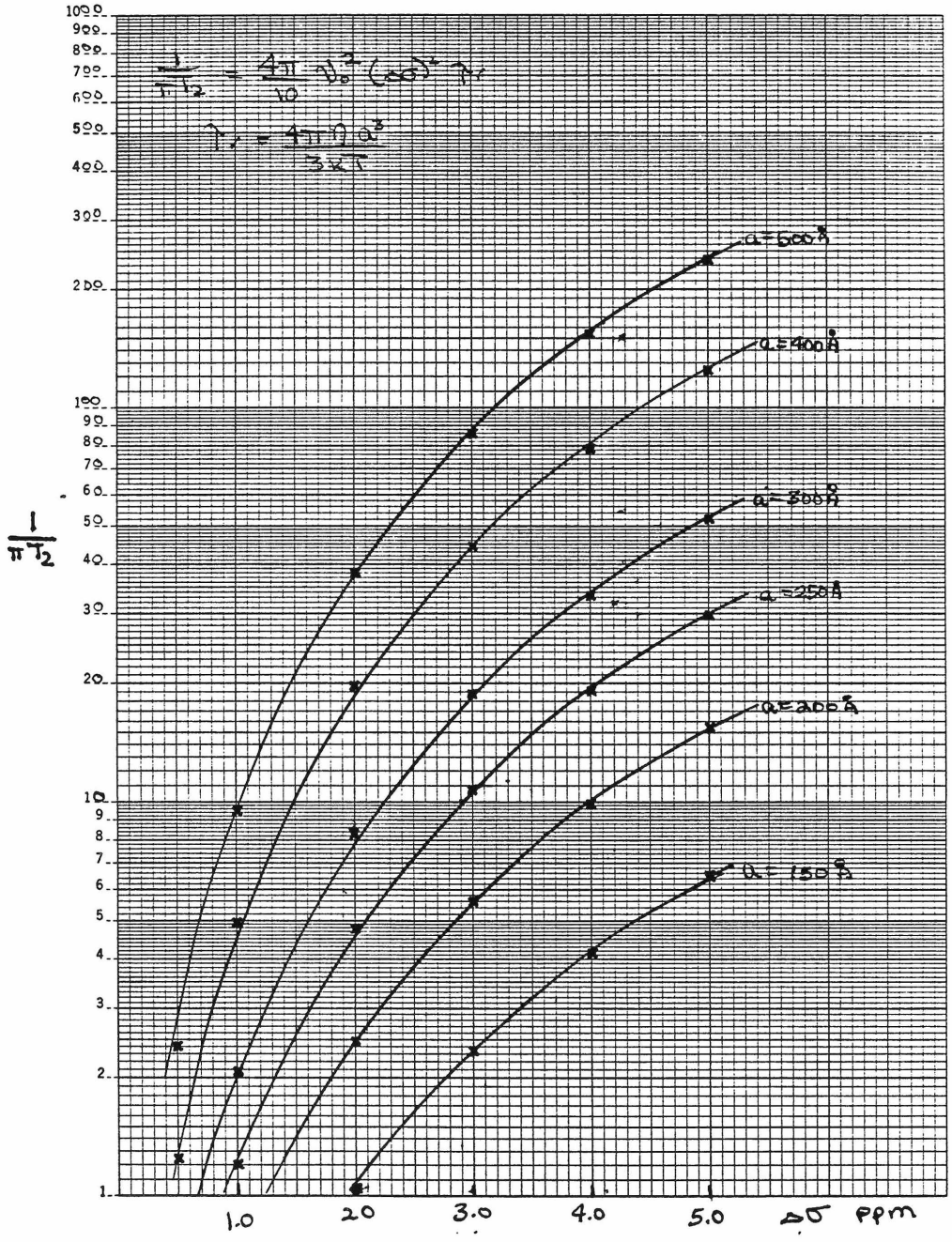

FIGURE A-7. Graph of equation (A-9).

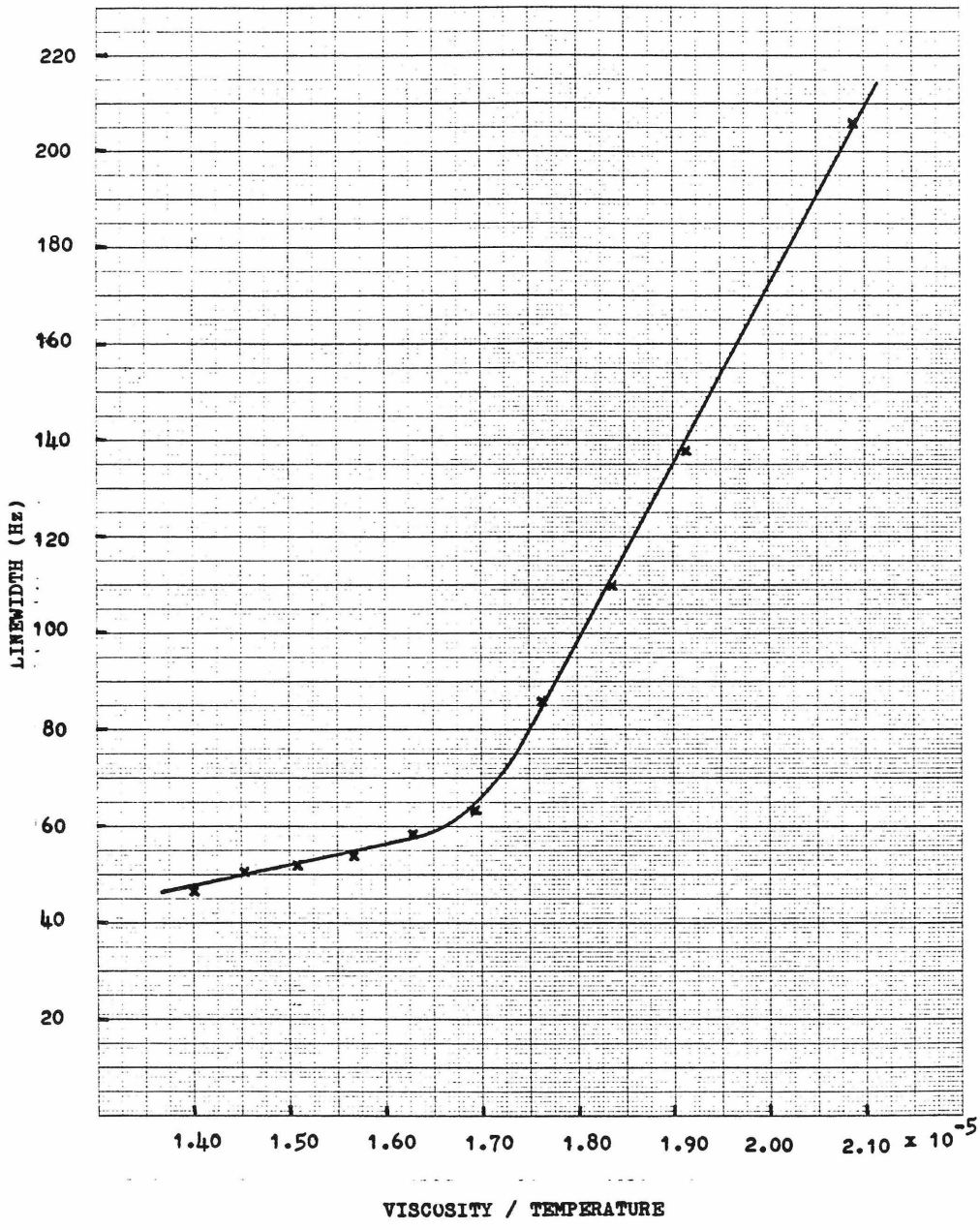

FIGURE A-8. Plot of the field-squared dependent component of the choline N-methyl resonance linewidth in 20% chlorophyll a/DSPC vesicles as a function of the viscosity in centipoise divided by temperature in degrees kelvin.

constant. It was determined in chapter II that chlorophyll a/DSPC vesicles were eluted in the void volume of a Sepharose 4B column and therefore are apparently much larger than DSPC vesicles; let us choose to use 500 angstroms as a reasonable estimate for the radius. For a vesicle radius of 500 angstroms, the measured slope indicates that $\Delta\sigma$ is 2.84 ppm above 50° anf 7.74 ppm below 50°. Since $\Delta\sigma$ is three times the ring current shift, these values translate to a ring current shift on the choline protons of 0.95 ppm in the solution phase, and 2.58 ppm in the compound phase. These are easily within the same order of magnitude of the shifts estimated in chapter V.

To our knowledge these results are the first evidence for a chemical shift anisotropy contribution to a proton nuclear spin relaxation, albeit in a rather atypical situation.

REFERENCES - APPENDIX A

1. A. Abragam, The Principles of Nuclear Magnetism, Clarendon Press, Oxford, 1961, pp. 315-316.

2. T. L. James, Nuclear Magnetic Resonance in Biochemistry, Academic Press, New York, 1975, pp. 38-40.

APPENDIX B

The Effect of Surface Curvature on the Headgroup Structure and Phase Transition Properties of Phospholipid Bilayer Vesicles

K. E. Eigenberg and S. I. Chan,
Biochim. Biophys. Acta, 599, 330-335 (1980)

Biological membranes often contain regions which have a small radius of curvature. It has been suggested[1,2] that this curvature could modify membrane properties thereby providing a means of regional differentiation of membrane function. The effect of curvature on the phase behavior of phospholipid bilayer membranes has been demonstrated by a variety of techniques. Differential scanning calorimetry[3-6] and fluorescence studies[6,7] have shown that the phase transition temperature, enthalpy and entropy are all lower in small sonicated vesicles than in planar bilayers. Nuclear magnetic resonance[1,8-12] and Raman studies[13-15] have shown that this is partly due to packing differences of the hydrocarbon chains as a result of the structural asymmetry imposed by a small radius of curvature. Because of this asymmetry, it is expected that curvature will affect the organization of the headgroup region as well.

In this communication we present the results of nuclear magnetic resonance experiments which suggest a substantial difference in the organization of inner and outer headgroups of small vesicles below the

thermal phase transition. This difference is reflected in the changes in chemical shift of inner and outer choline headgroup resonances as the phase transition is traversed. In particular, the chemical shifts indicate that the inner layer lipids undergo a structural change at the phase transition not observed for the outer layer.

Small single-walled bilayer vesicles were prepared by sonicating a dispersion of distearoylphosphatidylcholine, 30 mg/ml in ^2H_2O, at a temperature above the phase transition for 10 minutes. Following sonication the solution was centrifuged to remove any remaining large bilayer structures and titanium particles released from the sonicator tip. Previous studies[16] have shown that this treatment results in a fairly homogeneous population of small vesicles with an outer diameter of approximately 250 Å.

Fourier transform proton NMR spectra at 360 MHz of the resulting vesicle suspension were obtained at 2° intervals of temperature from 64 - 36°. A total of 100 transients were collected for each temperature using 16K data points (0.30 Hz digital resolution) with 2 seconds delay between pulses. The probe temperature was determined using ethylene glycol and can be considered reliable to within 0.5°. A coaxial capillary containing 1% $(CH_3)_4Si$ in $CHCl_3$ was used as an external reference.

The spectra of the vesicles show the characteristic splitting of the choline N-methyl resonance which has previously been assigned to headgroups on the inner and outer surfaces of the bilayer vesicle.[1,17] At the magnetic field of this experiment, 84.56 kilogauss, the inner

and outer peaks can be resolved throughout the temperature range of the experiment. At the lower temperatures the splitting becomes much more apparent. Resonances due to choline N-methylene and PO-methylene protons are also perceptibly split at the lower temperatures in the same manner as the choline N-methyl resonance, although the splittings of these resonances are either unresolved or absent at the higher temperatures. The relative intensities of the inner and outer peaks reflect the number of molecules in the inner and outer bilayer halves[1] and can be used to estimate the average outer radius of the vesicles to be 120 Å. The outer/inner choline intensity ratio is about 2.7 at both limits of the temperature range studied, indicating that the size distribution of the vesicle population has not changed during the course of the experiment. In addition, the total area of the choline peak remains constant with temperature, as was previously observed for dipalmitoylphosphatidylcholine vesicles.[1]

Figure B-1 shows the portion of the spectrum due to choline N-methyl protons at various temperatures. It can be seen that the chemical shift difference between the inner and outer choline N-methyl resonances increases as the temperature is lowered. In Figure B-2 the difference in chemical shift of the two resonances is plotted versus temperature. The data show an abrupt change in magnetic inequivalence over a relatively narrow range of temperature near 50°, decreasing from about 25 Hz below 50° to about 9 Hz at higher temperatures. The resonance linewidths also begin to increase at about 50° in agreement with previous observations that lipid resonances broaden below

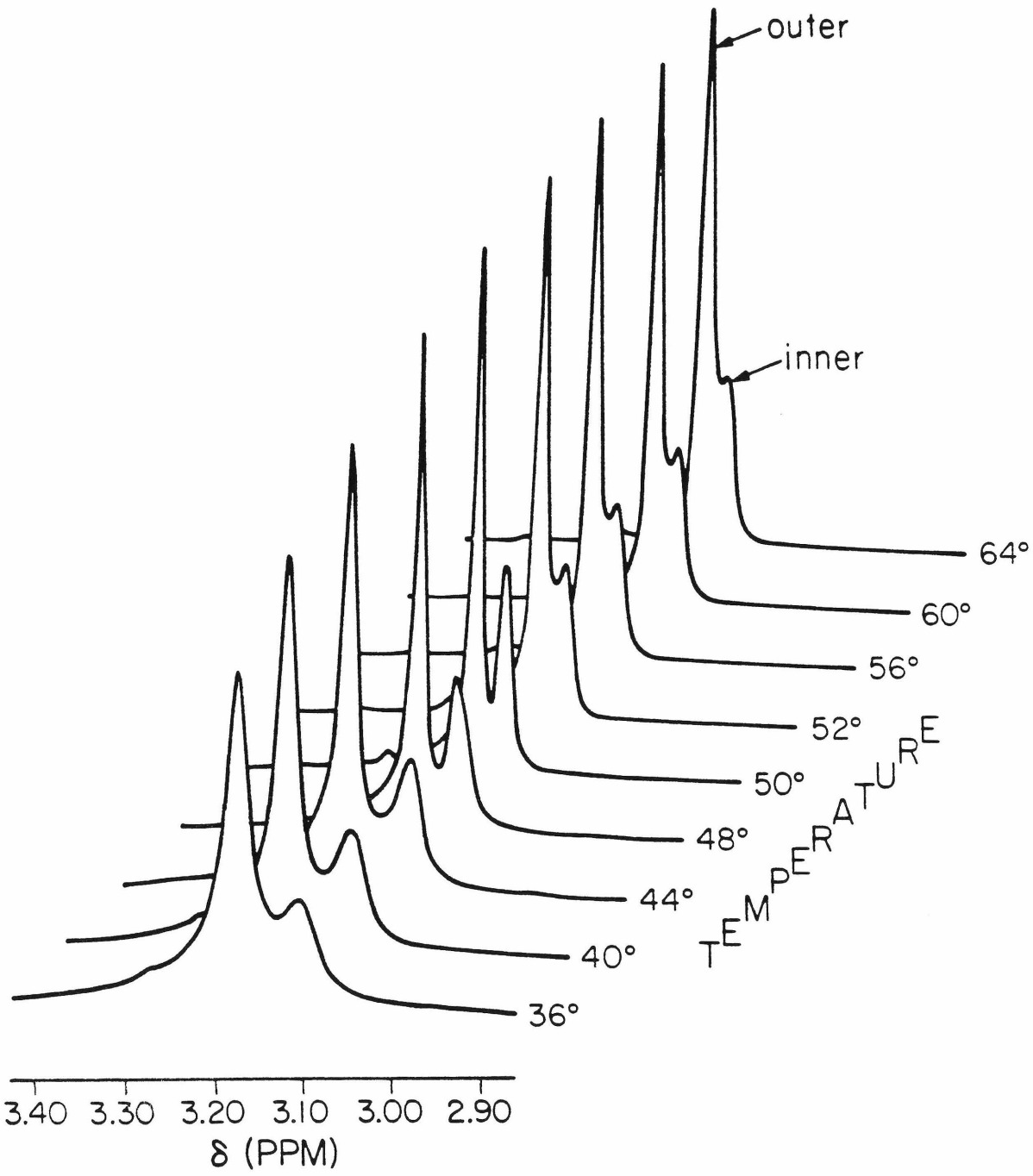

FIGURE B-1. Choline N-methyl portion of the 360 MHz ^{1}H-NMR spectrum of small sonicated vesicles at various indicated temperatures (°C). Resonances due to molecules on the inner and outer halves of the bilayer are indicated by arrows.

FIGURE B-2 (next page, top). Chemical shift difference in Hz between inner and outer choline N-methyl proton resonances at various temperatures ranging through the thermal phase transition of the bilayer vesicles. (360 Hz = 1 part per million).

FIGURE B-3 (next page, bottom). Resonance position (in Hz relative to $(CH_3)_4Si$) of outer (open circles) and inner (closed circles) choline N-methyl protons plotted versus temperature.

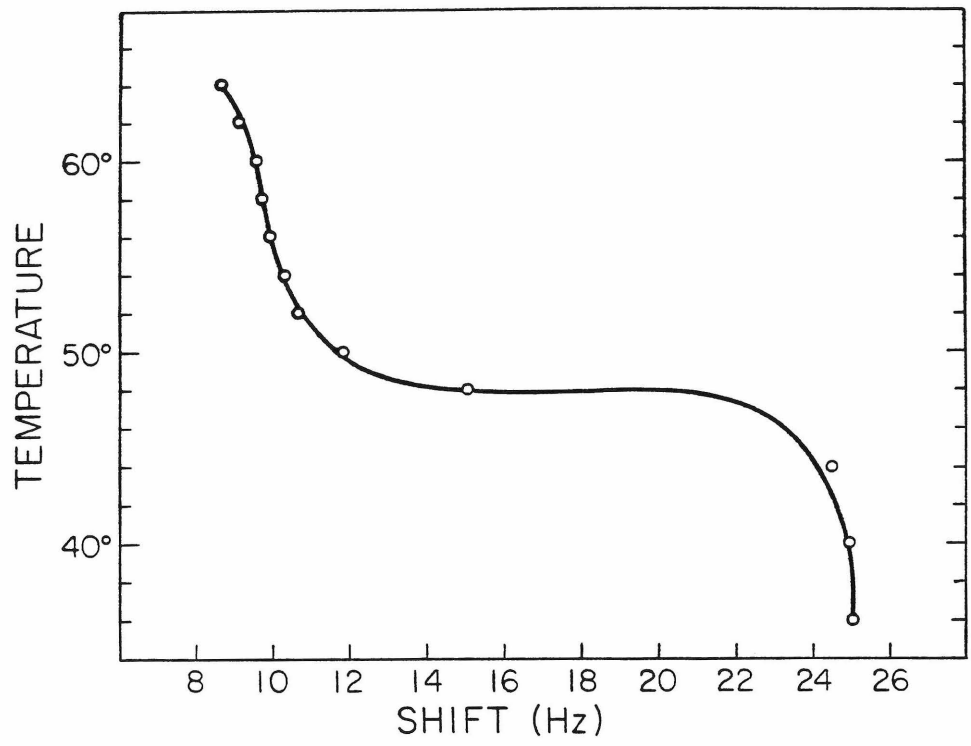
TEMPERATURE
60°
50°
40°
8
10
12
14
16
18
20
22
24
26
SHIFT (Hz)

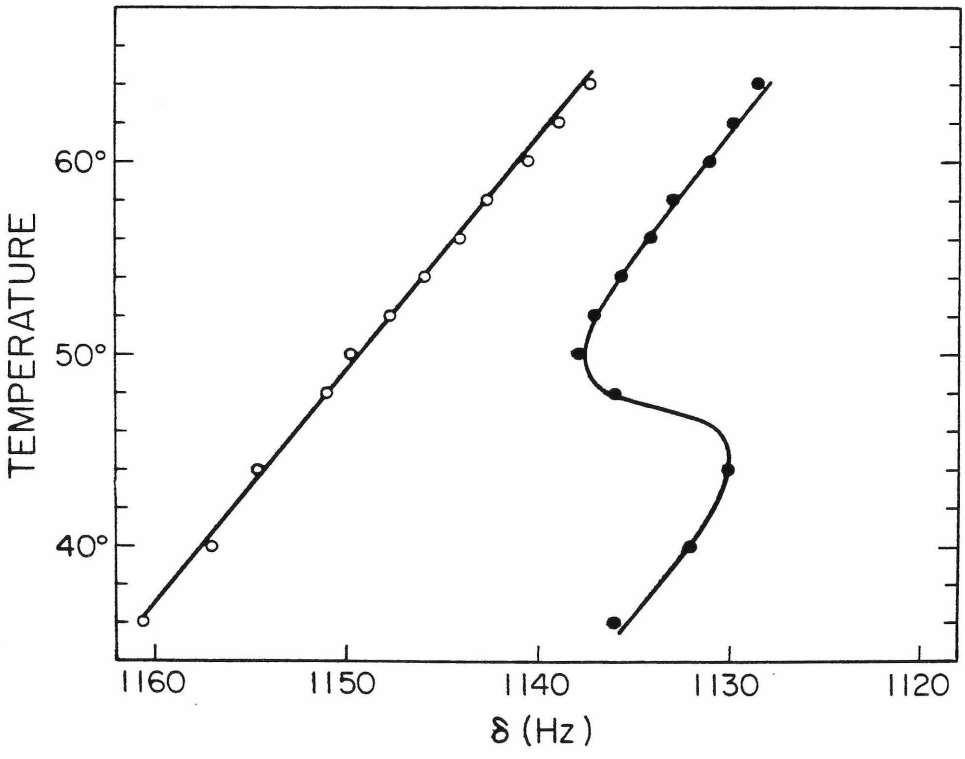
TEMPERATURE
60°
50°
40°
1160
1150
1140
1130
1120
δ (Hz)

the thermal phase transition. These observed changes correlate well with the phase transition temperature of 51.3° and width of 7.3° reported for distearoylphosphatidylcholine vesicles by fluorescent probe studies.[7]

In Figure B-3, the resonance frequencies of the individual inner and outer choline N-methyl protons are plotted versus temperature. These data reveal a change in the shift of inner layer headgroups at the phase transition which does not occur for the outer layer headgroups. Inasmuch as these chemical shifts are referenced to external $(CH_3)_4Si$, the data also reflect the change in solution bulk susceptibility with temperature. This effect is nearly linear over the temperature range of our experiment[18] and causes a small slope in the data. If the hydrocarbon methylene resonance is used as an internal reference, the outer layer shifts become constant with temperature, as do the inner layer resonances except for the inner layer transition at 50°. While it has been known previously that the chemical shifts of inner and outer layer choline N-methyl resonances are different, the data of Figures B-2 and B-3 show that there is an increase in the splitting below the phase transition and, furthermore, that this increase is the result of an upfield shift of the inner layer resonance.

As Kostelnik and Castellano have pointed out,[17] chemical shift differences of the magnitudes shown in Figures B-2 and B-3 cannot be accounted for solely by the shielding at the inner surface due to the bilayer (estimated to be $< 10^{-5}$ ppm). Any deviation of the vesicle shape from spherical symmetry could result in a more substantial shift

between inner and outer layers since the induced field at the outer layer does not average to zero over all orientations of the non-spherical surface. This possibility can be considered unlikely because the surface free energy of the vesicle favors a uniform spherical surface.[19] In this context it is pertinent that the ^{31}P spectrum of vesicles also consists of two resonances due to molecules on the inner and outer layers[20] and that the splitting between them is substantially larger than that observed for the choline N-methyl proton resonance. Thus bulk magnetic effects may be excluded as a cause of the magnetic inequivalence between layers. This leaves local magnetic effects due to headgroup organization as the important determinant of the difference in shift between inner and outer layers.

A difference in headgroup organization, reflecting differences in headgroup conformation or packing, may be a result of variations in the intermolecular electrostatic interactions of the zwitterionic headgroups. Yeagle has established[21] that phosphatidylcholine headgroup packing consists of the positively charged quaternary amine of each lipid associating with the negatively charged phosphates of adjacent neighbors. This interaction is electrostatically favorable and orients the headgroups parallel to the membrane surface.[22] Although the exact distance between intermolecular charged pairs is not known, ^{31}P nuclear Overhauser experiments suggest that it is less than 3 Å. It is known that under conditions which neutralize the electrostatic binding, this interaction can be disrupted.[23-26] This point is relevant because lipid packing is very different for the inner and outer halves of small bilayer

vesicles. In particular, the area occupied by each lipid headgroup in the outer layer of the vesicle is some 12 to 21% larger than for the inner layer, depending on the lipid. In vesicles of dipalmitoyl-phosphatidylcholine, the area per headgroup at the inner surface[27] (68 $Å^2$) is near to the value for planar bilayers,[29] while the larger area at the outer surface 76 $Å^2$) indicates that the outerlayer is somewhat expanded by curvature. This 12 - 21% difference in headgroup area translates to a 6 - 10% linear expansion between outer layer headgroups, irrespective of the packing lattice assumed by the lipid molecules. Assuming a reasonable distance of 8 - 10 Å between headgroups, this 6 - 10% difference in the average lipid-lipid distance would imply that headgroups are stretched almost an angstrom farther apart in the outer layer. Such an expansion would unquestionably influence the electrostatic interactions of the headgroups in the outer layer, causing them to be much weaker. If the interaction is sufficiently weakened, it might be expected that the headgroups of the outer layer could adopt some new, more energetically favored conformation in which the headgroups do not electrostatically interact to the same extent. In fact, minimum energy calculations of headgroup conformation predict an extended conformation of the headgroup when electrostatic interactions are excluded.[30] The conformation of the inner layer headgroups remains unperturbed by curvature since the inner headgroup areas remain roughly the same as in a planar bilayer.

The results of Figure B-3 suggest that there is no structural change in the outer layer headgroups over the temperature range of the

thermal phase transition of the bilayer. This conclusion may have some bearing on the apparent discrepancy between transition enthalpies of vesicles and flat multilamellar bilayers (multilayers). The transition enthalpy of small vesicles is about one-third of that for multilayers,[4,5] and increases with vesicle size.[5] Coincidentally, the fraction of molecules in the inner layer of small vesicles is about one-third and this fraction increases with vesicle size in a manner consistent with the dependence of enthalpy on vesicle size. It might be that the variation in heats is a reflection of the different headgroup organization of the inner and outer layers and it is conceivable that the different surface curvatures of the two layers can affect their thermal melting differently.

ACKNOWLEDGMENTS

This work was supported by United States Public Health Service Grant GM-22432 from the National Institute of General Medical Sciences. Nuclear magnetic resonance experiments were carried out at the Stanford Magnetic Resonance Laboratory which is supported by NSF Grant GP-23633 and NIH Grant RR-00711. KEE was supported by NIH Research Service Award 5T32 GM 07616-02 and gratefully acknowledges the assistance of Bill Croasmun and the SMRL staff in obtaining the data.

REFERENCES - APPENDIX B

1. M. P. Sheetz and S. I. Chan, Biochemistry, 11, 4573-4581 (1972).
2. T. C. Thompson, C. Huang, and B. J. Litman, in The Cell Surface in Development, (A. A. Moscona, ed.), Wiley, New York, 1974, pp. 1-16.
3. D. L. Melchior and J. M. Steim, Ann. Rev. Biophys. Bioeng., 5, 205-238 (1976).
4. J. M. Sturtevant, Stud. Nat. Sci. N.Y., 4, (Quant. Stat. Mech. Nat. Sci., [Coral Gables Conf. 1973]), 63-84 (1974).
5. B. Gruenewald, S. Stankowski, and A. Blume, FEBS Lett., 102, 227-229 (1979).
6. J. Suurkuusk, B. R. Lentz, Y. Barenholz, R. L. Biltonen, and T. E. Thompson, Biochemistry, 15, 1393-1401 (1976).
7. B. R. Lentz, Y. Barenholz, and T. E. Thompson, Biochemistry, 15, 4521-4528 (1976).
8. D. Lichtenberg, N. O. Petersen, J. Girardet, M. Kainosho, P. A. Kroon, C. H. A. Seiter, G. W. Feigenson, and S. I. Chan, Biochim. Biophys. Acta, 382, 10-21 (1975).
9. S. I. Chan, M. P. Sheetz, C. H. A. Seiter, G. W. Feigenson, M. Hsu, and A. Lau, Ann. N. Y. Acad. Sci., 222, 499-522 (1973).
10. C. H. A. Seiter and S. I. Chan, J. Am. Chem. Soc., 95, 7541-7553 (1973).
11. N. O. Petersen and S. I. Chan, Biochemistry, 16, 2657-2667 (1977).

REFERENCES (continued)

12. K. J. Longmuir and F. W. Dahlquist, Proc. Natl. Acad. Sci. USA, 73, 2716-2719 (1976).

13. B. P. Gaber and W. L. Peticolas, Biochim. Biophys. Acta, 465, 260-271 (1977).

14. R. C. Spiker and I. W. Levin, Biochim. Biophys. Acta, 455, 560-575 (1976).

15. R. Mendelson, S. Sunder, and H. J. Bernstein, Biochim. Biophys. Acta, 419, 563-569 (1976).

16. C. Huang, Biochemistry, 8, 344-352 (1969).

17. R. J. Kostelnik and S. M. Castellano, J. Magn. Reson., 9, 291-295 (1973).

18. C. J. Jameson, A. K. Jameson, and S. M. Cohen, J. Magn. Reson., 19, 385-392 (1975).

19. J. N. Israelachvili, D. J. Mitchell, and B. W. Ninham, J. Chem. Soc. Faraday Trans., 272, 1525-1568 (1976).

20. A. C. McLaughlin, P. R. Cullis, J. A. Berden, and R. E. Richards, J. Magn. Reson., 20, 146-165 (1975).

21. P. L. Yeagle, Acc. Chem. Res., 11, 321-327 (1978).

22. R. G. Griffin, L. Powers, and P. S. Pershan, Biochemistry, 17, 2718-2722 (1978).

23. M. F. Brown and J. Seelig, Nature, 269, 721-723 (1977).

24. H. Hauser, W. Guyer, B. Levine, P. Skrabal, and R. J. P. Williams, Biochim. Biophys. Acta, 508, 450-463 (1978).

REFERENCE (continued)

25. H. Hauser, M. C. Phillips, B. A. Levine, and R. J. P. Williams, Nature, 261, 390-394 (1976).

26. G. Lindblom, N. D. Persson, and G. Avidson, Adv. Chem. Ser., No. 152, 121-141 (1976).

27. A. Chrzeszczyk, A. Wishnia, and C. S. Springer, Biochim. Biophys. Acta, 470, 161-169 (1977).

28. C. Huang and J. T. Mason, Proc. Natl. Acad. Sci. USA, 75, 308-310 (1978).

29. F. Reiss-Husson, J. Mol. Biol., 25, 363-382 (1967).

30. E. Brosio, F. Conti, and A. DiNola, J. Theor. Biol., 67, 319-334 (1977).